

Experiments to Measure Armature Wear, Part 1: Wear Measurements on the KJ202 Armature

F. Stefani and J. Parker

*Institute for Advanced Technology
The University of Texas at Austin*

August 1998

IAT.R 0180

Approved for public release; distribution unlimited.

19990201 034

The views, opinions, and/or findings contained in this report are those of the author(s) and should not be construed as an official Department of the Army position, policy, or decision, unless so designated by other documentation.

REPORT DOCUMENTATION PAGE

Form Approved
OMB NO. 0704-0188

Public reporting burden for this collection of information is estimated to average 1 hour per response, including the time for reviewing instructions, searching existing data sources, gathering and maintaining the data needed, and completing and reviewing the collection of information. Send comments regarding this burden estimate or any other aspect of this collection of information, including suggestions for reducing this burden, to Washington Headquarters Services, Directorate for Information Operations and Reports, 1215 Jefferson Davis Highway, Suite 1204, Arlington, VA 22202-4302, and to the Office of Management and Budget, Paperwork Reduction Project (0704-0188), Washington, DC 20503.

1. AGENCY USE ONLY (Leave blank)		2. REPORT DATE August 1998		3. REPORT TYPE AND DATES COVERED Technical Report 1/97-12/97	
4. TITLE AND SUBTITLE Experiments to Measure Armature Wear, Part 1: Wear Measurements on the KJ202 Armature				5. FUNDING NUMBERS Contract # DAAA21-93-C-0101	
6. AUTHOR(S) F. Stefani and J. Parker					
7. PERFORMING ORGANIZATION NAME(S) AND ADDRESS(ES) Institute for Advanced Technology The University of Texas at Austin 4030-2 W. Braker Lane, #200 Austin, TX 78759				8. PERFORMING ORGANIZATION REPORT NUMBER IAT.R 0180	
9. SPONSORING / MONITORING AGENCY NAME(S) AND ADDRESS(ES) U.S. Army Research Laboratory ATTN: AMSRL-WM-B Aberdeen Proving Ground, MD 21005-5066				10. SPONSORING / MONITORING AGENCY REPORT NUMBER	
11. SUPPLEMENTARY NOTES The view, opinions and/or findings contained in this report are those of the author(s) and should not be considered as an official Department of the Army position, policy, or decision, unless so designated by other documentation.					
12a. DISTRIBUTION / AVAILABILITY STATEMENT Approved for public release; distribution unlimited.				12b. DISTRIBUTION CODE A	
13. ABSTRACT (Maximum 200 words) One of the research objectives of the Hypervelocity Launch group during 1997 was to understand armature wear, with the eventual goal of developing a predictive model. To this end we conducted sixteen experiments to measure wear at various conditions. This report describes the first ten experiments which directly measured wear in a typical "C-shaped" railgun armature. Section 2 of the report describes the objectives and our state of understanding at the outset of the research. We also comment on some prior work in related areas. Section 3 describes the techniques developed for making in-bore wear measurements. Section 4 summarizes the first ten experiments. Section 5 presents a physical interpretation of the data; our conclusion is based in part on the results of the mechanical wear tests, even though these are not discussed in detail in this report. Four appendices following Section 5 present the data from the experiments in a form that can be used to test models of armature wear.					
14. SUBJECT TERMS wear, armature, railgun, model, meltwave erosion, liquid film interface, viscous heating				15. NUMBER OF PAGES 92	
				16. PRICE CODE	
17. SECURITY CLASSIFICATION OF REPORT Unclassified	18. SECURITY CLASSIFICATION OF THIS PAGE Unclassified	19. SECURITY CLASSIFICATION OF ABSTRACT Unclassified	20. LIMITATION OF ABSTRACT UL		

Contents

Introduction.....	1
Background.....	1
Techniques for Measuring Armature Wear	4
Wear Pin Technique.....	4
In-Bore X-rays for Measuring Wear.....	6
Overview of Armature Wear Tests	7
Discussion.....	11
References.....	13
Appendix A: Typical Data Traces (I , V_{BRE} , V_{MUZ} , $B\text{-dot}$ etc.)	17
Appendix B: Summary of Test Conditions, Lab Notes, and Raw Wear Data.....	27
Appendix C: Wear Data	53
Appendix D: Wear Data Plotted as a Function of Location on Armature.....	83
Distribution List.....	91

Figures

Fig. 1. X-ray photographs showing the extent of material loss from KJ202 armature 3	3
during launch. a) static x-ray and b) in-flight x-ray at muzzle exit.	
Fig. 2. Patterns of residual aluminum on copper rails after a test on the MCL. 3	3
Fig. 3. Close-up of an armature used in a wear experiment. The small holes are 0.5 mm 5	5
in diameter and contain tungsten wear pins buried to various depths.	
Fig. 4. Close-up of wear tracks on a copper rail after aluminum has been removed 5	5
Fig. 5. Section of the MCL containment modified to allow partial X-ray access into the bore . 6	6
Fig. 6. In-bore X-ray of the rail/armature interface 7	7
Fig. 7. Drawing of KJ202 Armature used in the wear experiments 7	7
Fig. 8. Plot of current vs. position for a typical experiment on the MCL 8	8
Fig. 9. Results of Armature Wear Experiments for pins located on the first three rows 10	10
of pads nearest the trailing edge.	
Fig. 10. Results of Armature Wear Experiments for pins located in the central portion 10	10
of the armature.	
Figure 11. Contours of stress component normal to armature face 13	13
Fig. A-1. Rail B-dot signals for shot 97020701 on MCL (Arm. mass: 166.2 g) 18	18
Fig. A-2. MCL gun positions from rail B-dot coils for shot number 97020701 18	18
Fig. A-3. MCL gun velocities vs. time from rail B-dot coils for shot number 97020701 19	19
Fig. A-4. MCL gun velocities vs. position from rail B-dot coils for shot number 97020701 .. 19	19
Fig. A-5. Total current vs. time from module Rogowskis for shot number 97020701 20	20
Fig. A-6. Total current vs. position from module Rogowskis for shot number 97020701 20	20
Fig. A-7. Current ² and action vs. time from Rogowskis for shot number 97020701 21	21
Fig. A-8. Current ² and action vs. position from Rogowskis for shot number 97020701 21	21
Fig. A-9. Muzzle voltage vs. time for 97020701 22	22

Fig. A-10. Muzzle voltage vs. position for 97020701	22
Fig. A-11. Breech voltage vs. time for 97020701.....	23
Fig. B1. Coordinate system used for designating pin locations on armature face.....	28
Figure C1. Wear curve fits for all rows and columns.....	53
Fig. C2. Wear at standard conditions; all rows and columns	54
Fig. C3. Wear at standard conditions; all rows, inner columns.....	55
Fig. C4. Wear at standard conditions; all rows, outer columns.....	56
Fig. C5. Wear at low velocity, low current; all rows and columns.....	60
Fig. C6. Wear at low velocity, low current; all rows, inner columns	61
Fig. C7. Wear at low velocity, low current; all rows, outer columns	62
Fig. C8. Wear at high velocity, normal current; all rows and columns	66
Fig. C9. Wear at high velocity, normal current; all rows, inner columns.....	67
Fig. C10. Wear at high velocity, normal current; all rows, outer columns.....	68
Fig. C11. Wear at normal velocity, low current; all rows and columns	71
Fig. C12. Wear at normal velocity, low current; all rows, inner columns.....	72
Fig. C13. Wear at normal velocity, low current; all rows, outer columns.....	73
Fig. C14. Wear at low velocity, high current; all rows and columns	76
Fig. C15. Wear at low velocity, high current; all rows, inner columns	77
Fig. C16. Wear at low velocity, high current; all rows, outer columns	78
Fig. D1. Coordinate system used for designating pin locations on armature face.....	83
Fig. D2. Wear for row 1, columns 1-4	84
Fig. D3. Wear for row 2, columns 1-4	84
Fig. D4. Wear for row 2, columns 6-7.5	85

Fig. D5. Wear for row 3, columns 1-4	85
Fig. D6. Wear for row 3, columns 7-9	86
Fig. D7. Wear for row 4, columns 1-3	86
Fig. D8. Wear for row 4, columns 6-9	87
Fig. D9. Wear for row 5, columns 1-3	87
Fig. D10. Wear for row 5, columns 6-8	88
Fig. D11. Wear for row 6, columns 1-4	88
Fig. D12. Wear for row 6, columns 6-9	89
Fig. D13. Wear for row 7, columns 1-4	89
Fig. D14. Wear for row 8, columns 1-4	90

Experiments to Measure Armature Wear Part 1: Wear Measurements on the KJ202 Armature

Francis Stefani and Jerry Parker

1. Introduction

One of the research objectives of the Hypervelocity Launch group during 1997 was to understand armature wear, with the eventual goal of developing a predictive model. To this end we conducted sixteen experiments to measure wear at various conditions.

This report describes the first ten experiments which directly measured wear in a typical "C-shaped" railgun armature. A second report, "Experiments to Measure Mechanical Wear at Hypervelocity," describes six subsequent experiments which measured purely mechanical wear using a special test fixture.

This report is organized as follows. Section 2 describes the objectives and our state of understanding at the outset of the research. We also comment on some prior work in related areas. Section 3 describes the techniques developed for making in-bore wear measurements. Section 4 summarizes the first ten experiments. Section 5 presents a physical interpretation of the data; our conclusion is based in part on the results of the mechanical wear tests, even though these are not discussed in detail in this report. Four appendices following Section 5 present the data from the experiments in a form that can be used to test models of armature wear.

2. Background

Although wear in sliding electric contacts has been studied extensively at low velocities (100 m/s or less), the phenomenon constitutes uncharted territory at conditions of interest in railguns. This is because the conventional techniques used to study contact wear (pin-on-disk-type devices), are difficult to build for the velocities and pressures typical of railgun launches. An alternative approach is to make wear measurements directly inside the bore of a railgun.

In 1997, the Electrodynamics group at the Institute for Advanced Technology (IAT) set about measuring how much material is lost from an armature during launch. We were motivated by the belief that armature wear might be a factor in the transition of a solid armature to arcing contact, and that by understanding and controlling wear we might be able to delay the onset of transition.

Because the conditions at which armature wear occurs are so untypical, there was very little prior data from which to base our study. In the EML literature, there are no reports of armature wear measurements, (although several works have focused on the transition behavior of specific armatures). In the literature on sliding electric contacts and frictional wear, there are only a few papers reporting experiments at velocities greater than 500 m/s. These are

- wear measurements made at speeds 550 and 600 m/s on a large pin-on-disk device at the Franklin Institute [1, 2].
- basic studies of high speed wear by Bowden and co-authors [3, 4] using metal spheres magnetically suspended and spun to tip speeds of up to 800 m/s.

A general result found by all the investigators is that the coefficient of friction decreases with increasing speed (suggesting that the process is not truly friction in the conventional meaning of the term). There is more data for speeds below 500 m/s, but it is marginally relevant since over 90% of armature wear occurs at greater than 500 m/s.

Accordingly, at the outset of this study we knew very little with certainty about armature wear. What we knew was based on what can be deduced from comparing conditions before and after a shot.

- Muzzle x-ray photographs show that by the time an armature leaves the gun, a considerable amount of aluminum has been removed from the trailing arms of the armature (see Fig. 1). There is no way of knowing, however, how much aluminum is lost prior to the transition to arcing contact, although it is reasonable to assume that most is lost from exposure to the arc discharge.
- Rails removed from the launcher after a shot show a pattern of resolidified aluminum that suggests a uniform rate of material loss from the armature up to the point of transition. There is no way, however, of knowing whether the residual aluminum left on the rail is the only aluminum that was removed from the armature. The possibility exists that a significant portion of removed aluminum reacts in the bore to become aluminum oxide dust, and is expelled into the catch tank.
- Rails removed from the launcher show regions with differing patterns of resolidified aluminum, as shown in Fig. 2. The most interesting pattern of deposition is at the starting position of the armature. The central portion of the track shows a burnished finish indicating little or no wear, whereas the outer edges of the track show thick deposits of resolidified aluminum. This condition rapidly evolves (within three armature lengths, or 10 cm) to one of a uniform residue of resolidified aluminum, approximately 15-20 microns thick, that does not adhere well to the rails. This region persists for 20-40 cm and evolves into a similar region of aluminum that adheres to the rails.

What can be inferred from these observations is that initially, skin effect heating is the principal cause of aluminum loss from the armature, acting principally at the edges. Beyond the first 10 to 15 cm of travel, the root cause of wear is not obvious, since at this point the armature is moving faster than 500 m/s and therefore mechanical (viscous heat generation) and electrical heating are both potentially significant. With regards to the difference between the adhering film and nonadhering film, it is possible that the degree of adhesion is related to the peak temperature of the molten aluminum film at the interface (initially the film might not be hot enough to reduce the surface oxide layer and form a bond to the underlying copper). This remains an open question.

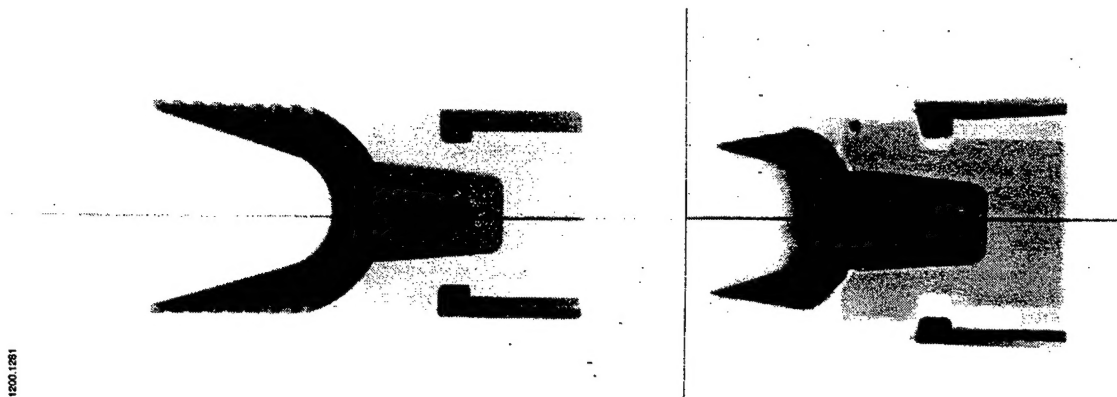


Fig. 1. X-ray photographs showing the extent of material loss from KJ202 armature during launch. a) static x-ray and b) in-flight x-ray at muzzle exit.

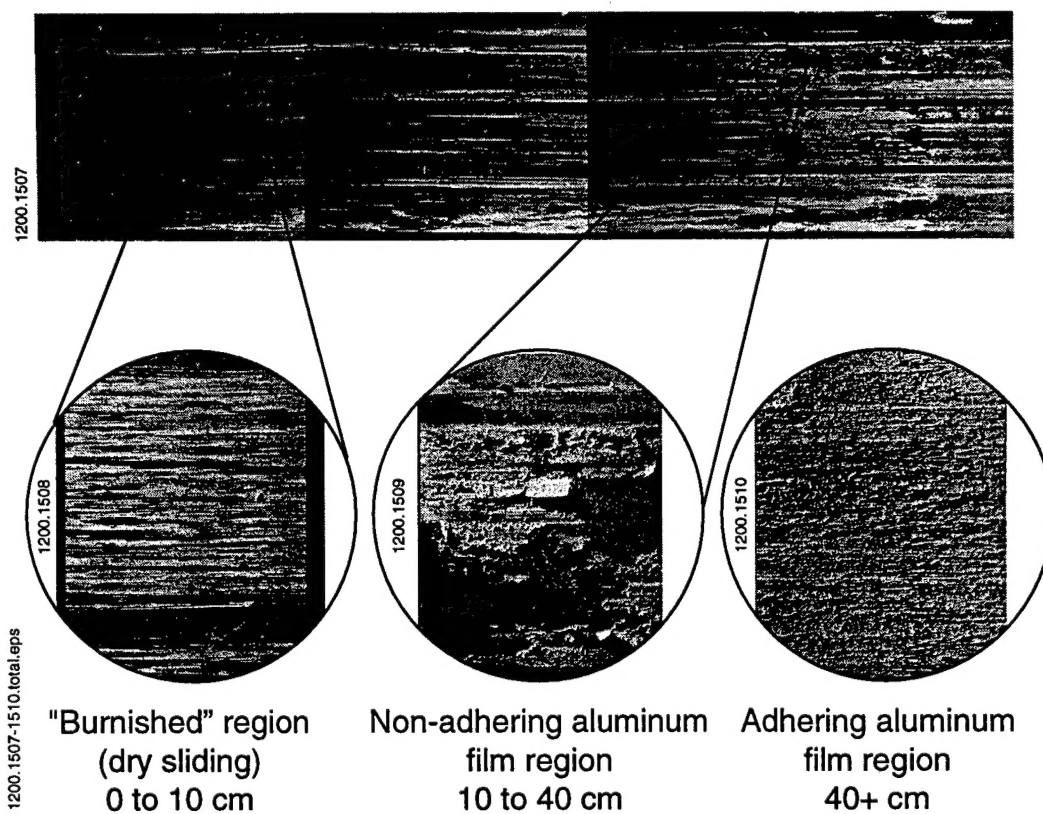


Fig. 2. Patterns of residual aluminum on copper rails after a test on the MCL.

3. Techniques for Measuring Armature Wear

The first problem encountered in this research was how to measure armature wear in a railgun. Recovering armatures in good enough condition to make measurements is not practical above 1 km/s. Inferring wear from material left on the rails is problematic for two reasons: i) it is difficult to accurately measure the volume of the resolidified aluminum, and ii) there is no way of knowing with certainty whether the deposited aluminum constitutes all the aluminum that was removed from the armature.

The first technique we developed, designated the "wear pin" technique, gives good results on softer rail materials up to a velocity of 1.7 km/s. This method involves using 0.5-mm diameter pins embedded in the armature. They become exposed through loss of material, leaving marks on the rails from which the wear can be inferred.

The second technique is to make measurements from X-ray photographs of the armature in the bore. The techniques are complementary. Wear pins are better suited for making measurements early in the launch, when the bulk of the armature is still relatively cold; in-bore X-rays provide more useful information later in the launch, when there is visible erosion of the armature.

Wear Pin Technique

The best way to explain the wear pin technique is to describe the steps involved in making a measurement. The procedure is as follows.

1. A batch of pins is prepared so that all the pins have the same length, diameter, and ends that are faced off. We have found that 0.50-mm diameter, tungsten welding electrodes work best. Tungsten is an ideal material because it is harder than copper, and retains its strength at the melting temperature of aluminum. The length of pins used in most of the tests was around 1.5 mm.
2. Holes for the pins are drilled to known depths at various points in an armature. The depth must be equal to the length of a pin, plus an amount equal to the wear to be measured by the pin. The technique works best for measuring wear from 0 to 1 mm. The ideal tool for making the holes is a high-speed, precision drill press with a gauge to indicate depth. The holes can be anywhere on the face of the armature; however, two holes should not be directly in line with each other in the direction of motion. We separate wear tracks by a couple of millimeters so that in the armature wear tests (Section 3) there are typically between 12 and 16 wear pins per armature face. See Fig. 3.
3. Pins are driven into the holes using a hammer and another pin until they are firmly seated against the bottom of the holes. Using the drill press as a depth gauge, the final depth of each pin below the surface is measured and recorded.

4. After shooting a prepared armature, the rails are recovered for inspection. At this point it is possible to see approximately where on the rail wear each track originates. Greater accuracy is achieved, however, if aluminum deposited by the armature is removed from the rail. This is accomplished using sodium hydroxide as an etchant. Because our armatures are made of 7075 aluminum, a second etching, with mild hydrochloric acid, is used to remove alloying elements (chromium and magnesium). Wear tracks on a completely etched rail are shown in Fig. 4.

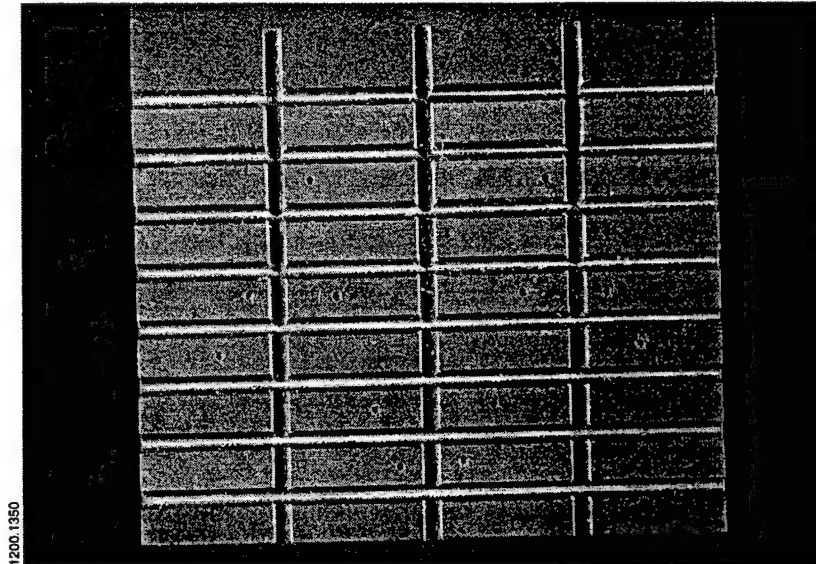


Fig. 3. Close-up of an armature used in a wear experiment. The small holes are 0.5 mm in diameter and contain tungsten wear pins buried to various depths.



Fig. 4. Close-up of wear tracks on a copper rail after aluminum has been removed through chemical etching. Seven tracks are distinctly visible. The middle track is emerging, that is, a pin is beginning to interact with the rail at this location. The axial distance required for a well-prepared pin to establish an unambiguous track is less than two centimeters.

In-Bore X-rays for Measuring Wear

The second technique for measuring wear is based on taking X-rays of the armature while it is in the bore. We were prompted to develop this technique because wear pins proved ineffective once thermal softening penetrates deeply enough that the pins are not supported by the armature material.

The biggest difficulties with taking X-rays in bore are: i) creating an X-ray window that does not compromise the strength of the railgun containment, and ii) developing a compact film holder that fits inside the bottom insulator segments of the gun.

The X-ray window we developed is shown in Fig. 5. It takes advantage of the fact that the containment of the Medium Caliber Launcher (MCL) is composed of many laminations. Removing two out of every three laminations over short sections of the barrel creates "partial" windows into the bore. To avoid bending the remaining laminations during launch, the empty spaces are filled with Lexan, three of which can be seen in Fig. 5. An in-bore X-ray of the KJ-200 armature (discussed below) taken during one experiment is shown in Fig. 6. The white vertical lines are shadows of the remaining containment laminates.

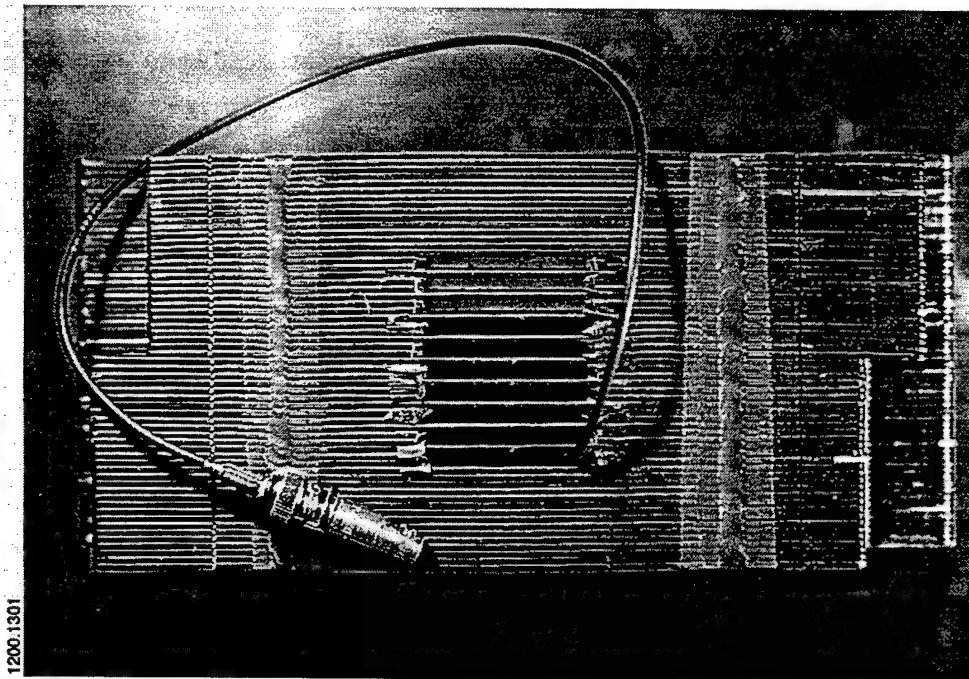


Fig. 5. Section of the MCL containment modified to allow partial X-ray access into the bore. The electrical connection emerging from the first slit is a two-turn coil (not visible) used to sense the arrival of the armature and trigger the X-rays.

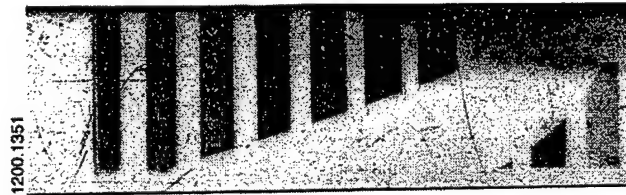


Fig. 6. In-bore X-ray of the rail/armature interface. The horizontal boundary at the bottom of the photograph is the rail. The white vertical bars are the shadows of retained containment laminations.

The film package is a custom-made assembly consisting of a strip of film (Kodak XAR5) sandwiched between two BioEarth Lanthium Oxybromide intensifier screens, wrapped in two turns of 0.1-mm thick black vinyl. The film package resides in a 1.25-mm deep slot on the bottom of the bore-insulating sections. Taking in-bore X-rays requires assembling the gun around the film package.

4. Overview of Armature Wear Tests

The first series of tests sought to characterize wear in an armature designated the KJ202. The KJ202 is a lightweight, compliant, armature made of 7075 Aluminum. It performs consistently well in the 40-mm square bore MCL. We used a version of the KJ202, shown in Fig. 5, in which channels are milled into each contact face to form 36 discrete pads. This modification adds compliance to the armature and was found in earlier tests to suppress the onset of gouging.

Initial pressure at the contact face is provided by an interference fit with the bore of 1 mm at the trailing edge. The interference fit creates an average pressure of about 1 ksi (7 MPa).

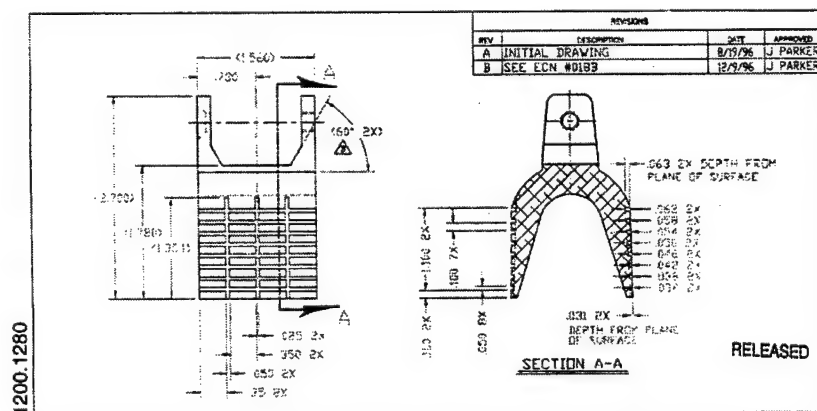


Fig. 7. Drawing of KJ202 Armature used in the wear experiments. The channels in the contact surface improve the performance of the armature.

A summary of the test matrix is shown in Table I. The first four tests were carried out under identical conditions in order to see the amount of statistical scatter intrinsic to the wear pin technique. The conditions for these tests, summarized in Table II, correspond to typical launch conditions for the KJ202 on the MCL. The current pulse, shown in Fig. 6, is nearly constant for the portion of the launch during which wear measurements are made. Examples of the other data traces recorded during the first four tests are included in Appendix A.

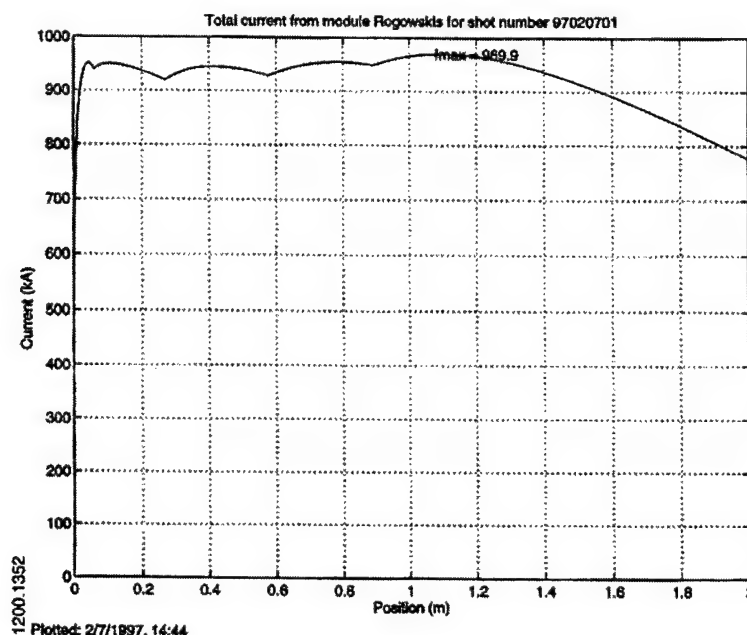


Fig. 8. Plot of current vs. position for a typical experiment on the MCL.

TABLE I
TEST MATRIX FOR ARMATURE WEAR MEASUREMENTS

NAME MCL:	DESCRIPTION	MASS (g)	V_{EXIT} (km/s)	$I_{AVG.}$ (kA)
57	STANDARD CONDITIONS	166.1	2350 ± 20	940 ± 10
58	STANDARD CONDITIONS	166.1	2350 ± 20	940 ± 10
59	STANDARD CONDITIONS	169.4	2440 ± 50	945 ± 10
63	STANDARD CONDITIONS	171.2	2250 ± 20	950 ± 10
71	LOW-VEL. LOW-CUR. #1	169.9	1940 ± 10	850 ± 10
73	HIGH-VEL, NORMAL-CUR.	136.7	2750 ± 20	960 ± 10
75	NORMAL-VEL. LOW-CUR.	136.8	2250 ± 50	855 ± 10
76	LOW-VEL. LOW-CUR. #2	170.7	1950 ± 50	855 ± 10
84	LOW-VEL. HIGH-CUR. #1	281.5	2000 ± 20	1175 ± 10
88	LOW-VEL. HIGH-CUR. #2	293.2	2150 ± 50	1150 ± 20

TABLE II
"STANDARD CONDITIONS" FOR ARMATURE WEAR MEASUREMENTS

LAUNCH PACKAGE	KJ202 VENTED BAR; LEXAN BORE RIDER
MASS	166.15 g
BANK CHARGE	14.0 kV
PEAK CURRENT	972.9 kA
AVERAGE CURRENT	940 \pm 10 KA (AVERAGE VALUE FOR FIRST 40 cm)
DERIVED L'	0.39 μ H/m
ACCELERATION	1.04 $\times 10^6$ m/s ²
EXIT VELOCITY	2350 \pm 20 m/s

Results of the first four tests are summarized in Figs. 9 and 10. Each plot shows wear in a specific region of the armature. Fig. 9 shows wear for the three rows of pads nearest the trailing edge. Fig. 10 shows wear for the next three rows of pads. No plot is shown for the two rows nearest the leading edge as we did not make enough measurements to extract any meaningful trends. Each plot contains two curves, corresponding to the inner and outer column of pads. Each data point corresponds to a particular wear pin in a particular experiment. The y-axis is the initial depth of the wear pin. The x-axis is the axial position on the rail at which the pin track first appears. The uncertainty in pin depth, typically ± 0.025 mm, is based on the resolution of the depth indicator on the drill press. The uncertainty in axial position reflects the precision with which we could establish visually the onset of a wear track.

The results of the tests can be summarized as follows:

1. There is a reasonably good straight line fit to the data. That is, the armature wears at a steady rate of about 0.65 ± 0.05 mm per meter of travel down the bore. This wear rate corresponds to laying down a film of aluminum with an average thickness of 0.015 mm. It is consistent with measurements we have made on residual aluminum that did not adhere to the rails. Using a precision micrometer with a small anvil, we have found the recovered aluminum to be about 0.020 mm thick. The discrepancy of 25% in the measurements is expected since the recovered aluminum is not a uniformly thick film.
2. The wear rate is reasonably even across the face of the armature. The outer edges initially wear faster than the inner regions, and the trailing edge wears on average slightly less than the center, but, on the whole, all parts of the armature appear to wear uniformly to within one or two-tenths of a millimeter. Individual plots of wear data for each pin location on the armature are presented in Appendix D.
3. The inner columns do not begin to wear until the armature has moved about 10 centimeters. This is evidenced in Fig. 9 by the x-intercept value of 18 cm in the regression fit. The same trend appears in Fig. 10 where the data for pins buried flush with the surface (depth = 0) of the armature do not begin to wear until the armature has traveled between five and ten centimeters.

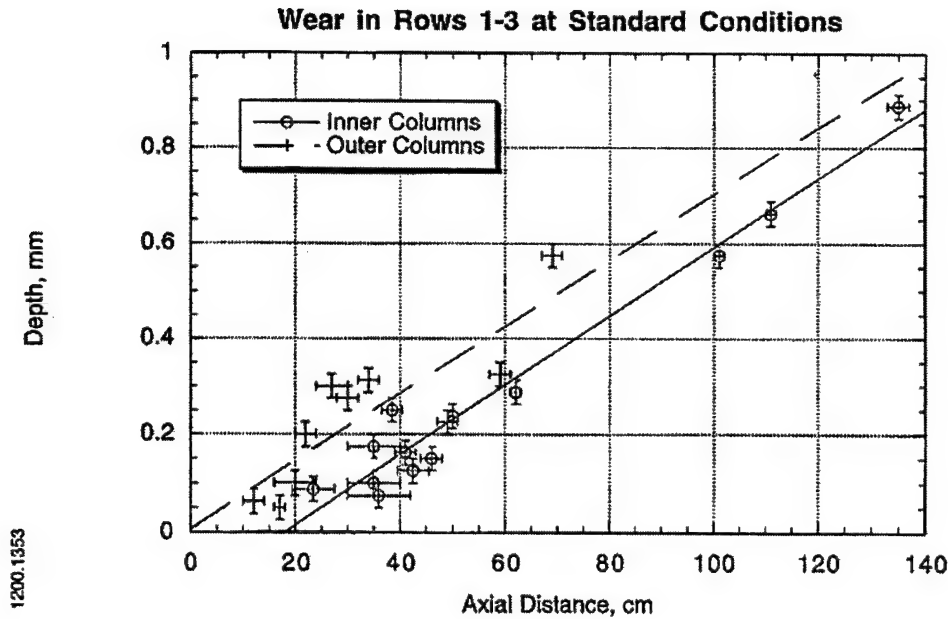


Fig. 9. Results of Armature Wear Experiments for pins located on the first three rows of pads nearest the trailing edge.

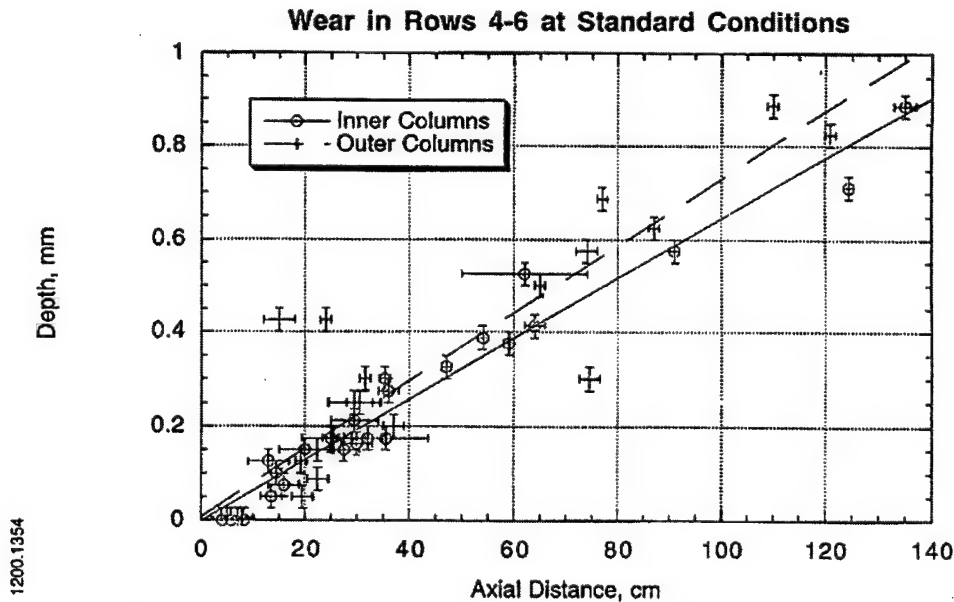


Fig. 10. Results of Armature Wear Experiments for pins located in the central portion of the armature.

Six additional tests were performed in which current and exit velocity were systematically varied without altering the basic experimental setup. Independent variations in exit velocity of ± 400 m/s ($\pm 17\%$), and variations in current of $+130/-90$ kA ($+13\%$ / -10%) were accomplished by adjusting the launch package mass, the bank voltage, or both. It should be noted that because "contact" surface pressure is coupled to current in "C-shaped" armatures, tests conducted with differing currents had differing face pressures.

The tests did not reveal any significant relationships discernible outside the scatter in the data; this is explored in greater depth in Appendix C. From this result we concluded that wear is fairly insensitive to small variations in velocity and current. Extending the range of experimental conditions to higher currents and exit velocities was not deemed possible. This is because in a "C-shaped" armature it is difficult to vary parameters appreciably, let alone independently, while retaining the same armature.

5. Discussion

The objective of this work was to develop an experimental database that can be used to guide the development of a predictive model of armature wear. To this end, we conducted 10 experiments in which we measured wear of a KJ202 armature inside the MCL launcher at the IAT. The aim of this section is to discuss our results in the context of a theoretical framework that can be applied to understanding armature wear.

We have identified three classes of models that attempt to explain surface erosion in metal armatures. These are

- **"Melt Wave Models"** of armature wear, which focus on skin effect heating as the principal cause of wear [5-10]. According to this view, skin-effect heating leads to localized melting and loss of aluminum at the perimeter of the rail/armature interface. This creates an erosion front which progresses in toward the center of the armature until magnetic forces cause the armature to separate from the rail. This is a well established view in the EML community of what causes armatures to wear and transition.
- **"Melt Lubrication Models,"** found in the literature on high-speed friction and wear, which consider the processes by which a molten liquid film between sliding and guiding surfaces is sustained by intense viscous heating [11-13].
- **"Sliding Electric Contact Models,"** which analyze the physics of imperfect electric contacts, focusing on electrical, thermal, and mechanical aspects of current flow through discrete microscopic asperities, or "a-spots" [14-15].

Our experiments show that in general, all three processes produce some wear in armatures. However wear due to "sliding electric contact" is probably of negligible importance since it involves contacting surfaces in the solid state, and evidence suggests that a liquid film interface is formed quite early in the launch, (see Section 2).

This leaves electrical and mechanical heating as potential mechanisms. Our results provide several clues as to their relative importance. The experiments suggest that electrical heating (melt wave erosion) is the dominant wear mechanisms for the first 10 cm of travel ($500 \text{ m/s} < V$). Between 500 and 1000 m/s, mechanical heating is as important as electrical heating. When the armature is traveling faster than 1 km/s, mechanical heating is the dominant wear mechanism.

The case for this interpretation is as follows:

We have accurate measurements of how a typical armature wears in the Medium Caliber Launcher (MCL) during the first 1.5 meters of travel; that is, up until close to the point of transition (typically at 1.8 ± 0.1 m and a velocity of 1,800 m/s.) The wear rate, 0.7 ± 0.005 mm per meter of travel down the bore corresponds to laying down a film of aluminum with an average thickness of 0.015 mm. This result provides a basis for estimating power dissipation at the rail/armature interface. Defining power as the energy needed to melt 0.015 mm of aluminum from the armature face divided by one transit time of the armature gives

$$P_{(\text{in Watts})} = \rho w \delta \Delta z (c_p \Delta T + h_f) / (\Delta z / \text{Velocity})$$
$$= 1,300 * \text{Velocity}_{(\text{in m/s})}$$

where

$$\begin{aligned} \rho &= 2,700 \text{ kg/m}^3 \text{ density of aluminum} \\ w &= 0.036 \text{ m contact width} \\ \delta &= 1.5 \times 10^{-5} \text{ m thickness of film} \\ \Delta z &= 0.025 \text{ m contact length} \\ c_p &= 960 \text{ J/kgK specific heat of aluminum} \\ \Delta T &= 500 \text{ K temperature rise} \\ h_f &= 3.9 \times 10^5 \text{ J/kg heat of fusion for aluminum} \end{aligned}$$

The value of 1,300 is only approximate, since 7075 Aluminum is an alloy, and as such there is a range of reasonable assumptions that can be made about the energy needed to remove material from the armature. The key point is that power is directly proportional to velocity, suggesting that the mechanism causing wear is something other than skin-effect heating, since the uniformity of mass removal across the surface of the armature is not consistent with velocity skin effect.

Additional evidence for the importance of mechanical heating at high velocity comes from six subsequent experiments in which we measured wear in the absence of electrical heating. In these experiments, we used a special launch package to apply face pressures ranging from 6 to 22 ksi to 7075 aluminum wear samples in sliding contact with the rails. The samples were electrically isolated to ensure that all wear was from mechanical heating. The tests (discussed in a separate report, "Experiments to Measure Mechanical Wear at Hypervelocity") show that at velocities greater than 700 m/s, a face pressure of 15 ksi produces wear that is comparable to wear measured in the armature tests, about 0.7 mm per meter of travel. From coupled electromagnetic/structural analysis of the KJ202 armature [16], we know that 15 ksi is approximately the face pressure in our tests, thus confirming that mechanical wear is the dominant process at high velocity. See Fig. 11.

TIME = 0.99996E-03 s
 CONTOURS OF X-STRESS
 MIN=-0.221E+09 IN ELEMENT 384
 MAX= 0.314E+09 IN ELEMENT 1344

CONTOUR VALUES (Pa)
 A=-2.00E+08
 B=-1.78E+08
 C=-1.56E+08
 D=-1.33E+08
 E=-1.11E+08
 F=-8.89E+07
 G=-6.67E+07
 H=-4.44E+07
 I=-2.22E+07
 J= 1.20E+01

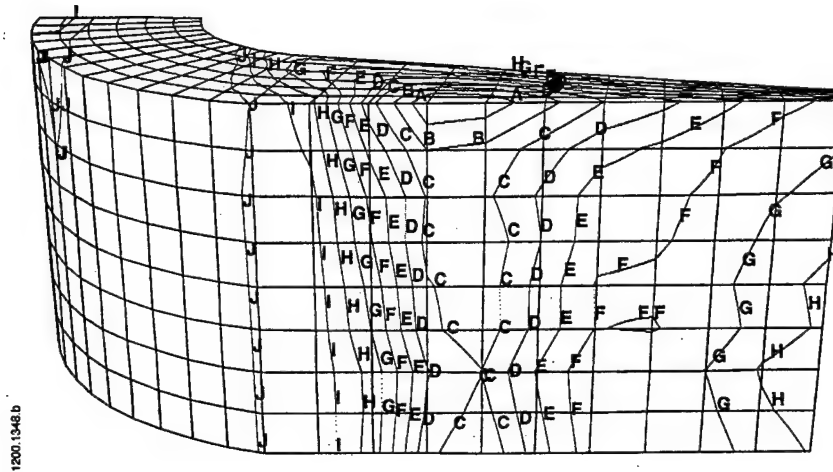


Figure 11. Contours of stress component normal to armature face, based on a dynamic EM/structural analysis of the KJ202 see Ref. [16].

In general, our results suggest that the melt wave models provide an accurate picture of wear in relatively slow, noncompliant armatures. On the other hand, our tests on a fast, compliant armature show that mechanical heating can be more important than electrical heating. Which mechanism dominates is determined by i) whether the armature attains a high velocity (>1 km/s) before the melt wave front has progressed appreciably, and ii) the magnetic pressure and compliance of the armature, which determine whether a uniform face pressure can be maintained to compensate for loss of material from the interface.

Acknowledgment

This work was supported by the U.S. Army Research Laboratory (ARL) under contract DAAA21-93-C-0101.

References

- [1] B. Sternlicht and H. Alpkarian, "Investigation of melt lubrication," *Transactions American Society of Lubrication Engineers*, Atlantic City, October 1956, pp. 248-256.
- [2] R. S. Montgomery, "Friction and wear at high sliding speeds," *Wear*, 36 (1976) pp. 275-298.
- [3] F. P. Bowden and E. H. Freitag, "The friction of solids at very high speeds," *Proc. Roy. Soc A*, vol. 260, p. 350-367, March 1958.

- [4] F. P. Bowden and P. A. Persson, "Deformation, heating and melting of solids in high-speed friction," *Proc. Roy. Soc A*, vol. 260, p. 433-458, March 1961.
- [5] J. P. Barber, A. Challita, B. Maas and L. Thurmond, "Contact transition in metal armatures," *IEEE Trans. on Magnetics*, vol. 27, no. 1, pp. 228-232, January 1991.
- [6] J. P. Barber and A. Challita, "Velocity effects on metal armature contact transition," *IEEE Trans. on Magnetics*, vol. 29, no. 1, pp. 733-37, January 1993.
- [7] P. B. Parks, "Current melt-wave model for transitioning solid armature," *J. Appl. Phys.*, vol. 67, no. 1, pp. 3511-16, April 1990.
- [8] T. E. James, "Current wave and magnetic saw-effect phenomena in solid armature," *IEEE Trans. on Magnetics*, vol. 31, no. 1, pp. 622-627, January 1995.
- [9] J. P. Barber and Y. A. Dreizin, "Model of contact transitioning with 'Realistic' Armature-Rail Interface," *IEEE Trans. on Magnetics*, vol. 31, no. 1, pp. 96-100, January 1995.
- [10] L. C. Woods, "The current melt wave model," *IEEE Trans. on Magnetics*, vol. 32, no. 1, January 1997.
- [11] W. R. D. Wilson, "Lubrication by a Melting Solid," *Transactions of the ASME*, p. 22- , January 1976.
- [12] A. K. Stiffler, "Friction and Wear With a Fully Melting Surface," *Transactions of the ASME*, vol. 106, p. 416, July 1984.
- [13] A. Bejan, "Lubrication by Close-Contact Melting," *Fundamental Issues in Small Scale Heat Transfer*, HTD-Vol. 227, p. 61, ASME 1992.
- [14] R. Holm, *Electric Contacts: Theory and Application*, New York: Springer-Verlag, 1967.
- [15] B. K. Kim, K. T. Hsieh, F. X. Bostick, "A Three-Dimensional Finite Element Model for Thermal Effect of Imperfect Electric Contacts," *IEEE Trans. on Magnetics*, vol. 34, January 1999.
- [16] D. Hopkins, F. Stefani, K. T. Hsieh, and B. K. Kim, "Analysis of startup behavior in a 'C-shaped' armature using linked EMAP3D/DYNA3D finite element codes," 9th EML Symposium, Edinburgh, UK, May 1998.

Summary of Appendices

The following four appendices contain most of the data collected in the ten armature wear experiments. They are organized as follows.

Appendix A: Typical Data Traces ($I, V_{BRE}, V_{MUZ}, B\text{-dot}$ etc.)

Appendix B: Summary of Test Conditions, Lab Notes, and Raw Wear Data

Appendix C: Wear Data Plotted on a Per-Test Basis as a Function of Location on Armature

Appendix D: Wear Data Plotted as a Function of Location on Armature

Appendix A

Typical Data Traces (I , V_{BRE} , V_{MUZ} , $B\text{-dot}$ etc.)

Appendix A contains data obtained from MCL 58 (97020701), one of the four "standard condition" tests. The time plots were obtained from LeCroy digitizers sampling at 1 MHz. Rail b-dot signals were processed to obtain the velocity time history, and position plots by using an analysis program that solves for a best fit to the probe data, subject to physics-based constraints. Armature mass and bore area are inputs to the fitting program; a best fit inductance gradient, L' , is computed. Note that the bore area is not automatically set equal to 1600 mm², the physical bore area, because the effect of air pressure is offset by loss of armature mass from arc erosion. The artificially reduced bore area does not affect the curve fit in the early portion of the launch, but provides a better velocity fit late in launch.

The muzzle voltage trace shows a transition to an arc discharge at 1.75 meters into the launch, that is, when the current has dropped to about 85% of the peak value. This transition behavior is typical for the KJ202 armature.

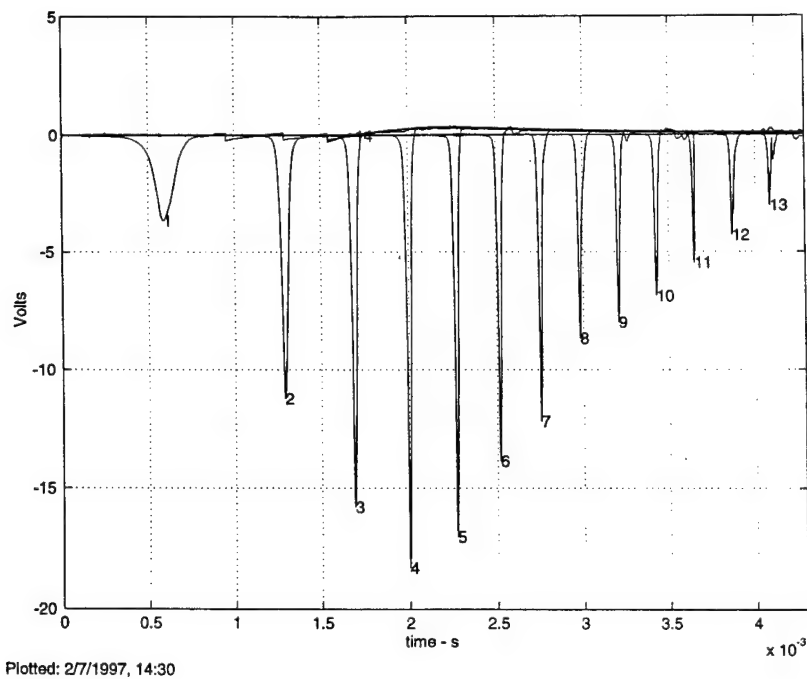


Fig. A-1. Rail B-dot signals for shot 97020701 on MCL (Arm. mass: 166.2 g).

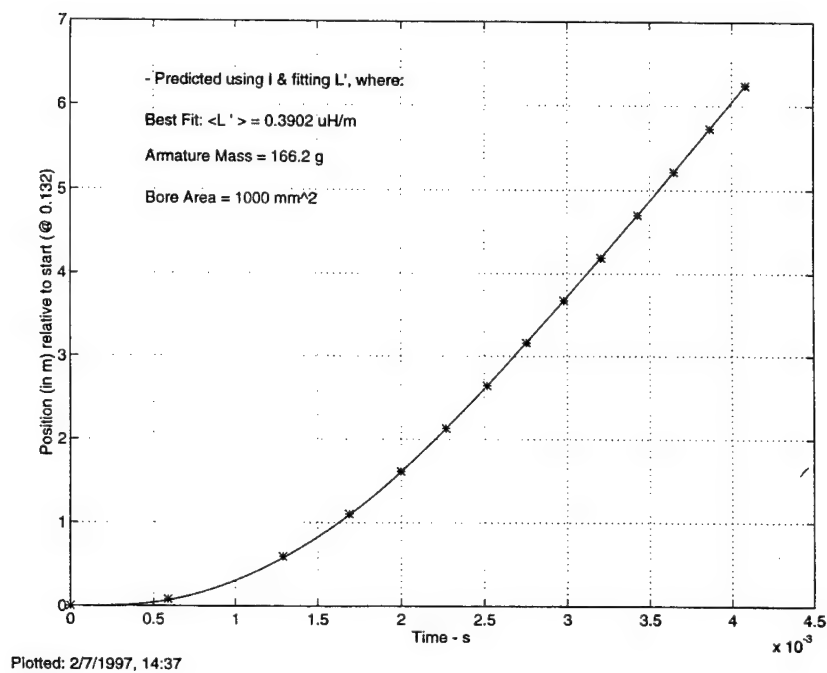


Fig. A-2. MCL gun positions from rail B-dot coils for shot number 97020701.

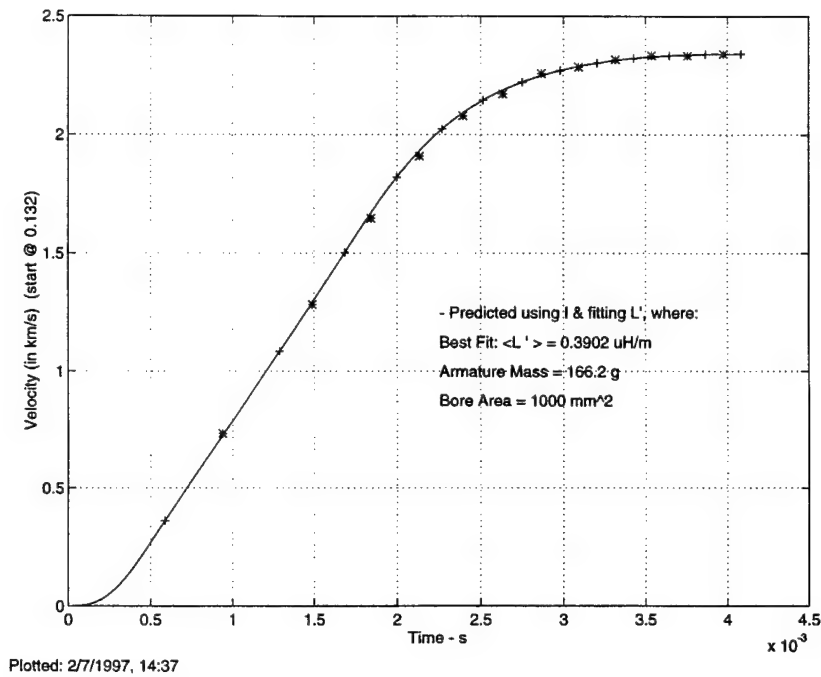


Fig. A-3. MCL gun velocities vs. time from rail B-dot coils for shot number 97020701.

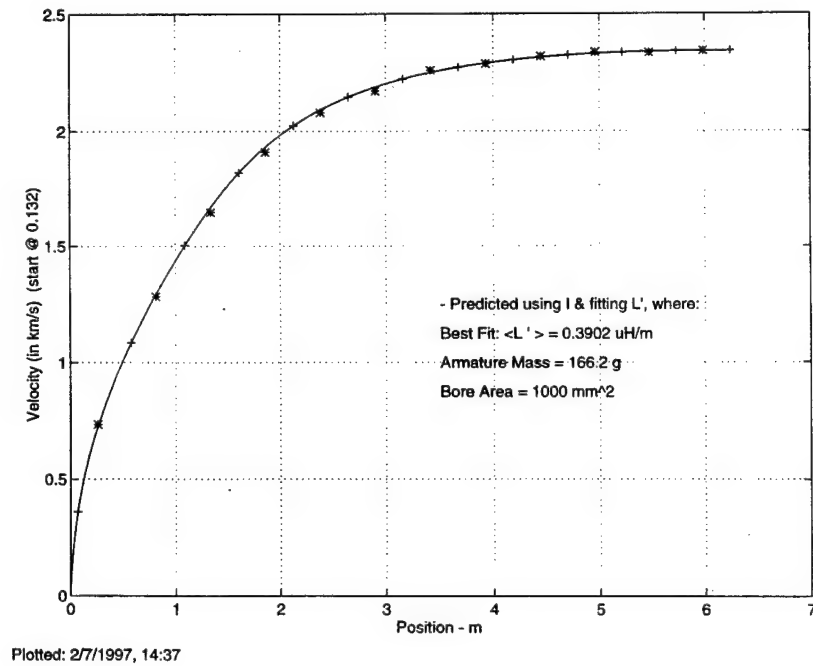
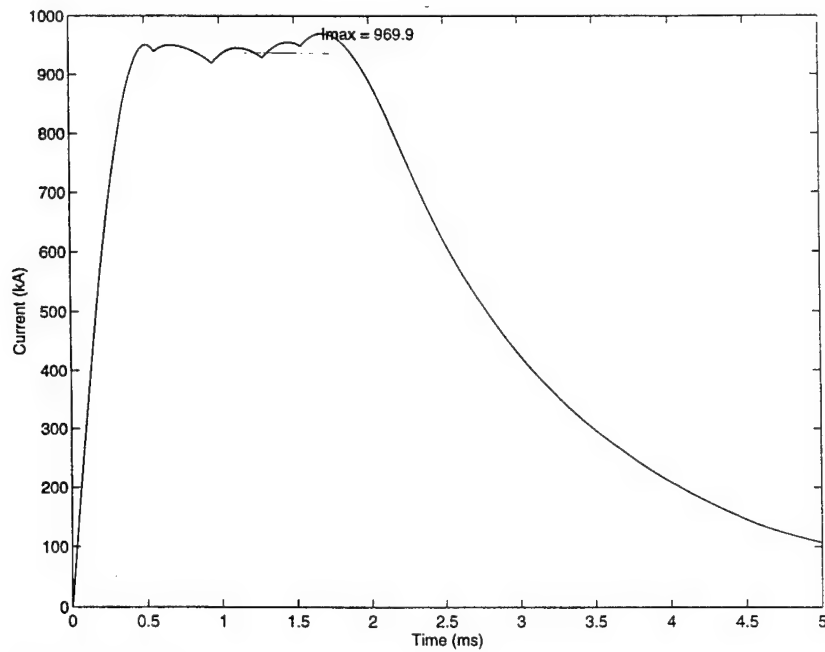
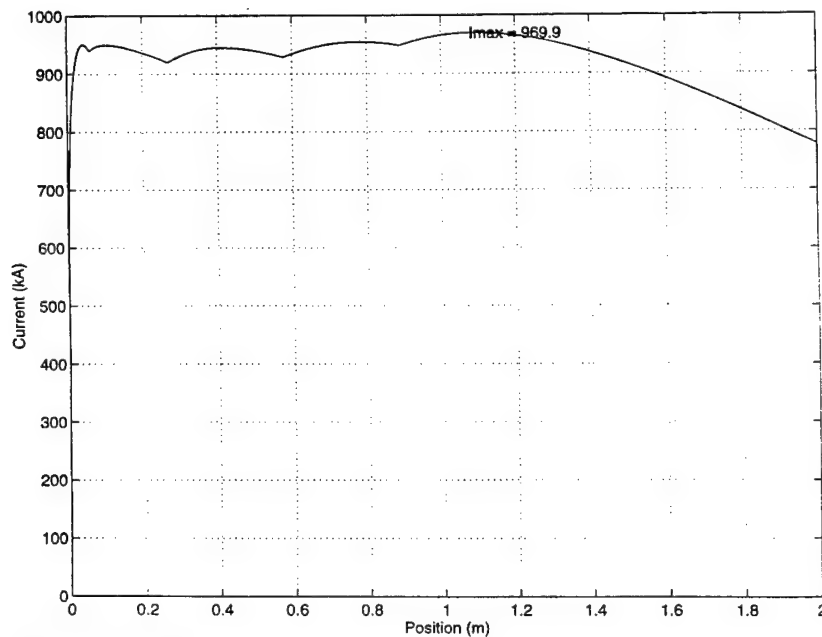


Fig. A-4. MCL gun velocities vs. position from rail B-dot coils for shot number 97020701.



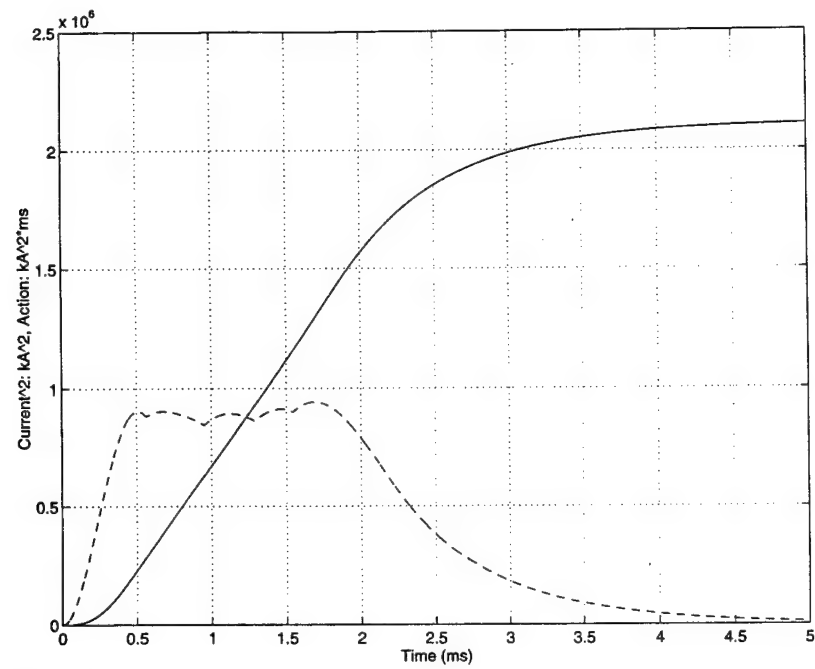
Plotted: 2/7/1997, 14:30

Fig. A-5. Total current vs. time from module Rogowskis for shot number 97020701.



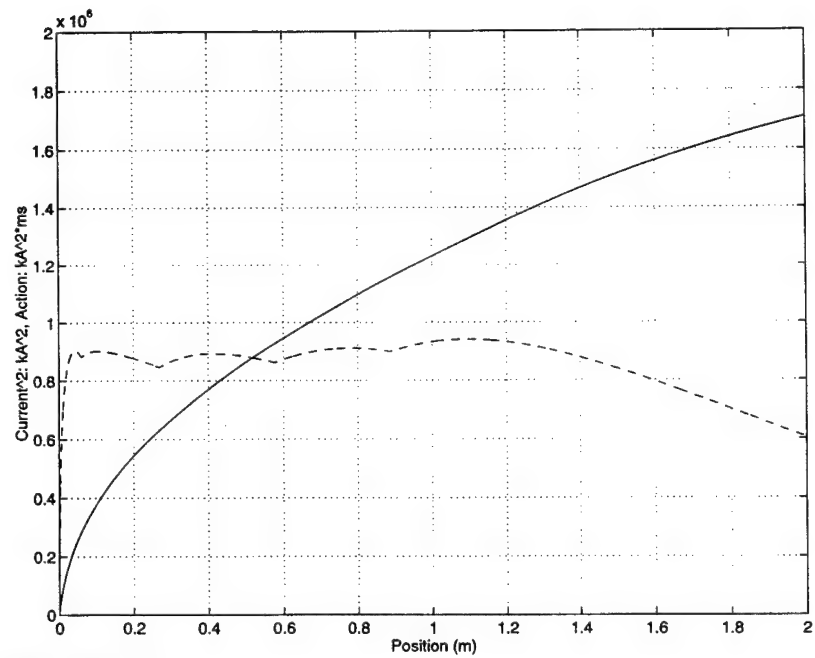
Plotted: 2/7/1997, 14:44

Fig. A-6. Total current vs. position from module Rogowskis for shot number 97020701.



Plotted: 2/7/1997, 14:44

Fig. A-7. Current² and action vs. time from Rogowskis for shot number 97020701.



Plotted: 2/7/1997, 14:44

Fig. A-8. Current² and action vs. position from Rogowskis for shot number 97020701.

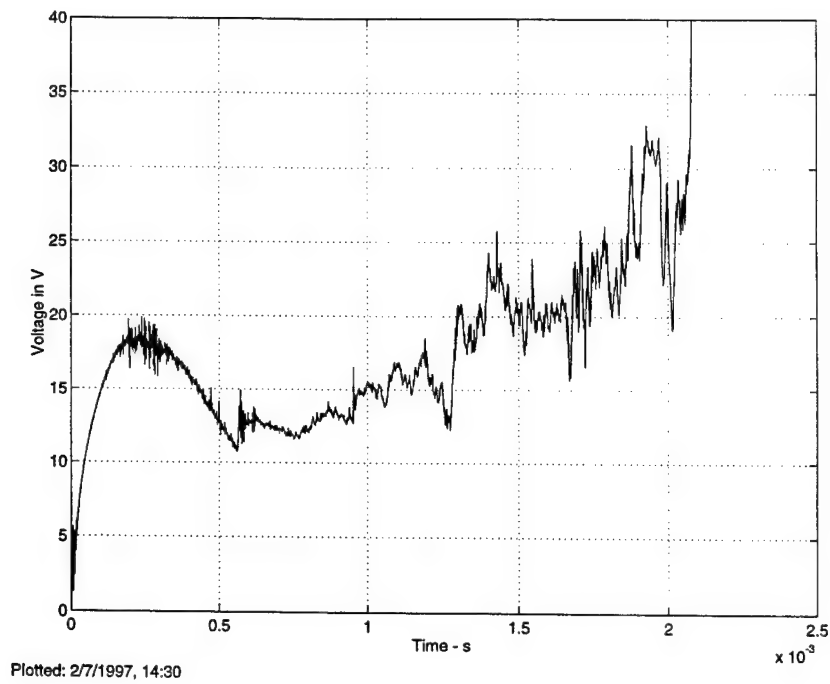


Fig. A-9. Muzzle voltage vs. time for 97020701.

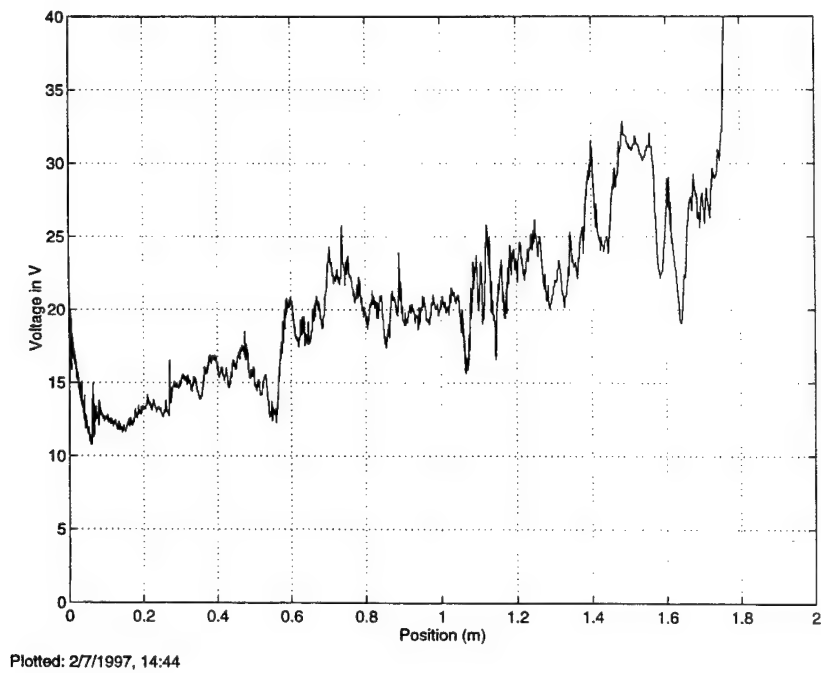


Fig. A-10. Muzzle voltage vs. position for 97020701.

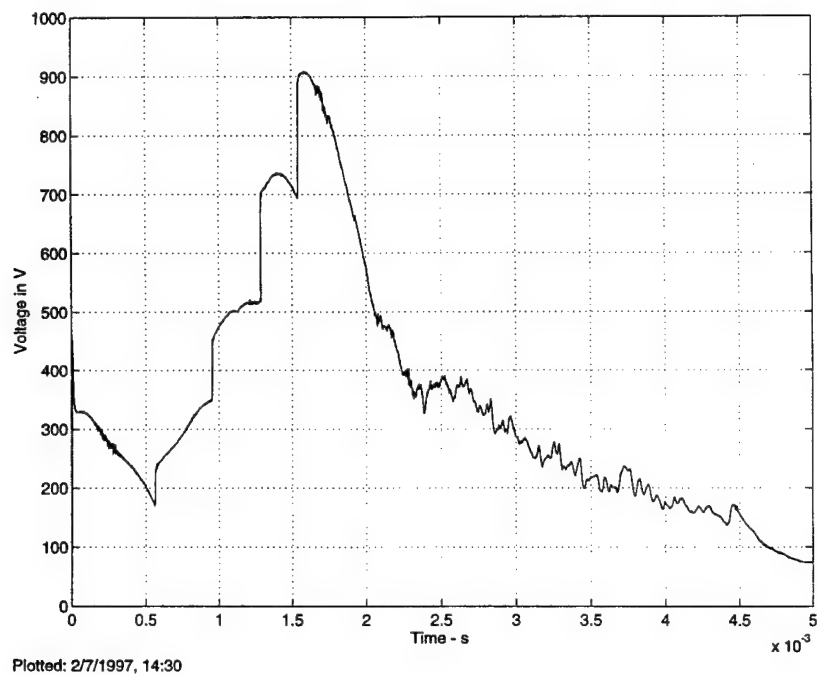


Fig. A-11. Breech voltage vs. time for 97020701.

Appendix B

Summary of Test Conditions, Lab Notes, and Raw Wear Data

Appendix B contains summaries of launch conditions, descriptions of resolidified aluminum on the recovered rails, and wear pin placement, depth, and axial location where pins interacted with rails.

Peak Current, *Average Current* and *Derived L'* are based on the plots shown in Appendix A. Acceleration is computed as $L'I^2/2m$, where I is average current during the "flat top" portion of the launch.

Post Shot Notes contain qualitative descriptions of resolidified aluminum on the rails after each shot. The photographs of recovered rails in Section 1 of this report show typical aluminum traces.

Wear Track Locations are summarized for each shot in two tables, one for each rail:

- The first column, **#**, contains a unique i.d. for every pin. The format consists of up to five fields. The first two are the shot number, followed by "n" or "p" to designate polarity, and then a number. For example 76n13 designates the thirteenth pin from shot MCL76, on the armature face in contact with the negative rail. Typically pins are numbered starting from the top (in the assembled gun) of the negative rails, and starting from the bottom of the positive rails.
- The second and third columns, **col.** and **row**, list the location of the pins on the armature. The KJ202 has 32 pads machined into each face, over which we have overlaid the coordinate system shown in Fig. B-1. Wear is assumed to be symmetrical about the center line of armature.
- The fourth column, **z**, lists the axial location at which the first interactions between pin and rail are observed. $z=0$ corresponds to the trailing edge of the armature. The error bar is based on degree of ambiguity in making a precise determination.
- The fifth column, **depth**, lists the depth of the pin below the surface of the armature face, measured at the time the armature was prepared. The procedure involves pressing each pin as far as it will go into its hole, then measuring depth using the dial indicator on the drill press. The units of mil ($1/1000'' = 25.4 \times 10^{-6} \text{ m}$) are retained throughout the appendices, with the unfortunate consequence that wear rate is expressed in mixed units of mil/cm. Unless specified otherwise, the uncertainty in pin depth is ± 1 mil. A parenthetical note of (Fe) in this column indicates that a steel drill bit broke and remained embedded at the recorded depth below the surface.
- The sixth column, **d/z**, lists the quotient of depth and axial distance in units of mil per centimeter of distance traveled. This is a measure of wear rate.
- The seventh and eighth columns, $\pm [\%]$, and $\pm [\text{mils/cm}]$, are the relative (%) and absolute error bars for the wear rate, d/z .
- The last column, **notes**, identifies spurious or unusual traces.

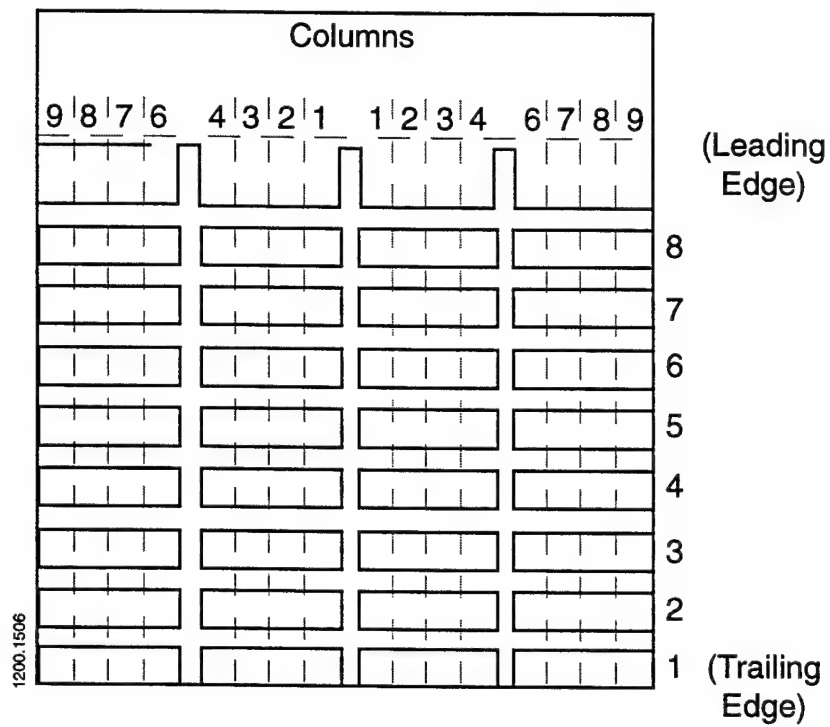


Fig. B1. Coordinate system used for designating pin locations on armature face.

Summary of Armature Wear Experiments

Name MCL	Date	Description	Mass [g]	Charge e [kV]	V _{EXT} [km/s]	I _{avg} [kA]	Accel. [m/s ²]
57	97013002	std. cond. 1st wear pin	166.15	14.0	2350±20	940±10	1.04x10 ⁶
58	97020701	std. cond. 2nd	166.15	14.0	2350±20	940±10	1.04x10 ⁶
59	97022601	std. cond. 3rd	169.37	14.0	2440±50	945±10	1.04x10 ⁶
63	97041101	std. cond. 4th	171.2	14.0	2250±20	950±10	1.04x10 ⁶
71	97053001	low-vel. low-cur. #1	169.9	12.5	1940±10	850±10	0.86x10 ⁶
73	97061201	high-vel. normal-cur.	136.74	14.0	2750±20	960±10	1.30x10 ⁶
75	97062501	normal-vel. low-cur.	136.84	12.8	2250±50	855±10	1.03x10 ⁶
76	97070701	low-vel. low-cur. #2	170.7	12.5	1950±50	855±10	0.82x10 ⁶
84	97090501	low-vel. high-cur. #1	281.5	16.5	2000±20	1150±10	0.90x10 ⁶
88	97102301	low-vel. high-cur. #2	293.2	16.5	2170	1150±10	0.86x10 ⁶

MCL 57 Shot Summary (97013002)

Description	First wear pin experiment ("standard conditions")
Launch Package	KJ202 Vented Bar with modifications; standard bore rider
Mass	166.15 g
Bank Charge	14.0 kV
Peak Current	972.9 kA
Average Current	940 ± 10 kA (average value for first 40 cm.)
Derived L'	0.39×10^{-6} H/m
Acceleration	1.04×10^6 m/s ²
Exit Velocity	2350 ± 20 m/s (based on MCL 58)

Pre-shot Notes: First experiment using wear pins. All pins were 20 mil tungsten tig electrodes except for one instance in which a steel drill bit broke off and remained embedded in the armature, acting effectively as a pin. In this experiment, as well as in MCL 58 and MCL 59, the axial grooves in the armature were changed from rectangular to trapezoidal. All subsequent shots have used rectangular grooves.

Post-shot Notes:

0-7 cm	burnished aluminum
7-17	loosely adhering aluminum (outer tracks)
7-27	loosely adhering aluminum (inner tracks)
17-22	transition to adhering aluminum (outer tracks)
27-32	transition to adhering aluminum (inner tracks)

notes: 1. Distance measured from trailing edge of armature (58 cm from end of rail).
2. At this time I had not begun to use scotch tape to remove all loose aluminum.

MCL 57 (97013002) Wear Track Locations:

Negative Rail ("driver's" side) Tracks numbered from top of rail

#	col.	row	z [cm]	depth [mil]	d/z [mil/cm]	± [%]	± [mils/cm]	Notes
57n1	—	—	—	—	—	—	—	
57n2	7.5	2	12 ± 2	2.5 ± 1	.21	.43	.09	
57n3	6	1	—	32	—	—	—	
57n4	4	1	35 ± 5	4	.11	.29	.03	poor
57n5	2.5	2	35 ± 5	7	.2	.20	.04	good
57n6	1	1	—	30	—	—	—	
57n7	1	1	—	30	—	—	—	
57n8	2.5	2	38.5 ± 2	10	.26	.11	.03	
57n9	4	3	—	8	—	—	—	
57n10	6	1	—	29	—	—	—	
57n11	7.5	2	30 ± 2	11	.37	.11	.04	good
57n12	9	3	22 ± 2	8	.36	.15	.05	

Positive Rail ("passenger's" side) Tracks numbered from bottom of rail

#	col.	row	z [cm]	depth [mil]	d/z [mil/cm]	± [%]	± [mils/cm]	Notes
57p1	9	6	24 ± 1	17 ± 1	0.7	.03	.04	??
57p2	7.5	5	19.25 ± 1	5	0.26	.21	.06	good
57p3	6	4	29.5 ± 5	10	0.34	.20	.07	
57p4	4	6	13 ± 4	5	0.38	.37	.14	
57p5	2.5	5	14.5 ± 1	4	0.28	.25	.07	
57p6	1	4	20 ± 5	6	0.3	.30	.09	
57p7	1	4	13.5 ± 2	2 (Fe)	0.15	.52	.08	
57p8	2.5	5	36 ± 2	11	0.31	.11	.035	
57p9	4	6	1.9 ± 0	0	—	—	—	
57p10	6	4	25.5 ± 6	7	0.27	.28	.08	
57p11	7.5	5	22.5 ± 3	6	0.27	.21	.06	
57p12	9	6	1.8 ± 0	0	—	—	—	

Comments: None of the deep pins (30 mils) survived to make scratches. Later experience will show that measurements are difficult to make at depths beyond 25 to 30 mils, and almost impossible this close to the trailing edge.

MCL 58 Shot Summary (97020701)

Description	Second wear pin experiment ("standard conditions")
Launch Package	KJ202 Vented Bar with modifications; standard bore rider
Mass	166.15 g
Bank Charge	14.0 kV
Peak Current	969.9 kA
Average Current	940 ± 10 kA (average value for first 40 cm.)
Derived L'	0.39×10^{-6} H/m
Acceleration	1.04×10^6 m/s ²
Exit Velocity	2350 ± 20 m/s

Pre-shot Notes: Second experiment using wear pins. All pins on inner two columns of pads were 20 mil tungsten tip electrodes. All pins on outer columns were 24 mil piano wire except for one instance in which a steel drill bit broke off and remained embedded in the armature, acting effectively as a pin. In this experiment, as well as in MCL 57 and MCL 59, the axial grooves in the armature were changed from rectangular to trapezoidal. All subsequent shots have used rectangular grooves. First attempt at using 4 pins per column.

Post-shot Notes:

0-7 cm	burnished aluminum
7-9	transition from burnished to loosely adhering aluminum in (outer tracks)
11-31	very "flaky" (-) rail
16-27	very "flaky" (+) rail
27-32	transition to adhering aluminum (inner tracks)
62	outer tracks disappear
72	inner tracks disappear
173	big gouge on (+) rail
178	transition on (-) rail

notes: 1. Distance measured from trailing edge of armature (58 cm from end of rail).
2. At this time I had not begun to use scotch tape to remove all loose aluminum.

MCL 58 (97020701) Wear Track Locations:

Negative Rail ("driver's" side) Tracks numbered from top of rail

#	col.	row	z [cm]	depth [mil]	d/z [mil/cm]	± [%]	± [mils/cm]	Notes
58n1	8	5	22.5 ± 2	3.5 (24 mil Fe)	.156	.30	.05	good
58n2	7	3	27 ± 3	12 "	.44	.14	.06	a.
58n3	6	1	49 ± 2	9 "	.18	.11	.02	good
58n4	4	1	42.5 ± 3	5	.12	.21	.025	
58n5	3	3	23.5 ± 4	3.5	.15	.33	.05	
58n6	2	5	16 ± 3	3	.19	.38	.07	
58n7	1	8	31 ± 2	2	.06	.5	.03	
58n8	1	7	41 ± 5	9	.22	.12	.036	
58n9	2	5	29.5 ± 4.5	8.5	.29	.19	.056	
58n10	3	3	50 ± 1	9.5	.19	.11	.02	
58n11	4	1	41 ± 2	6.5	.16	.16	.026	
58n14	7	3	59 ± 2	13 (24 mil Fe)	.22	.08	.018	
58n15	8	4	30.5 ± 2.5	10 "	.33	.13	.043	
58n16	9	6	31.5 ± 1	12 "	.39	.09	.033	

a. canal effect

Positive Rail ("passenger's" side) Tracks numbered from bottom of rail

#	col.	row	z [cm]	depth [mil]	d/z [mil/cm]	± [%]	± [mils/cm]	Notes
58p1	9	8	—	12 ± 1	—	—	—	
58p2	8	7	2.5 ± 0	0	—	—	—	
58p3	7	5	74.5 ± 2	12	.16	.08	.014	
58p4	6	2	69 ± 2	23	.33	.05	.017	
58p5	4	2	36 ± 6	3	.08	.37	.031	
58p6	3	4	30 ± 3	6.5	.22	.18	.040	
58p7	2	6	35.5 ± 8	7	.20	.27	.053	
58p8	1	8	43.5 ± 2	6.5 ± 3	.15	.47	.07	
58p9	1	8	64.5 ± 5	10.5	.16	.12	.02	
58p10	2	6	27.5 ± 3	6	.22	.20	.043	
58p11	3	4	32 ± 3	7	.22	.17	.037	
58p12	4	2	46 ± 2	6	.13	.18	.023	
58p13	6	2	20 ± 4	4	.20	.32	.064	
58p14	7	4	37 ± 2	8	.21	.14	.03	a.
58p15	8	6	—	0	—	—	—	
58p16	9	8	—	7	—	—	—	

a. fully developed wear track by z=39 cm; long ambiguous history up to then.

Comments: Still had not learned how to face-off pins, therefore error bars are larger than in later shots. Also, "canal effect" whereby smooth, wide shallow trenches coexist with wear tracks, was particularly pronounced in this shot.

MCL 59 Shot Summary (97022601)

Description	Third wear pin experiment ("standard conditions")
Launch Package	KJ202 Vented Bar with modifications; standard bore rider
Mass	169.37 g (included LED test)
Bank Charge	14.0 kV
Peak Current	979.2 kA
Average Current	945 ± 10 kA (average value for first 40 cm.)
Derived L'	0.393×10^{-6} H/m
Acceleration	1.04×10^6 m/s ²
Exit Velocity	2440 ± 50 m/s

Pre-shot Notes: Third experiment using wear pins. In this experiment (as well as in MCL 57 and MCL 58) the axial grooves in the armature were changed from rectangular to trapezoidal. All subsequent shots have used rectangular grooves. Might have used 10 mil tungsten pins in parts (did not keep a good record). Many of the pins were buried flush with the surface in order to measure when rows five, six, and seven make contact with the rails.

Post-shot Notes: none recorded

MCL 59 (97022602) Wear Track Locations:

Negative Rail ("driver's" side) Tracks numbered from top of rail

#	col.	row	z [cm]	depth [mil]	d/z [mil/cm]	± [%]	± [mils/cm]	Notes
59n1	9	4	8.0 ± .5	0 (Fe)	—	—	—	
59n2	7.5	6	7.75 ± 2.5	0	—	—	—	
59n3	6	5	5 ± 2.5	0	—	—	—	
59n4	4	6	35.25 ± 1	12	.28	.09	.03	
59n5	2.5	6	8.25 ± 1.5	0	—	—	—	
59n6	1	6	25 ± 1.5	7	.34	.15	.04	
59n7	1	6	5.75 ± 3.5	0 (Fe)	—	—	—	
59n8	2.5	6	62 ± 11.5	21 (Fe)	.28	.19	.07	
59n9	4	6	4 ± 2	0	—	—	—	
59n10	6	6	7 ± 2.5	0	—	—	—	
59n11	7.5	5	19.5 ± 2	21 (Fe)	.11	.11	.12	
59n12	9	6	7.75 ± 1	0	—	—	—	

Positive Rail ("passenger's" side) Tracks numbered from bottom of rail

#	col.	row	z [cm]	depth [mil]	d/z [mil/cm]	± [%]	± [mils/cm]	Notes
59p1	9	7	41 ± 1	15	.366	.07	.03	
59p2	7.5	7	—	25 (Fe)	—	—	—	no track
59p3	6	7	2.4 ± 0	0 ? (Fe)	—	—	—	
59p4	4	7	30.5 ± 2.5	13 (Fe)	.426	.11	.05	good
59p5	2.5	7	44.5 ± 16	0	—	—	—	
59p6	1	7	114 ± ?	25 (Fe)	.22	.04	.01	faint
59p7	1	7	11.25 ± 1.25	0 (Fe)	—	—	—	
59p8	2.5	7	23.5 ± 1	10	.426	.11	.05	good
59p9	4	7	55.5 ± 15	0	—	—	—	
59p10	6	7	22.5 ± 2	0	—	—	—	
59p11	7.5	7	—	16 (Fe)	—	—	—	no track
59p12	9	7	8 ± 1	0	—	—	—	

Comments: Still had not learned how to face-off pins, therefore error bars are larger than in later shots. Lots of pins buried flush with surface in rows six and seven to see when forward part of the armature makes contact with rails.

MCL 63 Shot Summary (97041101)

Description	Fourth wear pin experiment ("standard conditions")
Launch Package	KJ202 Vented Bar with modifications; standard bore rider
Mass	171.2 g
Bank Charge	14.0 kV
Peak Current	961.7 kA
Average Current	950 ± 10 kA (average value for first 50 cm.)
Derived L'	0.3885×10^{-6} H/m
Acceleration	1.04×10^6 m/s ²
Exit Velocity	2250 ± 20 m/s

Pre-shot Notes: Fourth experiment using wear pins. All pins 20 mil tungsten tig electrodes. All axial grooves in the armature rectangular. Pins are buried deeper than previous shots. Possibly the first shot in which I began to square off the face of the pins, since the error bars in "z" are smaller than in previous shots.

Post-shot Notes: none on record

MCL 63 (97041101) Wear Track Locations:

Negative Rail ("driver's" side) Tracks numbered from top of rail

#	col	row	z [cm]	depth [mil]	d/z [mil/cm]	± [%]	± [mils/cm]	Notes
63n1	7.5	2	17 ± 0	2	0.118	0.503	0.059	
63n2	7	5	65 ± 0	20	0.308	0.052	0.016	
63n3	6	6	121 ± 1	33	0.273	0.031	0.009	
63n4	4	7	135 ± 3	31.5	0.233	0.039	0.009	
63n5	3	5	135 ± 2	35.5	0.263	0.032	0.008	
63n6	2	3	135 ± 2	35.5	0.263	0.032	0.008	
63n7	1	5	54 ± 1	15.5	0.287	0.067	0.019	
63n8	1	5	—	43.5	—	—	—	no track
63n9	2	3	101 ± 0	23	0.228	0.045	0.01	
63n10	3	5	91 ± 1	23	0.253	0.045	0.011	
63n11	4	7	2.2 ± 0	28.5				
63n12	6	6	87 ± 1	25	0.287	0.042	0.012	
63n13	7	5	110 ± 1	35.5	0.323	0.03	0.01	
63n14	8	2	34 ± 2	12.5	0.368	0.099	0.037	

Positive Rail ("passenger's" side) Tracks numbered from bottom of rail

#	col	row	z [cm]	depth [mil]	d/z [mil/cm]	± [%]	± [mils/cm]	Notes
63p1	7.5	5	77 ± 0	27.5	0.357	0.039	0.014	
63p2	6	7	—	33	—	—	—	
63p3	4	2	62 ± 1	11.5	0.185	0.088	0.016	
63p4	3	4	47 ± 0	13	0.277	0.08	0.022	
63p5	2	6	64 ± 2	16.5	0.258	0.068	0.018	
63p6	1	8	—	23	—	—	—	
63p7	1	8	—	35	—	—	—	
63p8	2	6	124.5 ± 0	28.5	0.229	0.036	0.008	
63p9	3	4	59 ± 1	15	0.254	0.069	0.017	
63p10	4	2	111 ± 1	26.5	0.239	0.039	0.009	
63p11	6	7	—	40.5	—	—	—	
63p12	7.5	5	74 ± 2	23	0.311	0.051	0.016	

Comments:

MCL 71 Shot Summary (97053001)

Description	"low-speed", "low-current" wear pin (same as MCL 76)
Launch Package	KJ202 Vented Bar, standard bore rider
Mass	169.9 g
Bank Charge	12.5 kV
Peak Current	872.2 kA
Average Current	850 ± 10 kA
Derived L'	0.386×10^{-6} H/m
Acceleration	860×10^3 m/s ²
Exit Velocity	1.94 ± 10 m/s

Pre-shot Notes: Wear pin experiment using standard armature but at lower-than-usual current and consequently lower velocity. The current selected was such that, when used in a future test with the lightweight bore rider, it would result in a launch at "standard" velocity. Pins were fairly shallow in this shot. MCL 76 is a repeat of this shot in which the pins were buried deeper.

Post-shot Notes:

0 - 4 cm 50% burnished copper, 50% shiny aluminum (outer tracks)
0 - 6 cm 50% burnished copper, 50% shiny aluminum (inner tracks)
4 - 8 cm shiny burnished aluminum (outer tracks)
6 - 10 shiny burnished aluminum (inner tracks)
2 cm begin "magnetic saw" at outer edges
8 cm "melt wave" aluminum half-way into outer tracks
10 - 42 flaky aluminum on "-" rail
10 - 37 flaky aluminum on "+" rail
10 - 62 flaky aluminum on both rails if scotch tape is used to remove loose aluminum

notes: 1. Distance measured from trailing edge of armature (58 cm from end of rail).
2. At this time I began to use scotch tape to remove all loose aluminum.

MCL 71 (97053001) Wear Track Locations:

Negative Rail ("driver's" side) Tracks numbered from top of rail

#	col.	row	z [cm]	depth [mil]	d/z [mil/cm]	± [%]	± [mils/cm]	Notes
71n1	7	6	29 ± 1	7 ± 1	0.241	0.147	0.035	
71n2	6	8	3 ± 0	0	—			
71n3	4	1	.2 ± 0	-1	—			
71n4	3	3	19.5 ± 1	.5	0.026	2.001	0.051	
71n5	2	5	44.5 ± 1	10	0.225	0.102	0.023	
71n6	1	7	15 ± 2.5	1	0.067	1.014	0.068	
71n7	1	7	38.5 ± 3.5	8	0.208	0.155	0.032	
71n8	2	5	23 ± 1	4	0.174	0.254	0.044	
71n9	3	3	64.5 ± 2.5	8	0.124	0.131	0.016	
71n10	4	1	.2 ± 0	-1	—			
71n11	6	8	29 ± 1	3	0.103	0.335	0.035	
71n12	7	8	37.5 ± 1.5	6	0.16	0.171	0.027	

Positive Rail ("passenger's" side) Tracks numbered from bottom of rail

#	col.	row	z [cm]	depth [mil]	d/z [mil/cm]	± [%]	± [mils/cm]	Notes
71p1	7	6	32 ± 1	10 ± 1	0.313	0.105	0.033	
71p2	6	4	41.5 ± 2.5	0	0	###	###	
71p3	4	2	47.25 ± 1.25	8	0.169	0.128	0.022	
71p4	3	4	57.5 ± 2.5	14.5	0.252	0.082	0.021	
71p5	2	6	33.5 ± 1	8	0.239	0.129	0.031	
71p6	1	8	35 ± 1	4	0.114	0.252	0.029	
71p7	1	8	45.75 ± 1.25	5	0.109	0.202	0.022	
71p8	2	6	26.25 ± 1.25	5	0.19	0.206	0.039	
71p9	3	4	28.75 ± 1	6	0.209	0.17	0.036	
71p10	4	2	39.75 ± 1.25	5	0.126	0.202	0.025	
71p11	6	4	40.5 ± 1	0	0	###	###	
71p12	7	6	29 ± 1	8	0.276	0.13	0.036	

Comments:

MCL 73 Shot Summary (97061201)

Description	"high-speed", "normal-current" wear pin
Launch Package	KJ202 Vented Bar, lightweight lexan forebody
Mass	136.74 g
Bank Charge	14.0 kV
Peak Current	972.1 kA
Average Current	960 ± 10 kA
Derived L'	0.387×10^{-6} H/m
Acceleration	1.30×10^6 m/s ²
Exit Velocity	2750 ± 20 m/s

Pre-shot Notes: Wear pin experiment using lightweight armature at normal current and consequently higher velocity. MCL 75 is a complementary shot in that it uses the same launch package, with a low current to produce the standard acceleration of 10^6 m/s².

Post-shot Notes:

0 - 2 cm mostly burnished copper
 1.5 "melt wave" triangle begins at outer edges
 0 - 6 cm 50% burnished copper, 50% shiny aluminum (inner tracks)
 shiny burnished aluminum (outer tracks)
 6 - 11 shiny burnished aluminum (inner tracks)
 11 - 18 ...

notes: 1. Distance measured from trailing edge of armature (58 cm from end of rail).

MCL 73 (97061201) Wear Track Locations:

Negative Rail ("driver's" side) Tracks numbered from top of rail

#	col.	row	z [cm]	depth [mil]	d/z [mil/cm]	± [%]	± [mils/cm]	Notes
73n1	7.5	4	42.25 ± 1.5	11	0.26	0.098	0.025	
73n2	6	7	40.25 ± 1	11	0.273	0.094	0.026	
73n3	4	1	.5	3				bad
73n4	3	3	82 ± 1	18.5	0.226	0.055	0.013	
73n5	2	5	107 ± 1	48.5	0.453	0.023	0.01	a.
73n6	1	7	76 ± 4	16	0.211	0.082	0.017	
73n7	1	7	9 ± ?	0	0	###	###	b.
73n8	1.5	6	16.5 ± 3.5	2	0.121	0.543	0.066	
73n9	2	5	91 ± ?	12	0.132	###	###	c.
73n10	3	3	69.5 ± 1	14.5	0.209	0.07	0.015	
73n11	4	1	51 ± 1	6.5	0.127	0.155	0.02	
73n12	6	7	49 ± 1	12.5	0.255	0.083	0.021	
73n13	7.5	4	72.5 ± 1.5	24	0.331	0.047	0.015	

- a. possibly a spurious trace.
- b. shininess present from onset, track doesn't begin to carve copper until 9 cm.
- c. track appears abruptly but is very faint. Possible gougllets up to 8cm upstream

Positive Rail ("passenger's" side) Tracks numbered from bottom of rail

#	col.	row	z [cm]	depth [mil]	d/z [mil/cm]	± [%]	± [mils/cm]	Notes
73p1	7.5	2	40 ± 1	11	0.275	0.094	0.026	a.
73p2	6	6	57.5 ± 1	17	0.296	0.061	0.018	a.
73p3	4	2	82.5 ± ?	18.5	0.224	###	###	b.
73p4	3	4	105.5 ± ?	27.5	0.261	###	###	b.
73p5	2	6		36				missing
73p6	1	7	8.5 ± 1	0	0	###	###	
73p7	1	7	62 ± 1	13	0.21	0.079	0.016	c.
73p8	2	6	2.3 ± 0	0	0	###	###	
73p9	3	4	20 ± 6	10.5	0.525	0.315	0.165	d.
73p10	4	2	58 ± 1	10	0.172	0.101	0.017	
73p11	6	6	2.3 ± 0	0	0	###	###	
73p12	7.5	2	45 ± 1	8	0.178	0.127	0.023	

- a. strong track, appears abruptly.
- b. faint track, appears abruptly amid gougllets.
- c. long skinny precursor of uncertain depth from 50-61 cm. Strong interaction with track 73p8.
- d. long skinny scratch from 14.5 to 26 cm.

Comments:

MCL 75 Shot Summary (97062501)

Description	"normal-speed", "low-current" wear pin
Launch Package	KJ202 Vented Bar, lightweight lexan forebody
Mass	136.84 g
Bank Charge	12.8 kV
Peak Current	869.4 kA
Average Current	855 ± 10 kA
Derived L'	0.3856×10^{-6} H/m
Acceleration	1.03×10^6 m/s ²
Exit Velocity	2250 ± 50 m/s

Pre-shot Notes: Wear pin experiment using lightweight armature at low current so as to obtain normal acceleration/velocity. MCL 73 is a complementary shot in that it uses the same launch package, with a normal current to produce the higher than usual acceleration of 1.12×10^6 m/s².

Post-shot Notes:

0	2 cm	mostly burnished copper on all four tracks
2	10	"melt wave" triangle on outer edges
2	7	50% burnished copper, 50% shiny aluminum (inner tracks)
7	10	mostly shiny aluminum on inner tracks (similar to melt wave Al. on outer tracks); can't see Cu.
10	12	transition to flaky aluminum
12	42	mostly flaky aluminum on all four tracks
42	62	transition from flaky aluminum to solid (dull) aluminum
62	153	moderately dull aluminum
153		transition (abrupt) on "+" rail
178		more gouges on "-" rail
192		transition (mild) on "-" rail

notes: 1. Distance measured from trailing edge of armature (58 cm from end of rail).

MCL 75 (97062501) Wear Track Locations:

Negative Rail ("driver's" side) Tracks numbered from top of rail

#	col.	row	z [cm]	depth [mil]	d/z [mil/cm]	± [%]	± [mils/cm]	Notes
75n1	7.5	2	2.5 ± 0	0	0	###	###	
75n2	6	5	29 ± 1.5	7	0.241	0.152	0.037	
75n3	4	8	3 ± 0	0	0	###	###	
75n4	3	6	40.5 ± 1.5	9.5	0.235	0.112	0.026	
75n5	2	4	76 ± 1	13.0	0.171	0.078	0.013	
75n6	1	2	77 ± 1	13.75	0.179	0.074	0.013	
75n7	1	2	42.5 ± 1	7	0.165	0.145	0.024	
75n8	2	4	56 ± 1	14.5	0.259	0.071	0.018	
75n9	3	6	60 ± 1	15	0.25	0.069	0.017	
75n10	4	8	44.25 ± 1.25	6.5	0.147	0.156	0.023	
75n11	6	5	22 ± 1	3.5	0.159	0.289	0.046	
75n12	7.5	2	24 ± 1	4	0.167	0.253	0.042	

Positive Rail ("passenger's" side) Tracks numbered from bottom of rail

#	col.	row	z [cm]	depth [mil]	d/z [mil/cm]	± [%]	± [mils/cm]	Notes
75p1	7	6	27.5 ± 1	7	0.255	0.147	0.038	
75p2	6	4	28 ± 1	7	0.25	0.147	0.037	
75p3	4	1	0.2 ± 0	0	0	###	###	
75p4	3	3	31.25 ± 1	6	0.192	0.17	0.033	
75p5	2.5	4	108.5 ± 1	22.5	0.207	0.045	0.009	
75p6	2	5	50.5 ± 1.5	10.5	0.208	0.1	0.021	
75p7	1	7	2.3 ± 0	0	0	###	###	
75p8	1	7	33 ± 1.5	4.5	0.136	0.227	0.031	
75p9	2	5	29 ± 2	6	0.207	0.18	0.037	
75p10	2.5	4	24 ± 3	4.5	0.188	0.255	0.048	
75p11	3	3	40.5 ± 1.5	8	0.198	0.13	0.026	
75p12	4	1	30.5-44.5 see note	5	0.132	0.272	0.036	a
75p13	6	4	1.5 ± 0	0	0	###	###	
75p14	7	6	30.25 ± 1.25	8	0.264	0.132	0.035	

a. - skinny scratch 30.5 cm; deep and skinny at 37 cm; begins to widen at 43 cm; fully developed wear track at 45 cm.

Comments:

MCL 76 Shot Summary (97070701)

Description	"low-speed", "low-current" wear pin (same as MCL 71)
Launch Package	KJ202 Vented Bar, standard bore rider
Mass	170.7 g
Bank Charge	12.5 kV
Peak Current	872.8 kA
Average Current	855 \pm 10 kA
Derived L'	0.385x10 ⁻⁶ H/m
Acceleration	824x10 ³ m/s ²
Exit Velocity	1950 \pm 50 m/s

Pre-shot Notes: Wear pin experiment using standard armature but at lower-than-usual current and consequently lower velocity. The current selected was such that, when used in a future test with the lightweight bore rider, it would result in a launch at "standard" velocity. Pins were fairly deep in this shot, compared with MCL 71, for which conditions were nearly identical. Not this shot was the first attempt at obtaining in-bore x-rays. Therefore the containment was assembled slightly differently: three 20" containment sections w/ bdot cards, 4" window, bdot card, 4" window, bdot card, 20" containment...

Post-shot Notes:

0 apex of "melt wave" triangle on outer tracks
0 - 1.5 cm mostly copper color, faint shiny aluminum (outer tracks)
1.5 - 4 50% burnished copper, 50% shiny aluminum (inner tracks)
4 - 8.5 shiny burnished aluminum (outer tracks) not in triangle
4 - 8.5 shiny burnished aluminum (inner tracks)
8.5 - 10 transition to flaky aluminum all tracks
10 "melt wave" aluminum completely occupies outer tracks
27 flaky aluminum gives way to adhered aluminum on outer tracks
55 \pm 5 flaky aluminum end on "+" rail (inner tracks)
77 \pm 5 flaky aluminum end on "-" rail (inner tracks)
164 transition on "+" rail; some lift off
180 lift off on "-" rail
197 transition on "-" rail

notes: 1. Distance measured from trailing edge of armature (58 cm from end of rail).
2. Used scotch tape to remove all loose aluminum.

MCL 76 (97070701) Wear Track Locations:

Negative Rail ("driver's" side) Tracks numbered from top of rail

#	col.	row	z [cm]	depth [mil]	d/z [mil/cm]	± [%]	± [mils/cm]	Notes
76n1	9	8	30.5 ± 1.5	7	0.23	0.151	0.035	
76n2	7.5	2	18.5 ± 1	3.5	0.189	0.291	0.055	
76n3	7	6	74 ± 1.5	22	0.297	0.05	0.015	
76n4	6	4	49 ± 1.5	17	0.347	0.066	0.023	
76n5	4	2	54 ± 1.5	12	0.222	0.088	0.02	
76n6	3	4	79.5 ± 1	21	0.264	0.049	0.013	
76n7	2	6	53 ± 1	14.5	0.274	0.071	0.02	
76n8	1	8	75 ± 6.5	12.25	0.163	0.119	0.019	
76n9	1	8	115 ± 2	21.25	0.185	0.05	0.009	
76n10	2	6	117.5 ± 3.5	25	0.213	0.05	0.011	
76n11	3	4	26.75 ± 1	7.75	0.29	0.134	0.039	
76n12	4	2	62 ± 1	14.5	0.234	0.071	0.017	
76n13	6	4	37.5 ± 1	12.5	0.333	0.084	0.028	
76n14	7	6	36.5 ± 1	12	0.329	0.088	0.029	
76n15	7.5	2	27 ± 1	8.5	0.315	0.123	0.039	
76n16	9	8	18.5 ± 1	3.25	0.176	0.312	0.055	

Positive Rail ("passenger's" side) Tracks numbered from bottom of rail

#	col.	row	z [cm]	depth [mil]	d/z [mil/cm]	± [%]	± [mils/cm]	Notes
76p1	9	8	39.5 ± 1	8	0.203	0.128	0.026	
76p2	7.5	2	35.75 ± 1	13	0.364	0.082	0.03	
76p3	7	3	20.5 ± 1	4.5	0.22	0.228	0.05	
76p4	6	8	64 ± 1.5	12	0.188	0.087	0.016	
76p5	4	1	49 ± 3	10	0.204	0.117	0.024	
76p6	3	3	47 ± 2	13	0.277	0.088	0.024	
76p7	2	5	56 ± 1	17	0.304	0.061	0.019	
76p8	1	7	49.5 ± 1	6.5	0.131	0.155	0.02	
76p9	1	7	101.5 ± 4	19	0.187	0.066	0.012	
76p10	2	5	61.5 ± 1.5	18	0.293	0.061	0.018	
76p11	3	3	87 ± 1	21	0.241	0.049	0.012	
76p12	4	1	84 ± 1.5	16	0.19	0.065	0.012	
76p13	6	8	117 ± 2.5	17.5	0.15	0.061	0.009	
76p14	7	3	51 ± 1.5	15.5	0.304	0.071	0.022	
76p15	7.5	2	37 ± 1	9.25	0.25	0.111	0.028	
76p16	9	8	23 ± 1.5	4.5	0.196	0.232	0.045	

Comments:

MCL 84 Shot Summary (97090501)

Description	First experiemnt with heavy armature (lov-vel. high.cur.)
Launch Package	KJ202 Vented Bar; extra-long bore rider
Mass	281.5 g
Bank Charge	16.5 kV
Peak Current	< 1189 kA
Average Current	< 1175 ± 10 kA (use 1150 ± 10 kA for first 75 cm.)
Derived L'	> 0.3628×10^{-6} H/m (use 0.383×10^{-6} H/m)
Acceleration	0.90×10^6 m/s ²
Exit Velocity	2000 ± 20

Pre-shot Notes: This is the first of two shots in which we use an extremely heavy lexan bore rider in order to obtain high current and low velocity. This shot was combined with an in-bore diagnostic experiemnt to investigate the drop off in optical signal that occurs at 1.5 - 2.0 km/s.

Post-shot Notes:

There was a problem with the shot that makes data reduction difficult: a short across the breech occurred 1.6 ms into the launch. That is, 77-78 cm into the launch. The values for shot parameters in the table above that are in parentheses are based on information from the subsequent shot (MCL 88).

Trailing edge of armature at 73.2 cm from breech. This is becuase we're using a heavy bore rider and wanted to capture in bore x-ray just prior to transition. Starting location as per JVP's sims.

0 - 1	(outer tracks) 80% Cu, 20 %Al (is really mostly burnished Cu)
0 - 5 cm	(inner tracks) 80% Cu, 20 %Al (is really mostly burnished Cu)
1 - 11 cm	(outer tracks) beginning and ending point of melt wave traingle
5 - 11	(inner tracks) shiny aluminum
11	loosely adhering aluminum in
31 ± 5	transition to adhering aluminum (outer tracks)
43 ± 5	transition to adhering aluminum (inner tracks)
198	transition to plasma armature on (-) rail

No gouges except some gougelets from wear pins

notes: distace measured from trailing edge of armature (approx 73 cm from end of rail)
scotch tape used to remove loose aluminum

MCL 84 (97090501) Wear Track Locations:

Negative Rail ("driver's" side) Tracks numbered from top of rail

#	col.	row	z [cm]	depth [mil]	d/z [mil/cm]	± [%]	± [mils/cm]	Notes
84n1	7	5	51.25 ± 1	18 ± 1	0.351	0.059	0.021	
84n2	6	6	22 ± 1.5	4 ± 1	0.178	0.259	0.046	
84n3	4	7	32.75 ± 1.75	7 ± 1	0.214	0.153	0.033	
84n4	3	6	67.5 ± 1	16 ± 1	0.237	0.064	0.015	
84n5	2	4	48 ± 1	8 ± 1	0.167	0.127	0.021	
84n6	1	2	49 ± 1	4.5 ± 1	0.092	0.223	0.02	
84n7	1	2	33.5 ± 1	4.5 ± 1	0.134	0.224	0.03	
84n8	2	4	18 ± 1	2 ± 1	0.111	0.503	0.056	
84n9	3	6	40? ± 1	9 ± 1	0.225	0.114	0.026	
84n10	4	7	60.5 ± 1	17 ± 1	0.281	0.061	0.017	
84n11	6	6	22 ± 1	5 ± 1	0.227	0.205	0.047	
84n12	7	5	2 ± 0	0 ± 1				

Positive Rail ("passenger's" side) Tracks numbered from bottom of rail

#	col.	row	z [cm]	depth [mil]	d/z [mil/cm]	± [%]	± [mils/cm]	Notes
84p1	8	7	8 ± 1	3 ± 1 (Fe)	0.375	0.356	0.134	
84p2	7	5	26.5 ± 1	7.5 ± 1	0.283	0.139	0.039	
84p3	6	3	83.5 ± 1	23 ± 1	0.275	0.045	0.012	
84p4	4	2	.5 ± 0	+1 ± 1				
84p5	3	3	53.5 ± 1	8.5 ± 1	0.159	0.119	0.019	
84p6	2	5	61.5 ± 1	12.5 ± 1	0.203	0.082	0.017	
84p7	1	7	43 ± 1	9 ± 1	0.209	0.114	0.024	
84p8	1	7	45 ± 2	10 ± 1	0.222	0.109	0.024	
84p9	2	5	90 ± 1	22 ± 1	0.244	0.047	0.011	
84p10	3	3	80 ± 1	17 ± 1	0.213	0.06	0.013	
84p11	4	2	42 ± 1	5.5 ± 1	0.131	0.183	0.024	
84p12	6	3	65 ± 1	14.5 ± 1	0.223	0.071	0.016	
84p13	7	5	1.5 ± 0	0 ± 1				
84p14	8	7	13 ± 1	4 ± 1	0.308	0.262	0.08	

Comments:

MCL 88 Shot Summary (97102301)

Description	"low-speed", "high-current" wear pin (similar to MCL 84)
Launch Package	KJ202 Vented Bar, heavy lexan bore rider
Mass	293.2 g
Bank Charge	16.5 kV
Peak Current	1181 kA
Average Current	1150 ± 20 kA
Derived L'	0.383×10^{-6} H/m
Acceleration	0.86×10^3 m/s ²
Exit Velocity	2170 ± 50 m/s

Pre-shot Notes: This was the second of two tests in which a heavy armature was used to increase current and decrease speed (other shot was MCL 84). In this shot I buried pins deeper on average than in MCL 84. The shots are not identical several reasons. First, this armature is about 12 grams heavier than the MCL 84 armature. Second, this shot involved backfilling the bore with helium. Third, there was a bank misfire on MCL 84 so that current dropped off faster once the armature got to about 75-80 cm. The last event should not affect most of the points collected on MCL 84.

Post-shot Notes:

MCL 88 (97102301) Wear Track Locations:

Negative Rail ("driver's" side) Tracks numbered from top of rail

#	col.	row	z [cm]	depth [mil]	d/z [mil/cm]	± [%]	± [mils/cm]	Notes
88n1	7.5	7	33 ± 1	10 ± 1	0.303	0.104	0.032	
88n2	6	3	29 ± 1	5.5 ± 1	0.19	0.185	0.035	
88n3	4	2	49 ± 1	8 ± 1	0.163	0.127	0.021	
88n4	3	3	93.5 ± 1	21.5 ± 1	0.23	0.048	0.011	
88n5	2	5	89 ± 1	21 ± 1	0.236	0.049	0.012	
88n6	1	7	95 ± 1	23 ± 1	0.242	0.045	0.011	
88n7	1	7	72.5 ± 1	19 ± 1	0.262	0.054	0.014	
88n8	2	5	80.5 ± 1	18 ± 1	0.224	0.057	0.013	
88n9	3	3	93 ± 1	22 ± 1	0.237	0.047	0.011	
88n10	4	2	52 ± 1	8 ± 1	0.154	0.126	0.019	
88n11	6	3	---	0 (Fe)				a.
88n12	7.5	7	25 ± 1	10 ± 1	0.4	0.108	0.043	

a. Broken bit (flush with surface) no usable wear track

Positive Rail ("passenger's" side) Tracks numbered from bottom of rail

#	col.	row	z [cm]	depth [mil]	d/z [mil/cm]	± [%]	± [mils/cm]	Notes
88p1	7	4	22 ± 2	4.5 ± 1	0.205	0.24	0.049	
88p2	6	5	32.5 ± 1	10 ± 1	0.308	0.105	0.032	
88p3	4	7	47 ± 1	13 ± 1	0.277	0.08	0.022	b.
88p4	3	5	85.5 ± 1	22 ± 1	0.257	0.047	0.012	
88p5	2	3	68.5 ± 1	12 ± 1	0.175	0.085	0.015	
88p6	1	2	22.5 ± 2	3 ± 1	0.133	0.345	0.046	
88p7	1	2	23.5 ± 2	2 ± 1	0.085	0.507	0.043	
88p8	2	3	89 ± 1	18 ± 1	0.202	0.057	0.011	
88p9	3	5	37.5 ± 5	10 ± 1 (Fe)	0.267	0.167	0.044	c.
88p10	4	7	65 ± 1	17.5 ± 1	0.269	0.059	0.016	
88p11	6	4	44 ± 1	14 ± 1	0.318	0.075	0.024	
88p12	7	3	29.5 ± 1	9 ± 1	0.305	0.116	0.035	

b. canal effect adjacent to wear track.

c. broken bit; wear track starts out as 10cm long skinny scratch.

Comments:

Appendix C

Wear Data Plotted on a Per-Test Basis

Appendix C contains results of the wear tests plotted on a test by test basis to show the effect on wear of changing current and velocity. The data from each test is presented in three plots. Plots labeled "inner columns" display points located in columns 1-4; plots labeled "outer columns" display points located in columns 5-9; "all columns" display columns 1-9. Also included are tables of the data from which the plots are generated, and details of a regression fit to all the data for that set of conditions (all rows and columns).

Plot	Tests	Page
Wear at Standard Conditions:	MCL 57, 58, 59, 63	54
Wear at Low Velocity, Low Current:	MCL 71, 76	60
Wear at High Velocity, Normal Current:	MCL 73	66
Wear at Normal Velocity, Low Current:	MCL 75	71
Wear at Low Velocity, High Current:	MCL 84, 88	76

A result of the tests is summarized in Fig. C1 below, which shows the regression fit obtained for each set of conditions. Although there are noticeable variations, they are slight and in most cases smaller than one standard error of the regression (63% of the data points lie within one standard error of the regression).

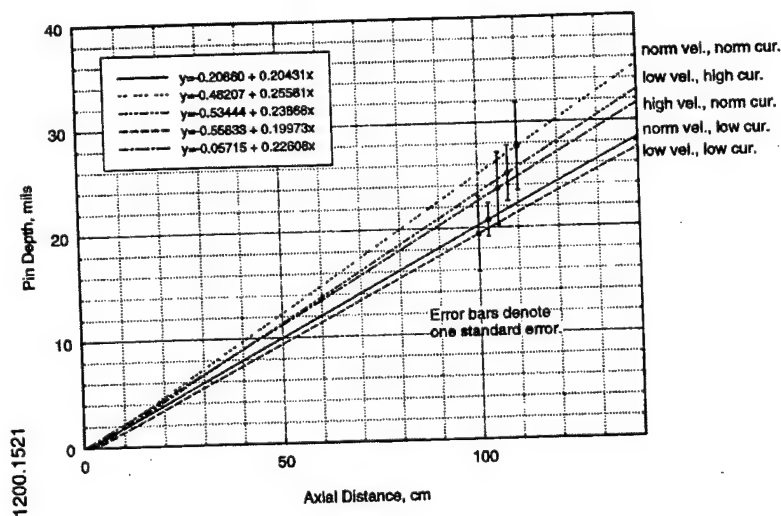


Figure C1. Wear curve fits for all rows and columns.

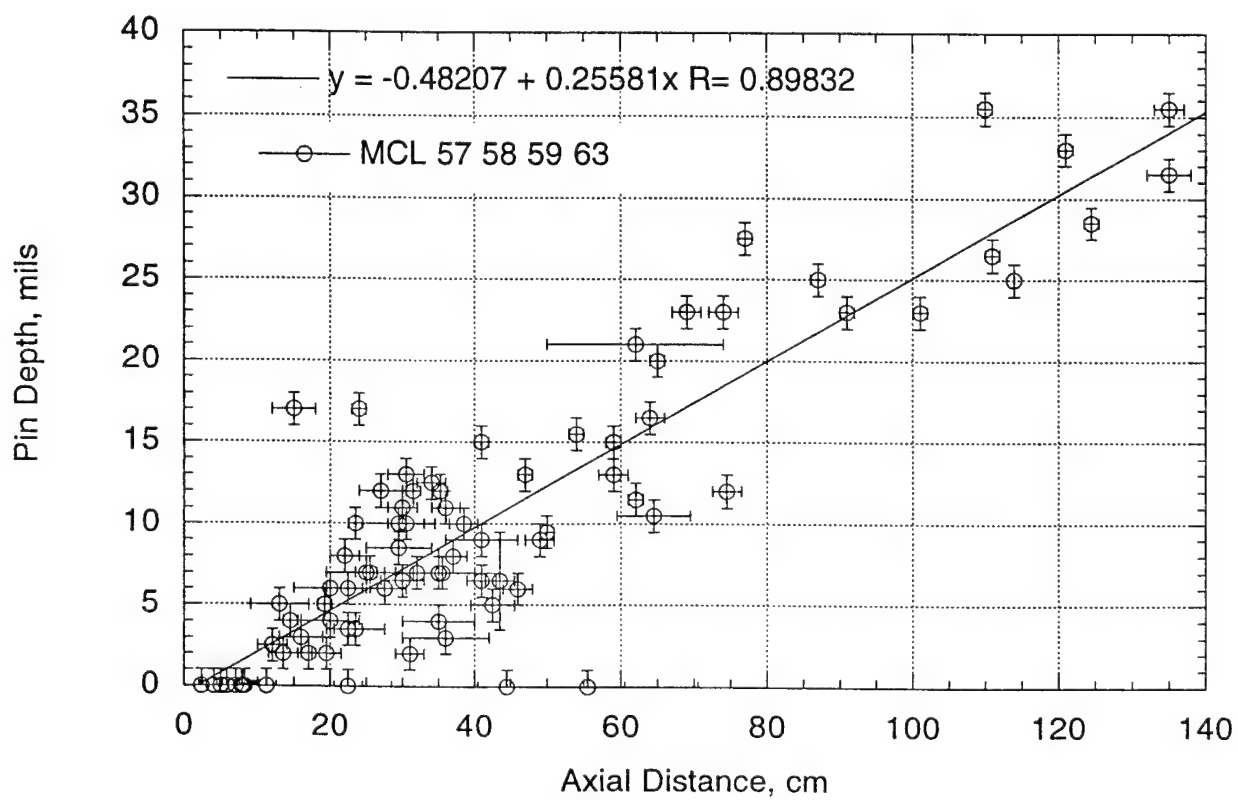


Fig. C2. Wear at standard conditions; all rows and columns.

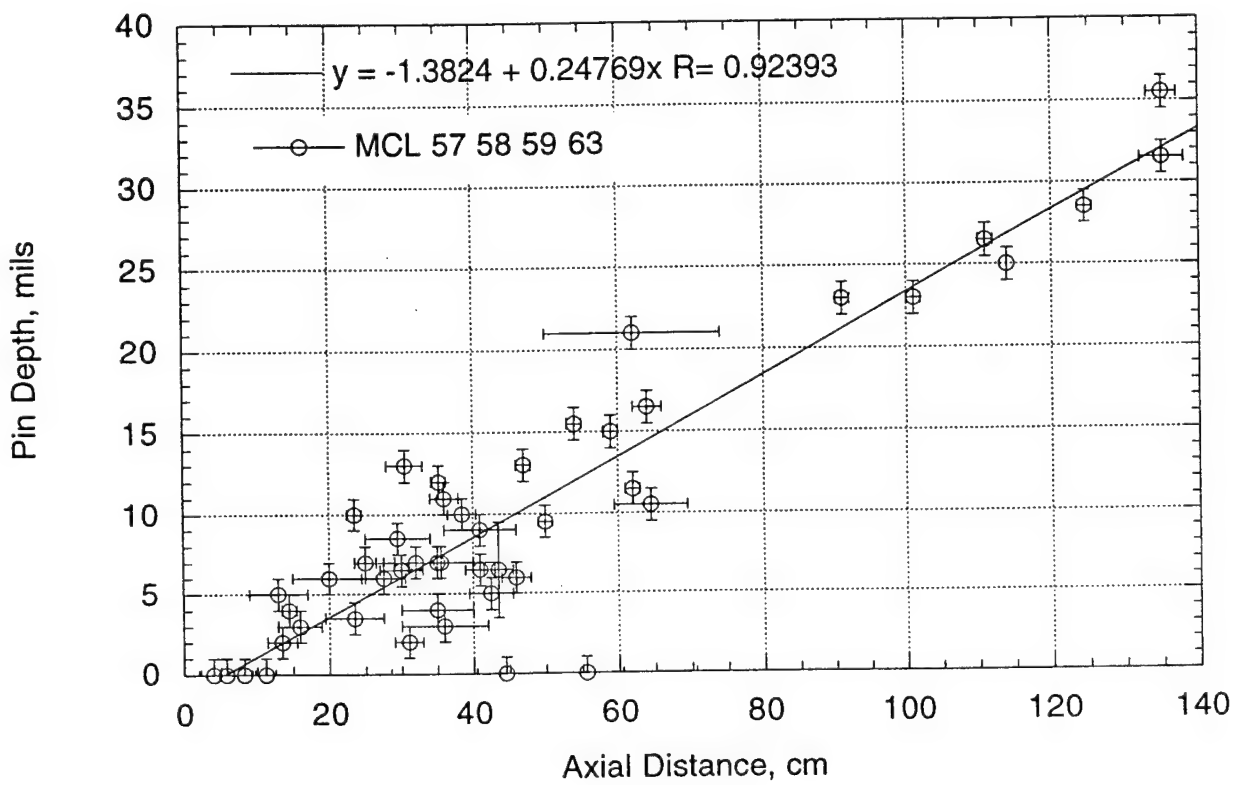


Fig. C3. Wear at standard conditions; all rows, inner columns.

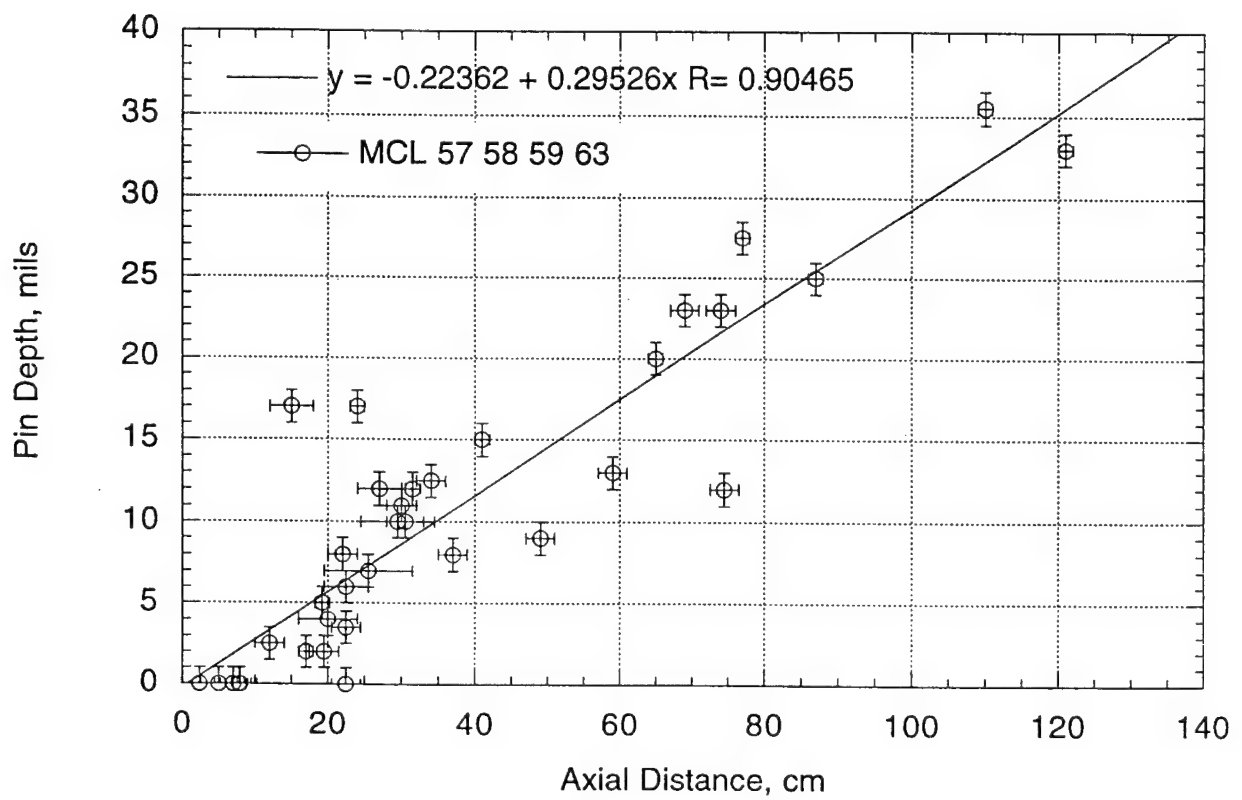


Fig. C4. Wear at standard conditions; all rows, outer columns.

**Wear At Standard Conditions
All Rows and Columns**

	$(D-D_{fit})^2$
Minimum	0.007682533
Maximum	188.1118
Sum	1485.1019
Points	85
Mean	17.471788
Median	5.1661205
RMS	38.414485
Std Deviation	34.414281
Variance	1184.3427
Std Error	3.7327528
Skewness	3.6024076
Kurtosis	13.582335

Regression depth = $-0.48207 + 0.22581z$; R = 0.89832

Standard Error $S_y = [(D-D_{fit})^2/N]^{1/2} = [1485.1019 / 85]^{1/2} = 4.18$

	Pin	Column	Row	Z-bar	Depth	Z error	D error	D/Z	D-fit	(D-Dfit)^2
0	59p7	1.0000	7.0000	11.250	0.0000	1.3000	1.0000	0.0000	2.3958	5.7398
1	59p6	1.0000	7.0000	114.00	25.000	0.0000	1.0000	0.21900	28.680	13.544
2	58p8	1.0000	8.0000	43.500	6.5000	2.0000	3.0000	0.14900	10.646	17.187
3	58n7	1.0000	8.0000	31.000	2.0000	2.0000	1.0000	0.065000	7.4480	29.681
4	63n7	1.0000	5.0000	54.000	15.500	1.0000	1.0000	0.28700	13.332	4.7017
5	58n8	1.0000	7.0000	41.000	9.0000	5.0000	1.0000	0.22000	10.006	1.0123
6	57p6	1.0000	4.0000	20.000	6.0000	5.0000	1.0000	0.30000	4.6341	1.8656
7	57p7	1.0000	4.0000	13.500	2.0000	2.0000	1.0000	0.14800	2.9714	0.94355
8	58p9	1.0000	8.0000	64.500	10.500	5.0000	1.0000	0.16300	16.018	30.445
9	59n6	1.0000	6.0000	25.000	7.0000	1.5000	1.0000	0.28000	5.9132	1.1812
10	59n7	1.0000	6.0000	5.7500	0.0000	3.5000	1.0000	0.0000	0.98884	0.97780
11	63n6	2.0000	3.0000	135.00	35.500	2.0000	1.0000	0.26300	34.052	2.0959
12	63n9	2.0000	3.0000	101.00	23.000	1.0000	1.0000	0.22800	25.355	5.5448
13	58n6	2.0000	5.0000	16.000	3.0000	3.0000	1.0000	0.18800	3.6109	0.37319
14	63p8	2.0000	6.0000	124.50	28.500	1.0000	1.0000	0.22900	31.366	8.2155
15	58n9	2.0000	5.0000	29.500	8.5000	4.5000	1.0000	0.28800	7.0643	2.0612
16	58p10	2.0000	6.0000	27.500	6.0000	3.0000	1.0000	0.21800	6.5527	0.30548
17	63p5	2.0000	6.0000	64.000	16.500	2.0000	1.0000	0.25800	15.890	0.37238
18	58p7	2.0000	6.0000	35.500	7.0000	8.0000	1.0000	0.19700	8.5992	2.5574
19	59p5	2.5000	7.0000	44.500	0.0000	16.000	1.0000	0.0000	10.901	118.84
20	59n5	2.5000	6.0000	8.2500	0.0000	1.5000	1.0000	0.0000	1.6284	2.6516
21	59p8	2.5000	7.0000	23.500	10.000	1.0000	1.0000	0.42600	5.5295	19.986
22	57n5	2.5000	2.0000	35.000	7.0000	5.0000	1.0000	0.20000	8.4713	2.1647
23	57p5	2.5000	5.0000	14.500	4.0000	1.0000	1.0000	0.27600	3.2272	0.59726
24	57p8	2.5000	5.0000	36.000	11.000	2.0000	1.0000	0.30600	8.7271	5.1661
25	59n8	2.5000	6.0000	62.000	21.000	12.000	1.0000	0.33900	15.378	31.605
26	57n8	2.5000	2.0000	38.500	10.000	2.0000	1.0000	0.26000	9.3666	0.40118
27	63n5	3.0000	5.0000	135.00	35.500	2.0000	1.0000	0.26300	34.052	2.0959
28	63n10	3.0000	5.0000	91.000	23.000	1.0000	1.0000	0.25300	22.797	0.041355
29	58p6	3.0000	4.0000	30.000	6.5000	3.0000	1.0000	0.21700	7.1922	0.47918
30	58n10	3.0000	3.0000	50.000	9.5000	1.0000	1.0000	0.19000	12.308	7.8873
31	58n5	3.0000	3.0000	23.500	3.5000	4.0000	1.0000	0.14900	5.5295	4.1187
32	58p11	3.0000	4.0000	32.000	7.0000	3.0000	1.0000	0.21900	7.7038	0.49540
33	63p9	3.0000	4.0000	59.000	15.000	1.0000	1.0000	0.25400	14.611	0.15154
34	63p4	3.0000	4.0000	47.000	13.000	1.0000	1.0000	0.27700	11.541	2.1287
35	59n9	4.0000	6.0000	4.0000	0.0000	2.0000	1.0000	0.0000	0.54117	0.29286
36	57p4	4.0000	6.0000	13.000	5.0000	4.0000	1.0000	0.38500	2.8435	4.6507
37	59n4	4.0000	6.0000	35.250	12.000	1.0000	1.0000	0.34000	8.5352	12.005
38	63p10	4.0000	2.0000	111.00	26.500	1.0000	1.0000	0.23900	27.913	1.9961
39	63p3	4.0000	2.0000	62.000	11.500	1.0000	1.0000	0.18500	15.378	15.040
40	58p5	4.0000	2.0000	36.000	3.0000	6.0000	1.0000	0.083000	8.7271	32.800
41	58p12	4.0000	2.0000	46.000	6.0000	2.0000	1.0000	0.13000	11.285	27.933
42	63n4	4.0000	7.0000	135.00	31.500	3.0000	1.0000	0.23300	34.052	6.5141
43	58n11	4.0000	1.0000	41.000	6.5000	2.0000	1.0000	0.15900	10.006	12.293
44	58n4	4.0000	1.0000	42.500	5.0000	3.0000	1.0000	0.11800	10.390	29.051
45	57n4	4.0000	1.0000	35.000	4.0000	5.0000	1.0000	0.11400	8.4713	19.992
46	59p4	4.0000	7.0000	30.500	13.000	2.5000	1.0000	0.42600	7.3201	32.261
47	59p9	4.0000	7.0000	55.500	0.0000	15.000	1.0000	0.0000	13.715	188.11
48	59n10	6.0000	6.0000	7.0000	0.0000	2.5000	1.0000	0.0000	1.3086	1.7124
49	63n12	6.0000	6.0000	87.000	25.000	1.0000	1.0000	0.28700	21.773	10.411
50	59p3	6.0000	7.0000	2.4000	0.0000	0.0000	1.0000	0.0000	0.13187	0.017391
51	59p10	6.0000	7.0000	22.500	0.0000	2.0000	1.0000	0.0000	5.2737	27.811

	Pin	Column	Row	Z-bar	Depth	Z error	D error	D/Z	D-fit	(D-Dfit)^2
52	63n3	6.0000	6.0000	121.00	33.000	1.0000	1.0000	0.27300	30.471	6.3961
53	57p3	6.0000	4.0000	29.500	10.000	5.0000	1.0000	0.33900	7.0643	8.6182
54	57p10	6.0000	4.0000	25.500	7.0000	6.0000	1.0000	0.27500	6.0411	0.91952
55	59n3	6.0000	5.0000	5.0000	0.0000	2.5000	1.0000	0.0000	0.79698	0.63518
56	58p4	6.0000	2.0000	69.000	23.000	2.0000	1.0000	0.33300	17.169	34.003
57	58n3	6.0000	1.0000	49.000	9.0000	2.0000	1.0000	0.18400	12.053	9.3185
58	58p13	6.0000	2.0000	20.000	4.0000	4.0000	1.0000	0.20000	4.6341	0.40212
59	58p14	7.0000	4.0000	37.000	8.0000	2.0000	1.0000	0.21600	8.9829	0.96609
60	58n14	7.0000	3.0000	59.000	13.000	2.0000	1.0000	0.22000	14.611	2.5944
61	58n2	7.0000	3.0000	27.000	12.000	3.0000	1.0000	0.44400	6.4248	31.083
62	63n2	7.0000	5.0000	65.000	20.000	1.0000	1.0000	0.30800	16.146	14.857
63	63n13	7.0000	5.0000	110.00	35.500	1.0000	1.0000	0.32300	27.657	61.512
64	58p3	7.0000	5.0000	74.500	12.000	2.0000	1.0000	0.16100	18.576	43.241
65	57n2	7.5000	2.0000	12.000	2.5000	2.0000	1.0000	0.20800	2.5877	0.0076825
66	57n11	7.5000	2.0000	30.000	11.000	2.0000	1.0000	0.36700	7.1922	14.499
67	63n1	7.5000	2.0000	17.000	2.0000	1.0000	1.0000	0.11800	3.8667	3.4846
68	59n2	7.5000	6.0000	7.7500	0.0000	2.5000	1.0000	0.0000	1.5005	2.2514
69	59n11	7.5000	5.0000	19.500	2.0000	2.0000	1.0000	0.10300	4.5062	6.2812
70	63p1	7.5000	5.0000	77.000	27.500	1.0000	1.0000	0.35700	19.215	68.636
71	63p12	7.5000	5.0000	74.000	23.000	2.0000	1.0000	0.31100	18.448	20.722
72	57p11	7.5000	5.0000	22.500	6.0000	3.0000	1.0000	0.26700	5.2737	0.52758
73	57p2	7.5000	5.0000	19.250	5.0000	1.0000	1.0000	0.26000	4.4423	0.31106
74	63n14	8.0000	2.0000	34.000	12.500	2.0000	1.0000	0.36800	8.2155	18.357
75	58n1	8.0000	5.0000	22.500	3.5000	2.0000	1.0000	0.15600	5.2737	3.1459
76	58n15	8.0000	4.0000	30.500	10.000	2.5000	1.0000	0.32800	7.3201	7.1817
77	59p12	9.0000	7.0000	8.0000	0.0000	1.0000	1.0000	0.0000	1.5644	2.4474
78	59p1	9.0000	7.0000	41.000	15.000	1.0000	1.0000	0.36600	10.006	24.939
79	59n12	9.0000	6.0000	7.7500	0.0000	1.0000	1.0000	0.0000	1.5005	2.2514
80	58n16	9.0000	6.0000	31.500	12.000	1.0000	1.0000	0.38100	7.5759	19.572
81	57p1	9.0000	6.0000	15.000	17.000	3.0000	1.0000	1.1330	3.3551	186.18
82	59n1	9.0000	4.0000	8.0000	0.0000	0.50000	1.0000	0.0000	1.5644	2.4474
83	57n12	9.0000	3.0000	22.000	8.0000	2.0000	1.0000	0.36400	5.1458	8.1467
84	57p1'	9.0000	6.0000	24.000	17.000	1.0000	1.0000	0.70800	5.6574	128.66

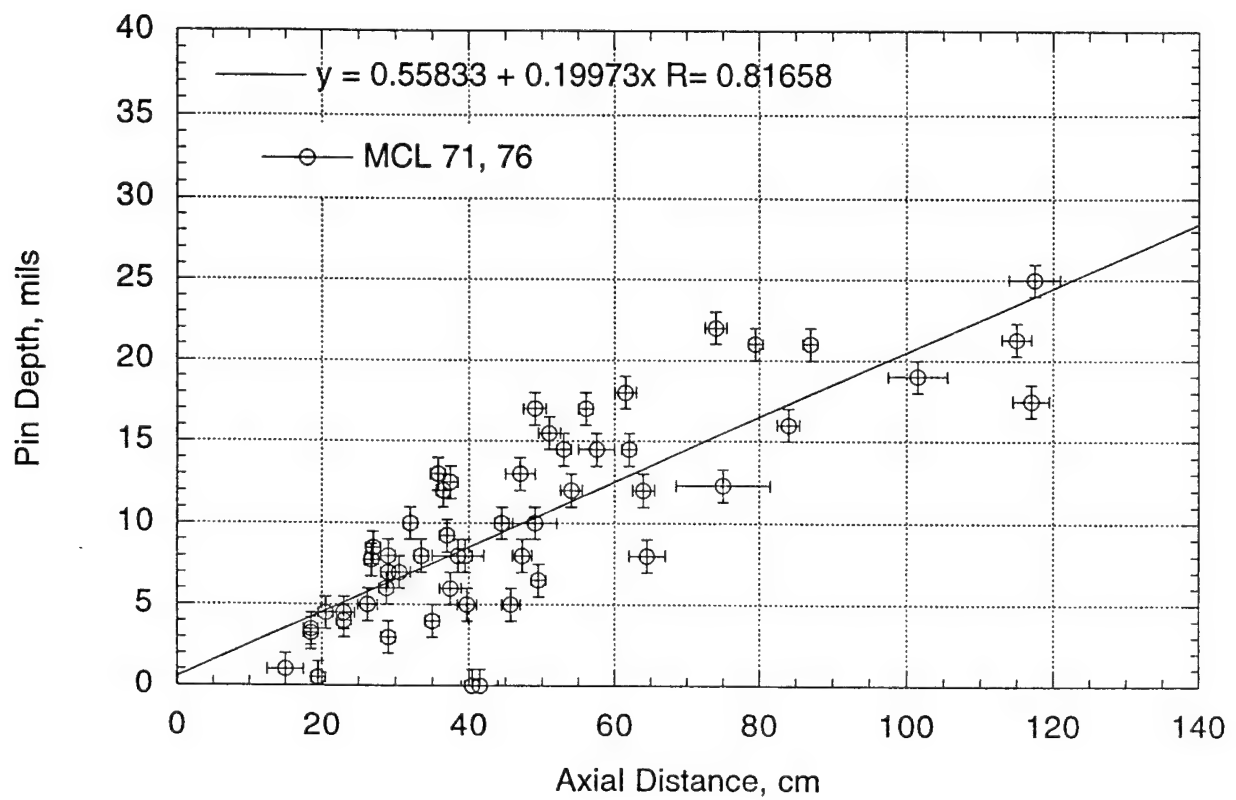


Fig. C5. Wear at low velocity, low current; all rows and columns.

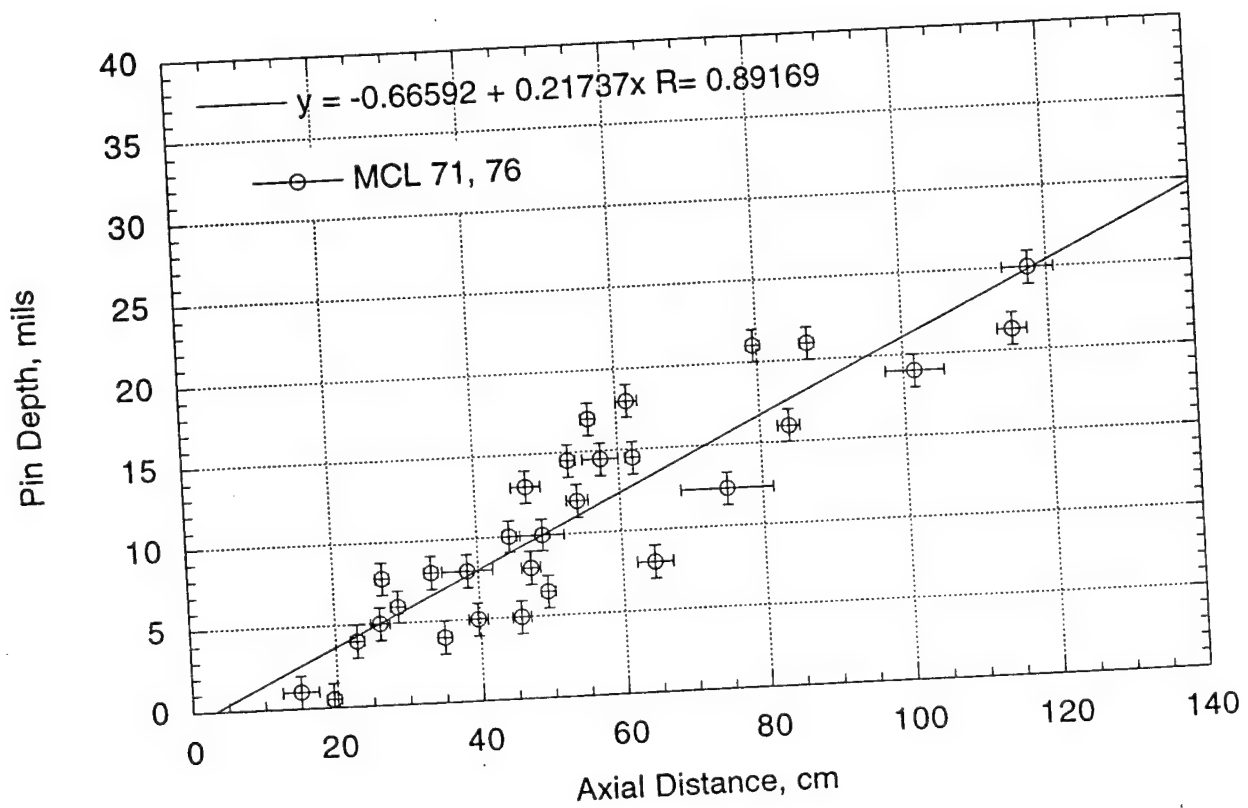


Fig. C6. Wear at low velocity, low current; all rows, inner columns.

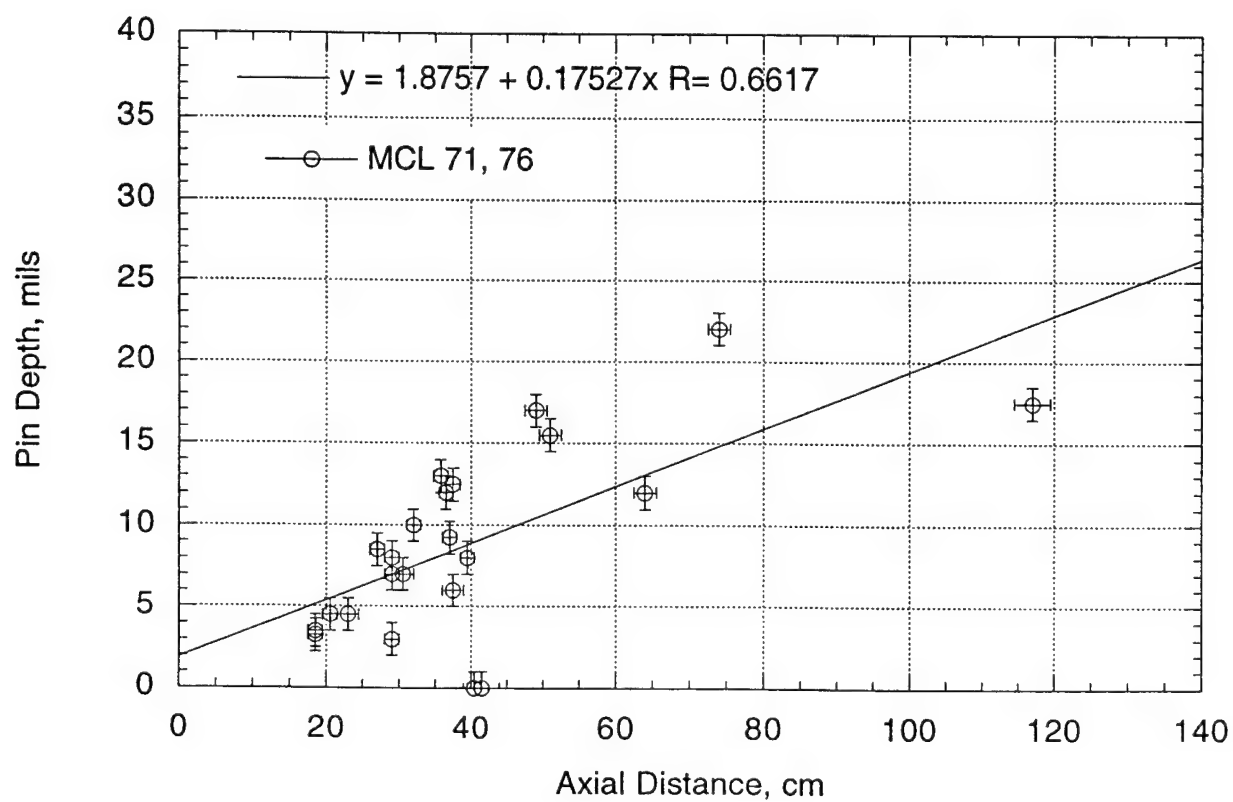


Fig. C7. Wear at low velocity, low current; all rows, outer columns.

Wear At Low Velocity , Low Current (MCL 71,76)
All Rows, All Columns

	$(D-D_{fit})^2$
Minimum	0.023346262
Maximum	78.271622
Sum	671.17887
Points	53
Mean	12.663752
Median	6.0378084
RMS	21.396228
Std Deviation	17.411138
Variance	303.14772
Std Error	2.3916037
Skewness	2.1598554
Kurtosis	4.8499061

Regression depth = $0.55833 + 0.19973z$; R = 0.81658

Standard Error $S_y = [(D-D_{fit})^2/N]^{1/2} = [671.177887/ 53]^{1/2} = 3.56$

	Pin	Column	Row	Z-bar	Depth	Z error	D error	D/Z	D-fit	(D-Dfit)^2
0	76p9	1.0000	7.0000	101.50	19.000	4.0000	1.0000	0.18700	20.831	3.3523
1	76p8	1.0000	7.0000	49.500	6.5000	1.0000	1.0000	0.13100	10.445	15.563
2	71n7	1.0000	7.0000	38.500	8.0000	3.5000	1.0000	0.20800	8.2479	0.061472
3	71n6	1.0000	7.0000	15.000	1.0000	2.5000	1.0000	0.067000	3.5543	6.5243
4	76n8	1.0000	8.0000	75.000	12.300	6.5000	1.0000	0.16300	15.538	10.485
5	76n9	1.0000	8.0000	115.00	21.300	2.0000	1.0000	0.18500	23.527	4.9608
6	71p6	1.0000	8.0000	35.000	4.0000	1.0000	1.0000	0.11400	7.5489	12.595
7	71p7	1.0000	8.0000	45.750	5.0000	1.3000	1.0000	0.10900	9.6960	22.052
8	71n8	2.0000	5.0000	23.000	4.0000	1.0000	1.0000	0.17400	5.1521	1.3274
9	71n5	2.0000	5.0000	44.500	10.000	1.0000	1.0000	0.22500	9.4463	0.30657
10	71p8	2.0000	6.0000	26.250	5.0000	1.3000	1.0000	0.19000	5.8012	0.64199
11	71p5	2.0000	6.0000	33.500	8.0000	1.0000	1.0000	0.23900	7.2493	0.56357
12	76n7	2.0000	6.0000	53.000	14.500	1.0000	1.0000	0.27400	11.144	11.263
13	76n10	2.0000	6.0000	117.50	25.000	3.5000	1.0000	0.21300	24.027	0.94750
14	76p10	2.0000	5.0000	61.500	18.000	1.5000	1.0000	0.29300	12.842	26.608
15	76p7	2.0000	5.0000	56.000	17.000	1.0000	1.0000	0.30400	11.743	27.634
16	76n11	3.0000	4.0000	26.750	7.7500	1.0000	1.0000	0.29000	5.9011	3.4184
17	71p4	3.0000	4.0000	57.500	14.500	2.5000	1.0000	0.25200	12.043	6.0378
18	76p6	3.0000	3.0000	47.000	13.000	2.0000	1.0000	0.27700	9.9456	9.3291
19	76p11	3.0000	3.0000	87.000	21.000	1.0000	1.0000	0.24100	17.935	9.3952
20	71n9	3.0000	3.0000	64.500	8.0000	2.5000	1.0000	0.12400	13.441	29.604
21	71p9	3.0000	4.0000	28.750	6.0000	1.0000	1.0000	0.20900	6.3006	0.090341
22	76n6	3.0000	4.0000	79.500	21.000	1.0000	1.0000	0.26400	16.437	20.822
23	71n4	3.0000	3.0000	19.500	0.50000	1.0000	1.0000	0.026000	4.4531	15.627
24	71p3	4.0000	2.0000	47.250	8.0000	1.3000	1.0000	0.16900	9.9956	3.9823
25	71p10	4.0000	2.0000	39.750	5.0000	1.3000	1.0000	0.12600	8.4976	12.233
26	76p12	4.0000	1.0000	84.000	16.000	1.5000	1.0000	0.19000	17.336	1.7840
27	76p5	4.0000	1.0000	49.000	10.000	3.0000	1.0000	0.20400	10.345	0.11909
28	76n5	4.0000	2.0000	54.000	12.000	1.5000	1.0000	0.22200	11.344	0.43066
29	76n12	4.0000	2.0000	62.000	14.500	1.0000	1.0000	0.23400	12.942	2.4286
30	76p13	6.0000	8.0000	117.00	17.500	2.5000	1.0000	0.15000	23.927	41.303
31	76p4	6.0000	8.0000	64.000	12.000	1.5000	1.0000	0.18800	13.341	1.7984
32	71n11	6.0000	8.0000	29.000	3.0000	1.0000	1.0000	0.10300	6.3505	11.226
33	71p11	6.0000	4.0000	40.500	0.0000	1.0000	1.0000	0.0000	8.6474	74.777
34	71p2	6.0000	4.0000	41.500	0.0000	2.5000	1.0000	0.0000	8.8471	78.272
35	76n13	6.0000	4.0000	37.500	12.500	1.0000	1.0000	0.33300	8.0482	19.818
36	76n4	6.0000	4.0000	49.000	17.000	1.5000	1.0000	0.34700	10.345	44.288
37	71n12	7.0000	8.0000	37.500	6.0000	1.5000	1.0000	0.16000	8.0482	4.1951
38	71p12	7.0000	6.0000	29.000	8.0000	1.0000	1.0000	0.27600	6.3505	2.7208
39	76n3	7.0000	6.0000	74.000	22.000	1.5000	1.0000	0.29700	15.338	44.378
40	76p14	7.0000	3.0000	51.000	15.500	1.5000	1.0000	0.30400	10.745	22.614
41	76p3	7.0000	3.0000	20.500	4.5000	1.0000	1.0000	0.22000	4.6528	0.023346
42	76n14	7.0000	6.0000	36.500	12.000	1.0000	1.0000	0.32900	7.8485	17.235
43	71p1	7.0000	6.0000	32.000	10.000	1.0000	1.0000	0.31300	6.9497	9.3044
44	71n1	7.0000	6.0000	29.000	7.0000	1.0000	1.0000	0.24100	6.3505	0.42185
45	76n15	7.5000	2.0000	27.000	8.5000	1.0000	1.0000	0.31500	5.9510	6.4972
46	76n2	7.5000	2.0000	18.500	3.5000	1.0000	1.0000	0.18900	4.2533	0.56751
47	76p15	7.5000	2.0000	37.000	9.2500	1.0000	1.0000	0.25000	7.9483	1.6943
48	76p2	7.5000	2.0000	35.750	13.000	1.0000	1.0000	0.36400	7.6987	28.104
49	76p1	9.0000	8.0000	39.500	8.0000	1.0000	1.0000	0.20300	8.4477	0.20040
50	76n16	9.0000	8.0000	18.500	3.2500	1.0000	1.0000	0.17600	4.2533	1.0067
51	76n1	9.0000	8.0000	30.500	7.0000	1.5000	1.0000	0.23000	6.6501	0.12243

	Pin	Column	Row	Z-bar	Depth	Z error	D error	D/Z	D-fit	(D-Dfit)^2
52	76p16	9.0000	8.0000	23.000	4.5000	1.5000	1.0000	0.19600	5.1521	0.42526

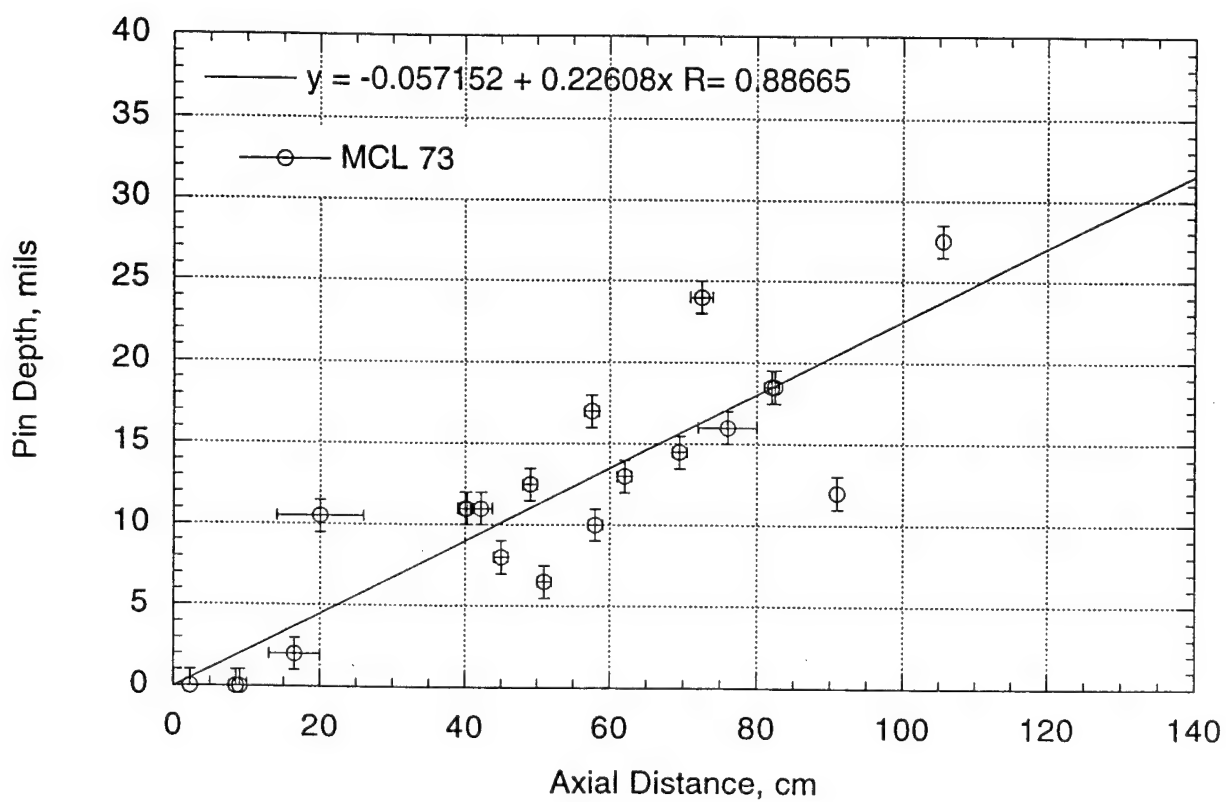


Fig. C8. Wear at high velocity, normal current; all rows and columns.

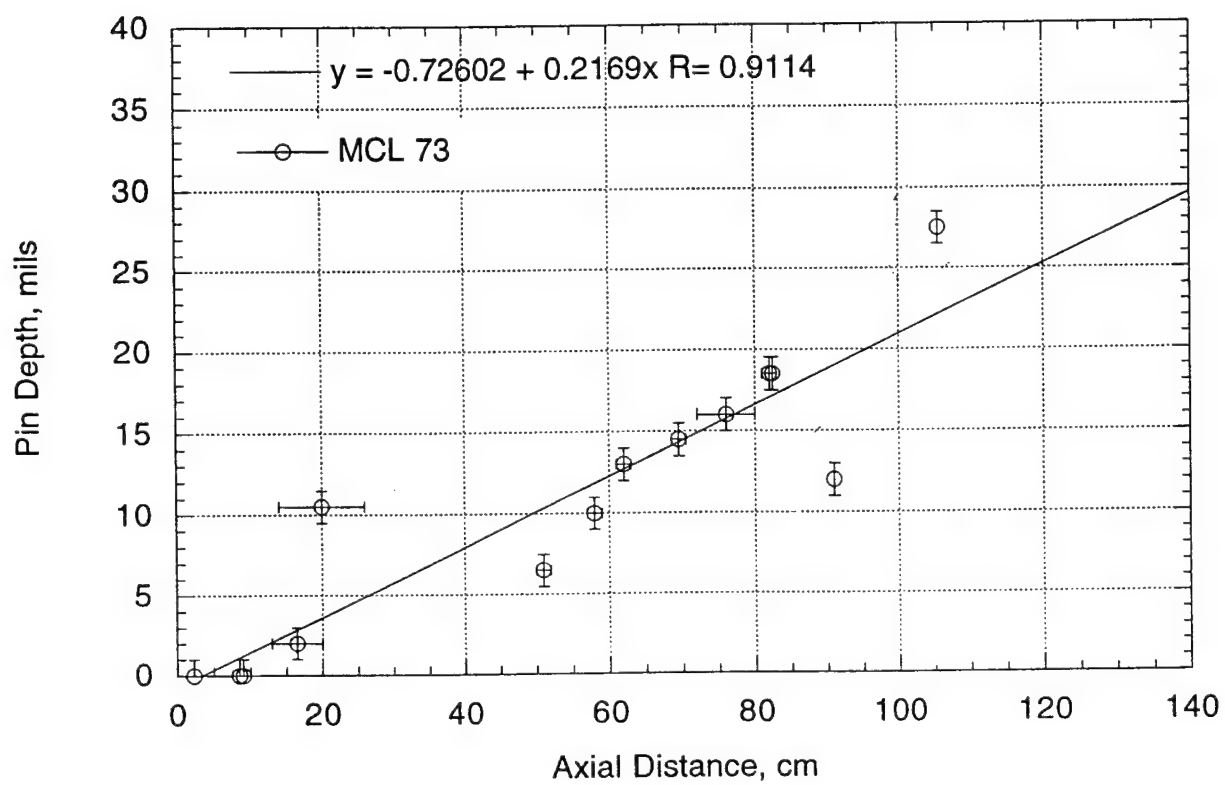


Fig. C9. Wear at high velocity, normal current; all rows, inner columns.

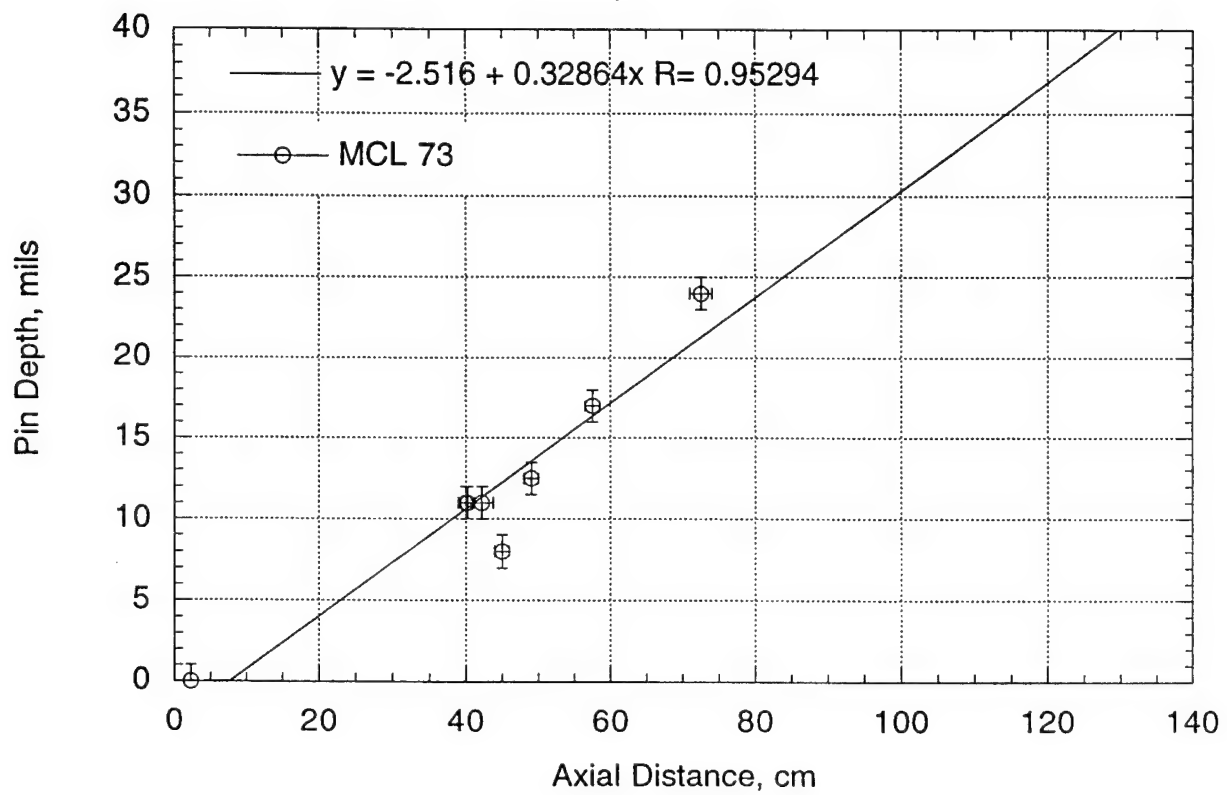


Fig. C10. Wear at high velocity, normal current; all rows, outer columns.

Wear At High Velocity , Normal Current (MCL 73)
All Rows, All Columns

	$(D-D_{fit})^2$
Minimum	0.00034569349
Maximum	72.524445
Sum	262.95427
Points	22
Mean	11.952467
Median	3.6540018
RMS	22.663616
Std Deviation	19.708733
Variance	388.43414
Std Error	4.2019159
Skewness	2.0762386
Kurtosis	3.2218084

Regression depth = $-0.057152 + 0.22608z$; $R = 0.88665$

Standard Error $S_y = [(D-D_{fit})^2/N]^{1/2} = [262.95427/22]^{1/2} = 3.46$

	Pin	Column	Row	Z-bar	Depth	Z error	D error	D/Z	D-fit	(D-Dfit)^2
0	73n7	1.0000	7.0000	9.0000	0.0000	0.0000	1.0000	0.0000	1.9776	3.9108
1	73n6	1.0000	7.0000	76.000	16.000	4.0000	1.0000	0.21100	17.125	1.2655
2	73p7	1.0000	7.0000	62.000	13.000	1.0000	1.0000	0.21000	13.960	0.92123
3	73p6	1.0000	7.0000	8.5000	0.0000	1.0000	1.0000	0.0000	1.8645	3.4765
4	73n8	1.5000	6.0000	16.500	2.0000	3.5000	1.0000	0.12100	3.6732	2.7995
5	73n9	2.0000	5.0000	91.000	12.000	0.0000	1.0000	0.13200	20.516	72.524
6	73p8	2.0000	6.0000	2.3000	0.0000	0.0000	1.0000	0.0000	0.46283	0.21421
7	73n5	2.0000	5.0000	107.00	48.500	1.0000	1.0000	0.45300		
8	73p4	3.0000	4.0000	105.50	27.500	0.0000	1.0000	0.26100	23.794	13.732
9	73p9	3.0000	4.0000	20.000	10.500	6.0000	1.0000	0.52500	4.4644	36.428
10	73n10	3.0000	3.0000	69.500	14.500	1.0000	1.0000	0.20900	15.655	1.3350
11	73n4	3.0000	3.0000	82.000	18.500	1.0000	1.0000	0.22600	18.481	0.00034569
12	73n11	4.0000	1.0000	51.000	6.5000	1.0000	1.0000	0.12700	11.473	24.730
13	73p10	4.0000	2.0000	58.000	10.000	1.0000	1.0000	0.17200	13.055	9.3360
14	73p3	4.0000	2.0000	82.500	18.500	0.0000	1.0000	0.22400	18.594	0.0089204
15	73p11	6.0000	6.0000	2.3000	0.0000	0.0000	1.0000	0.0000	0.46283	0.21421
16	73n12	6.0000	7.0000	49.000	12.500	1.0000	1.0000	0.25500	11.021	2.1881
17	73p2	6.0000	6.0000	57.500	17.000	1.0000	1.0000	0.29600	12.942	16.464
18	73n2	6.0000	7.0000	40.250	11.000	1.0000	1.0000	0.27300	9.0426	3.8315
19	73p12	7.5000	2.0000	45.000	8.0000	1.0000	1.0000	0.17800	10.116	4.4794
20	73n13	7.5000	4.0000	72.500	24.000	1.5000	1.0000	0.33100	16.334	58.773
21	73p1	7.5000	2.0000	40.000	11.000	1.0000	1.0000	0.27500	8.9860	4.0560
22	73n1	7.5000	4.0000	42.250	11.000	1.5000	1.0000	0.26000	9.4947	2.2658

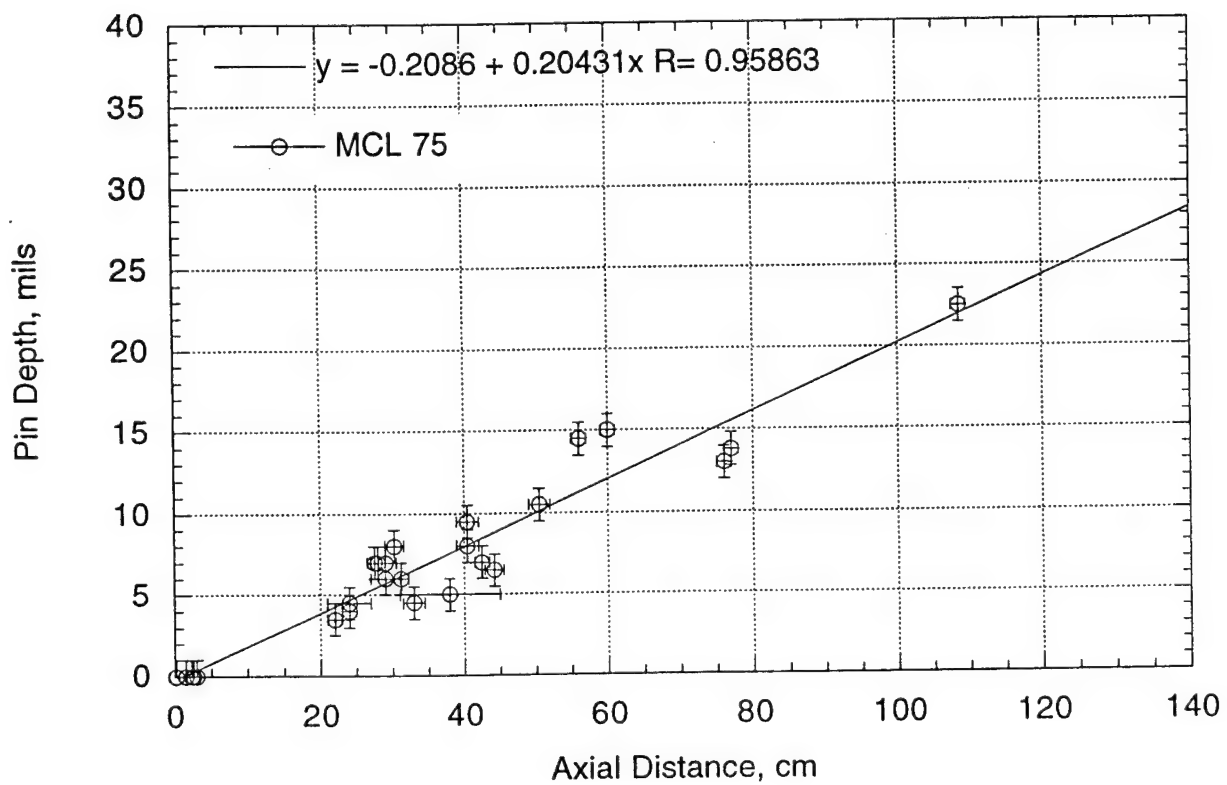


Fig. C11. Wear at normal velocity, low current; all rows and columns.

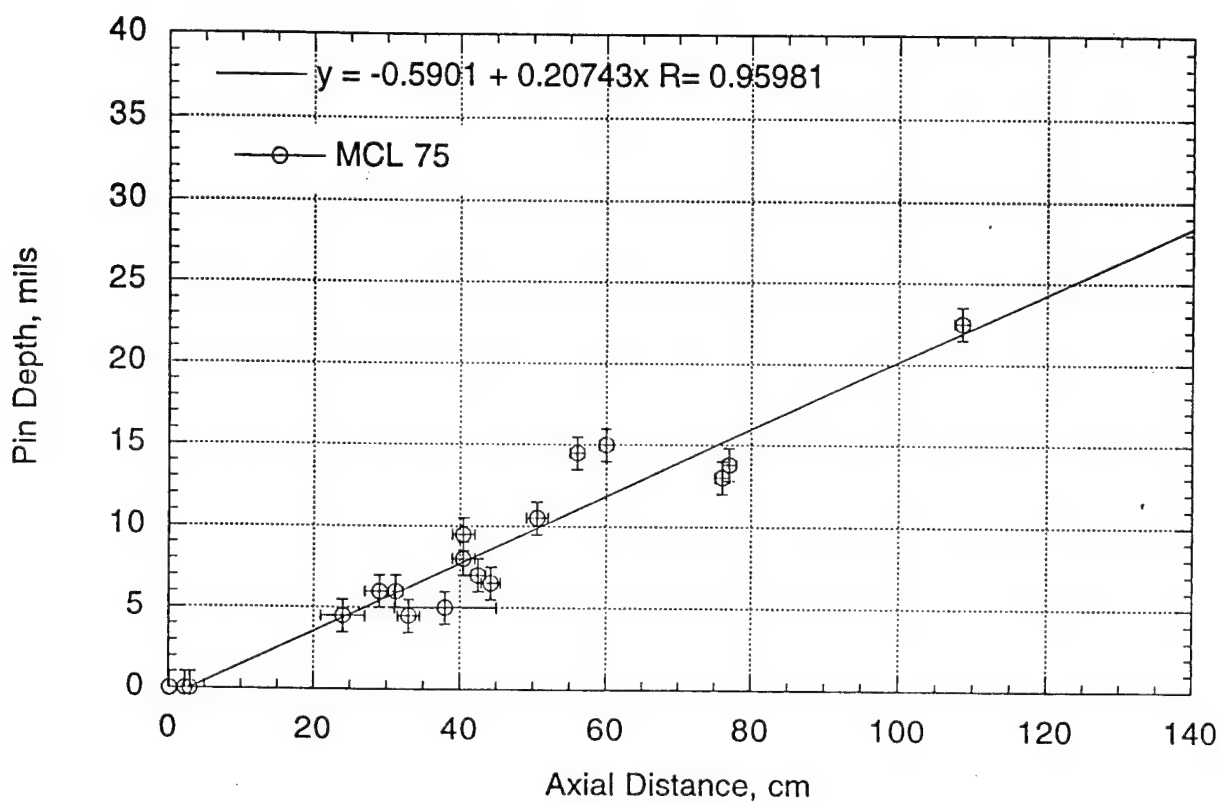


Fig. C12. Wear at normal velocity, low current; all rows, inner columns.

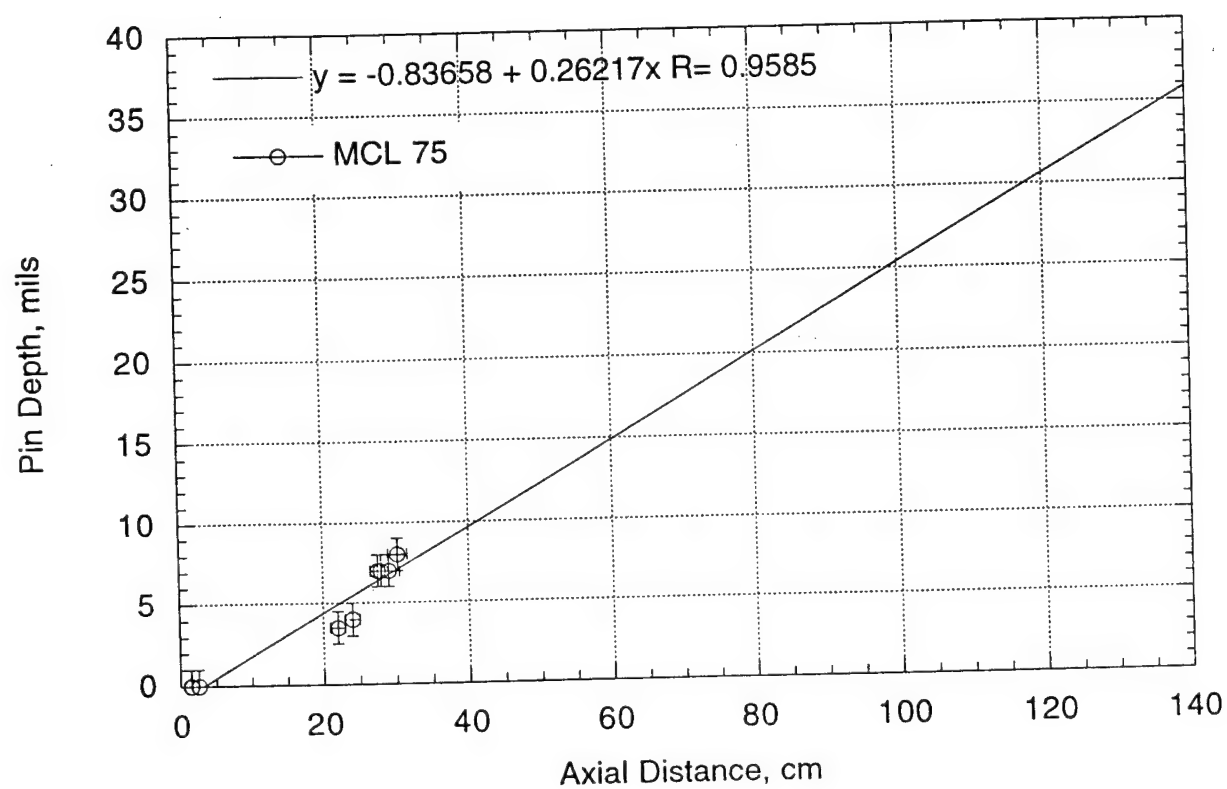


Fig. C13. Wear at normal velocity, low current; all rows, outer columns.

Wear At Normal Velocity , Low Current (MCL 75)
All Rows, All Columns

	$(D-D_{fit})^2$
Minimum	0.0043500834
Maximum	10.674854
Sum	60.623363
Points	26
Mean	2.3316678
Median	1.1328982
RMS	3.7075594
Std Deviation	2.9396759
Variance	8.6416947
Std Error	0.57651788
Skewness	1.3597108
Kurtosis	1.0692865

Regression depth = $-0.2086 + 0.20431z$; R = 0.95863

Standard Error $S_y = [(D-D_{fit})^2/N]^{1/2} = [60.623363/26]^{1/2} = 1.57$

	Pin	Column	Row	Z-bar	Depth	Z error	D error	D/Z	D-fit	(D-Dfit)^2
0	75n7	1.0000	2.0000	42.500	7.0000	1.0000	1.0000	0.16500	8.4746	2.1744
1	75n6	1.0000	2.0000	77.000	13.800	1.0000	1.0000	0.17900	15.523	2.9697
2	75p8	1.0000	7.0000	33.000	4.5000	1.5000	1.0000	0.13600	6.5336	4.1357
3	75p7	1.0000	7.0000	2.3000	0.0000	0.0000	1.0000	0.0000	0.26131	0.068284
4	75n8	2.0000	4.0000	56.000	14.500	1.0000	1.0000	0.25900	11.233	10.675
5	75p6	2.0000	5.0000	50.500	10.500	1.5000	1.0000	0.20800	10.109	0.15284
6	75p9	2.0000	5.0000	29.000	6.0000	2.0000	1.0000	0.20700	5.7164	0.080435
7	75n5	2.0000	4.0000	76.000	13.000	1.0000	1.0000	0.17100	15.319	5.3776
8	75p10	2.5000	4.0000	24.000	4.5000	3.0000	1.0000	0.18800	4.6948	0.037963
9	75p5	2.5000	4.0000	108.50	22.500	1.0000	1.0000	0.20700	21.959	0.29264
10	75p4	3.0000	3.0000	31.250	6.0000	1.0000	1.0000	0.19200	6.1761	0.031007
11	75n9	3.0000	6.0000	60.000	15.000	1.0000	1.0000	0.25000	12.050	8.7025
12	75n4	3.0000	6.0000	40.500	9.5000	1.5000	1.0000	0.23500	8.0660	2.0565
13	75p11	3.0000	3.0000	40.500	8.0000	1.5000	1.0000	0.19800	8.0660	0.0043501
14	75n3	4.0000	8.0000	3.0000	0.0000	0.0000	1.0000	0.0000	0.40433	0.16348
15	75n10	4.0000	8.0000	44.250	6.5000	1.3000	1.0000	0.14700	8.8321	5.4388
16	75p12	4.0000	1.0000	38.000	5.0000	7.0000	1.0000	0.13200	7.5552	6.5289
17	75p3	4.0000	1.0000	0.20000	0.0000	0.0000	1.0000	0.0000	-0.16774	0.028136
18	75n11	6.0000	5.0000	22.000	3.5000	1.0000	1.0000	0.15900	4.2862	0.61814
19	75n2	6.0000	5.0000	29.000	7.0000	1.5000	1.0000	0.24100	5.7164	1.6477
20	75p2	6.0000	4.0000	28.000	7.0000	1.0000	1.0000	0.25000	5.5121	2.2139
21	75p13	6.0000	4.0000	1.5000	0.0000	0.0000	1.0000	0.0000	0.097865	0.0095776
22	75p14	7.0000	6.0000	30.250	8.0000	1.3000	1.0000	0.26400	5.9718	4.1137
23	75p1	7.0000	6.0000	27.500	7.0000	1.0000	1.0000	0.25500	5.4099	2.5283
24	75n1	7.5000	2.0000	2.5000	0.0000	0.0000	1.0000	0.0000	0.30217	0.091310
25	75n12	7.5000	2.0000	24.000	4.0000	1.0000	1.0000	0.16700	4.6948	0.48280

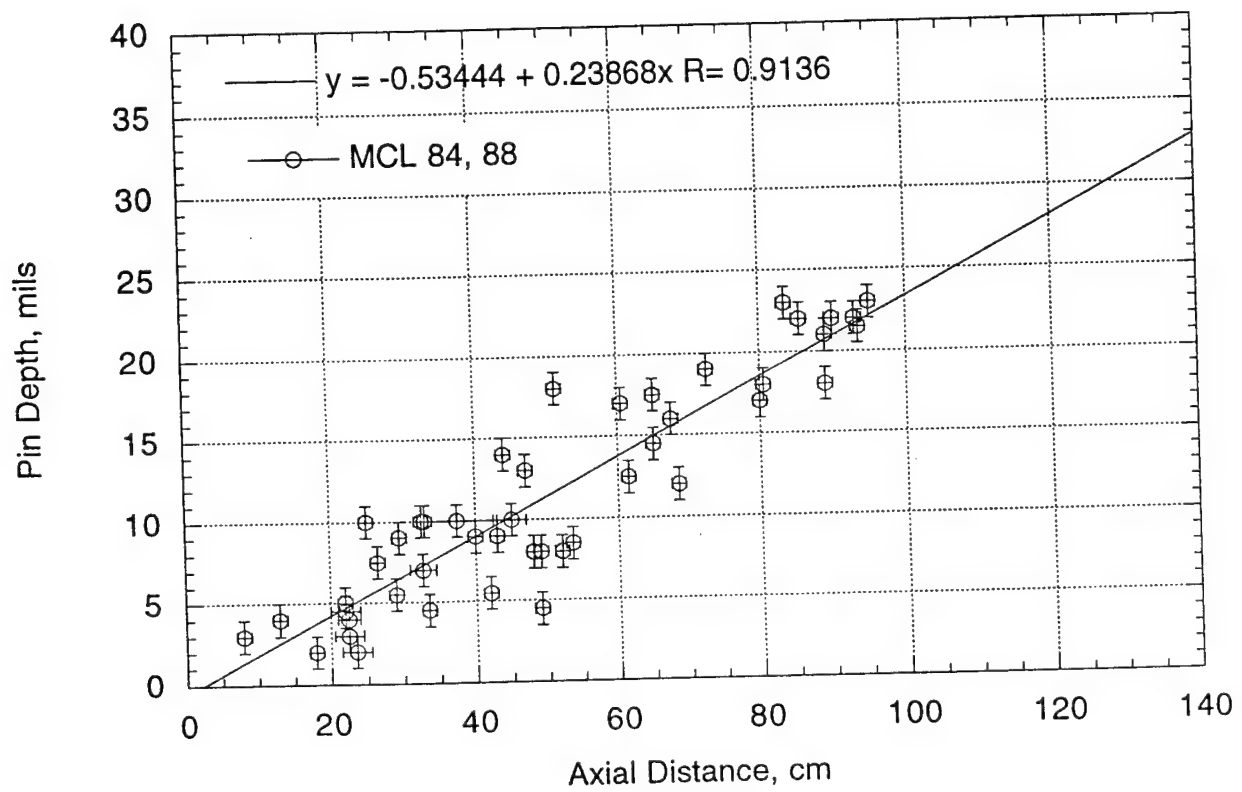


Fig. C14. Wear at low velocity, high current; all rows and columns.

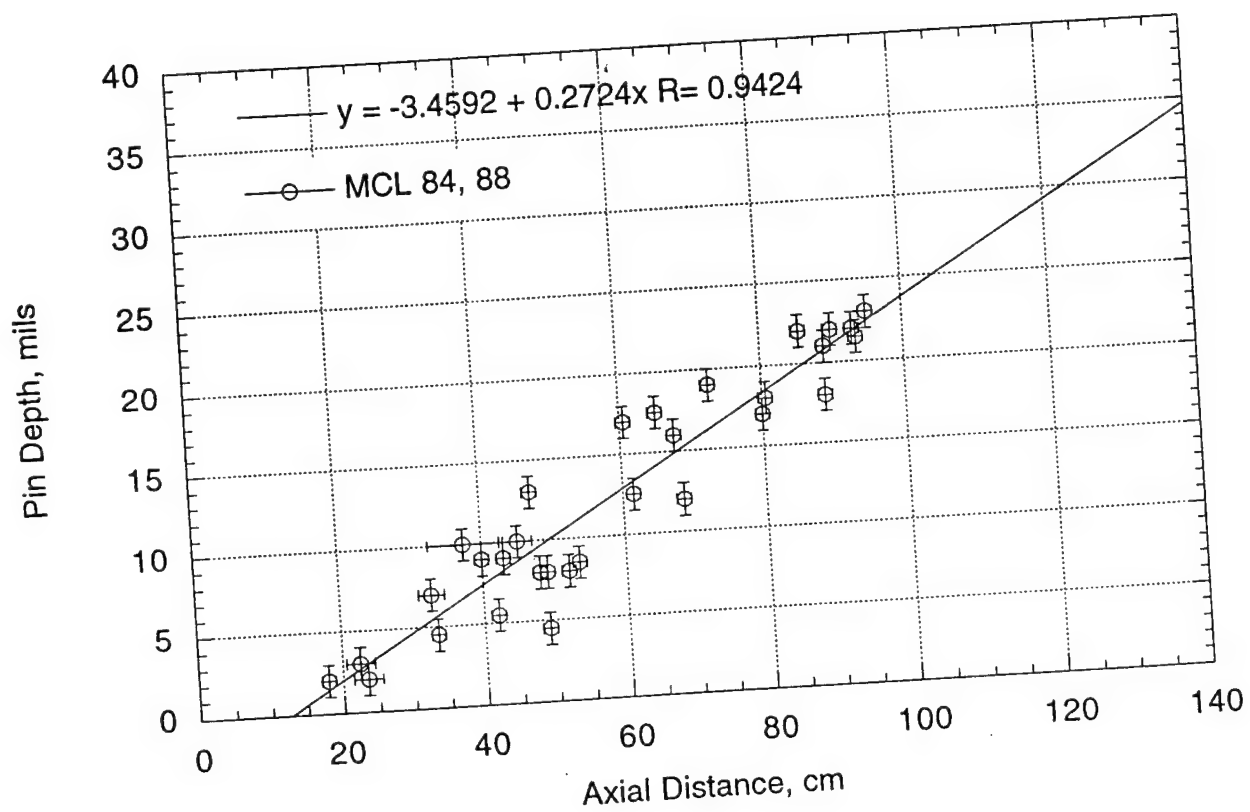


Fig. C15. Wear at low velocity, high current; all rows, inner columns.

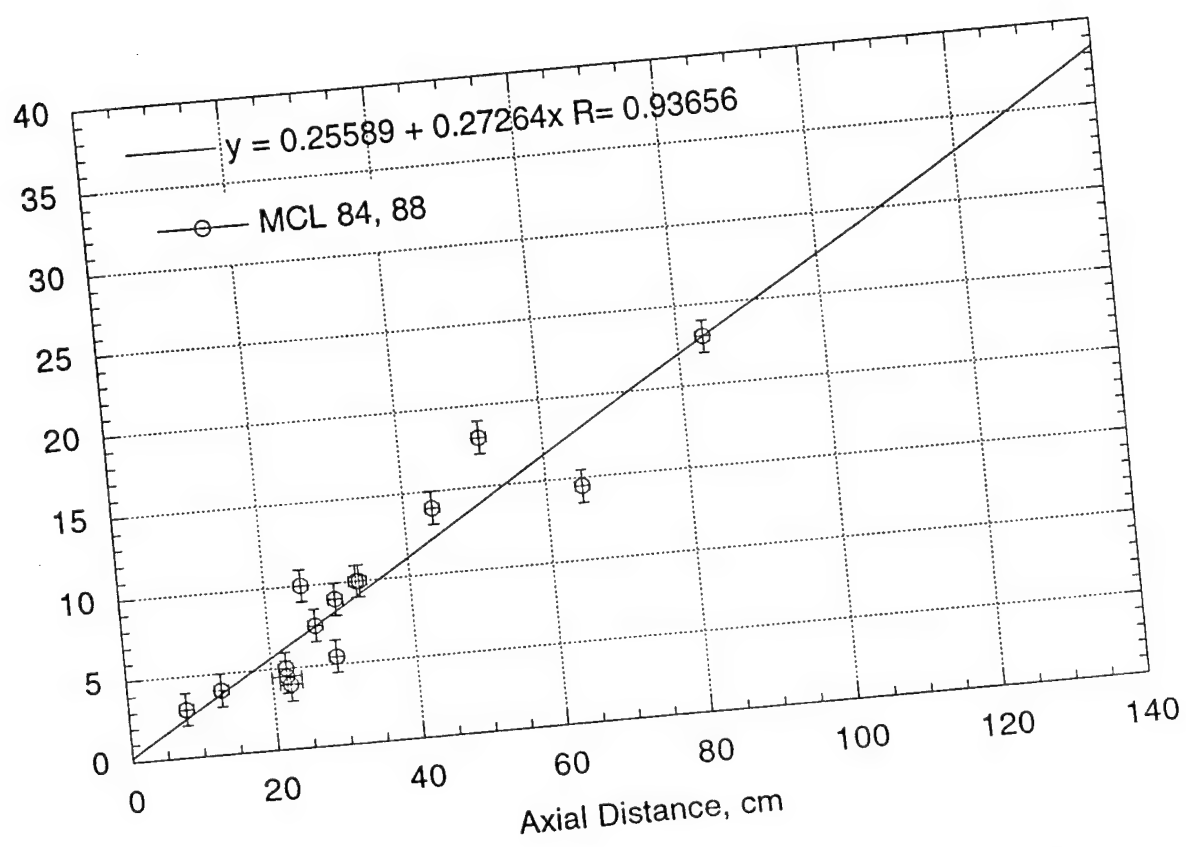


Fig. C16. Wear at low velocity, high current; all rows, outer columns.

Wear At Low Velocity , High Current (MCL 84,88)
All Rows, All Columns

	$(D-D_{fit})^2$
Minimum	0.00016282174
Maximum	44.367325
Sum	316.52761
Points	46
Mean	6.8810349
Median	3.2371603
RMS	11.525754
Std Deviation	9.3484883
Variance	87.394234
Std Error	1.3783594
Skewness	2.4441355
Kurtosis	6.6190506

Regression depth = $-0.53444 + 0.23868z$; R = 0.9136

Standard Error $S_y = [(D-D_{fit})^2/N]^{1/2} = [316.52761/ 46]^{1/2} = 2.62$

	Pin	Column	Row	Z-bar	Depth	Z error	D error	D/Z	D-fit	(D-Dfit)^2
0	84n1	7.0000	5.0000	51.250	18.000	1.0000	1.0000	0.35100	11.698	39.716
1	84n2	6.0000	6.0000	22.500	4.0000	1.5000	1.0000	0.17800	4.8359	0.69866
2	84n3	4.0000	7.0000	32.750	7.0000	1.8000	1.0000	0.21400	7.2823	0.079710
3	84n4	3.0000	6.0000	67.500	16.000	1.0000	1.0000	0.23700	15.576	0.17939
4	84n5	2.0000	4.0000	48.000	8.0000	1.0000	1.0000	0.16700	10.922	8.5393
5	84n6	1.0000	2.0000	49.000	4.5000	1.0000	1.0000	0.092000	11.161	44.367
6	84n7	1.0000	2.0000	33.500	4.5000	1.0000	1.0000	0.13400	7.4613	8.7695
7	84n8	2.0000	4.0000	18.000	2.0000	1.0000	1.0000	0.11100	3.7618	3.1039
8	84n9	3.0000	6.0000	40.000	9.0000	1.0000	1.0000	0.22500	9.0128	0.00016282
9	84n10	4.0000	7.0000	60.500	17.000	1.0000	1.0000	0.28100	13.906	9.5747
10	84n11	6.0000	6.0000	22.000	5.0000	1.0000	1.0000	0.22700	4.7165	0.080361
11	84p1	8.0000	7.0000	8.0000	3.0000	1.0000	1.0000	0.37500	1.3750	2.6406
12	84p2	7.0000	5.0000	26.500	7.5000	1.0000	1.0000	0.28300	5.7906	2.9221
13	84p3	6.0000	3.0000	83.500	23.000	1.0000	1.0000	0.27500	19.395	12.994
14	84p5	3.0000	3.0000	53.500	8.5000	1.0000	1.0000	0.15900	12.235	13.950
15	84p6	2.0000	5.0000	61.500	12.500	1.0000	1.0000	0.20300	14.144	2.7040
16	84p7	1.0000	7.0000	43.000	9.0000	1.0000	1.0000	0.20900	9.7288	0.53115
17	84p8	1.0000	7.0000	45.000	10.000	2.0000	1.0000	0.22200	10.206	0.042502
18	84p9	2.0000	5.0000	90.000	22.000	1.0000	1.0000	0.24400	20.947	1.1093
19	84p10	3.0000	3.0000	80.000	17.000	1.0000	1.0000	0.21300	18.560	2.4335
20	84p11	4.0000	2.0000	42.000	5.5000	1.0000	1.0000	0.13100	9.4901	15.921
21	84p12	6.0000	3.0000	65.000	14.500	1.0000	1.0000	0.22300	14.980	0.23017
22	84p14	8.0000	7.0000	13.000	4.0000	1.0000	1.0000	0.30800	2.5684	2.0495
23	88n1	7.5000	7.0000	33.000	10.000	1.0000	1.0000	0.30300	7.3420	7.0650
24	88n2	6.0000	3.0000	29.000	5.5000	1.0000	1.0000	0.19000	6.3873	0.78727
25	88n3	4.0000	2.0000	49.000	8.0000	1.0000	1.0000	0.16300	11.161	9.9912
26	88n4	3.0000	3.0000	93.500	21.500	1.0000	1.0000	0.23000	21.782	0.079603
27	88n5	2.0000	5.0000	89.000	21.000	1.0000	1.0000	0.23600	20.708	0.085217
28	88n6	1.0000	7.0000	95.000	23.000	1.0000	1.0000	0.24200	22.140	0.73933
29	88n7	1.0000	7.0000	72.500	19.000	1.0000	1.0000	0.26200	16.770	4.9735
30	88n8	2.0000	5.0000	80.500	18.000	1.0000	1.0000	0.22400	18.679	0.46145
31	88n9	3.0000	3.0000	93.000	22.000	1.0000	1.0000	0.23700	21.663	0.11370
32	88n10	4.0000	2.0000	52.000	8.0000	1.0000	1.0000	0.15400	11.877	15.031
33	88n12	7.5000	7.0000	25.000	10.000	1.0000	1.0000	0.40000	5.4326	20.862
34	88p1	7.0000	4.0000	22.000	4.5000	2.0000	1.0000	0.20500	4.7165	0.046881
35	88p2	6.0000	5.0000	32.500	10.000	1.0000	1.0000	0.30800	7.2227	7.7136
36	88p3	4.0000	7.0000	47.000	13.000	1.0000	1.0000	0.27700	10.684	5.3661
37	88p4	3.0000	5.0000	85.500	22.000	1.0000	1.0000	0.25700	19.873	4.5254
38	88p5	2.0000	3.0000	68.500	12.000	1.0000	1.0000	0.17500	15.815	14.555
39	88p6	1.0000	2.0000	22.500	3.0000	2.0000	1.0000	0.13300	4.8359	3.3704
40	88p7	1.0000	2.0000	23.500	2.0000	2.0000	1.0000	0.085000	5.0745	9.4528
41	88p8	2.0000	3.0000	89.000	18.000	1.0000	1.0000	0.20200	20.708	7.3337
42	88p9	3.0000	5.0000	37.500	10.000	5.0000	1.0000	0.26700	8.4161	2.5089
43	88p10	4.0000	7.0000	65.000	17.500	1.0000	1.0000	0.26900	14.980	6.3516
44	88p11	6.0000	4.0000	44.000	14.000	1.0000	1.0000	0.31800	9.9675	16.261
45	88p12	7.0000	3.0000	29.500	9.0000	1.0000	1.0000	0.30500	6.5066	6.2169

Appendix D

Wear Data Plotted as a Function of Location on Armature

Appendix D contains results of the wear tests, plotted to show how wear varies with location on the armature face. Ideally, this appendix would contain a scatter plot for each unique "pad" location (16 locations, given the symmetry about the centerline of the armature). However, three peripheral pad locations (outer columns at rows 1, 7 and 8) did not yield usable wear pin measurements. This is consistent with the high degree of skin-effect heating (and thus softening) predicted by the 3D EM-FEA calculations at these locations on the KJ202 armature.

Results from all ten experiments are included in the plots, in spite of the fact that there were slight variations in current and velocity among the tests. This is in keeping with the conclusion, presented in Appendix C, that variations in wear were small compared to the scatter inherent in the measurements.

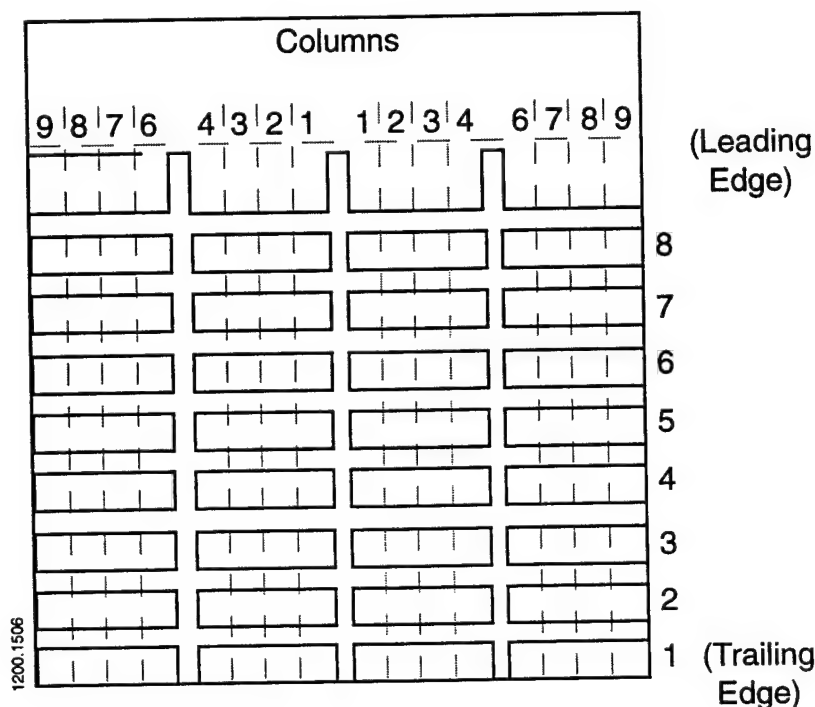


Fig. D1. Coordinate system used for designating pin locations on armature face.

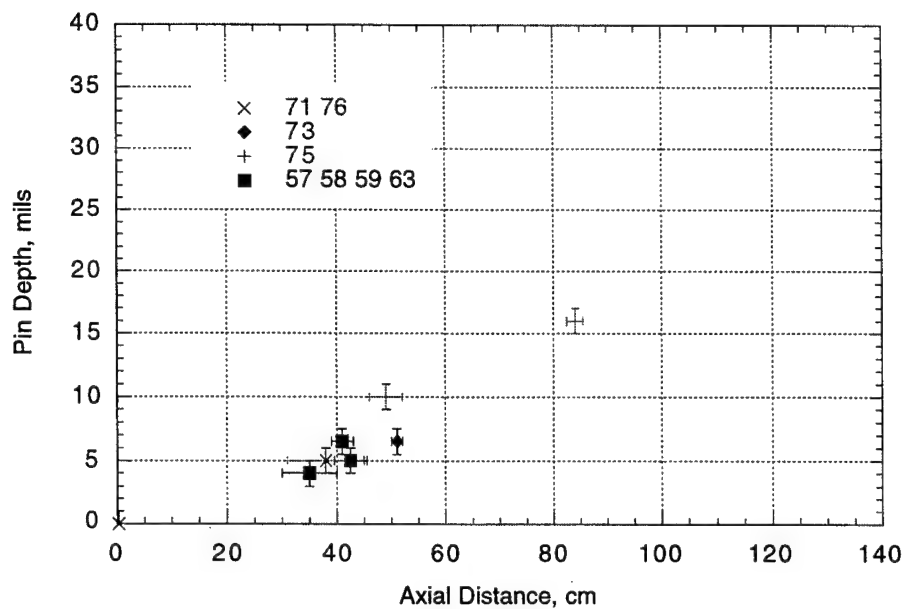


Fig. D2. Wear for row 1, columns 1-4.

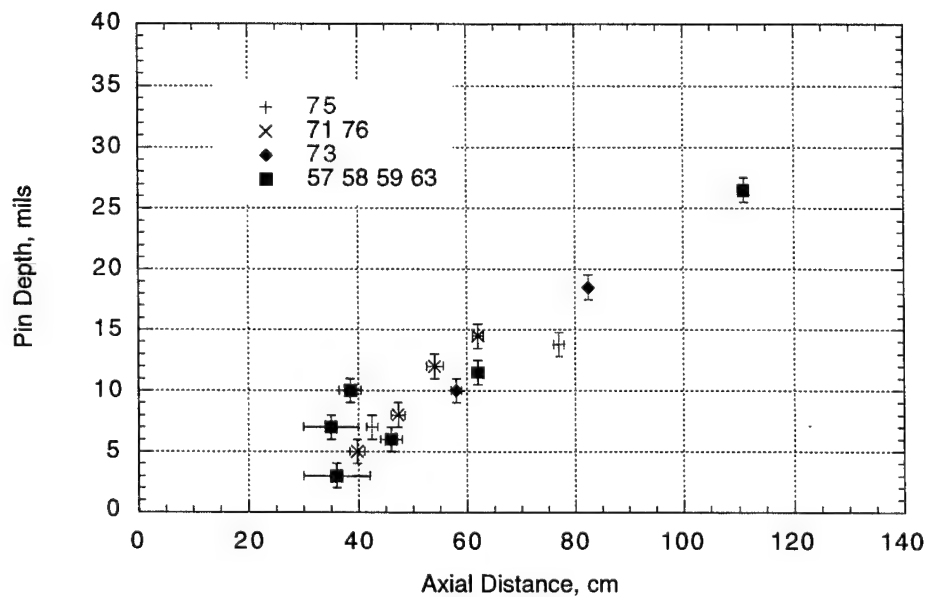


Fig. D3. Wear for row 2, columns 1-4.

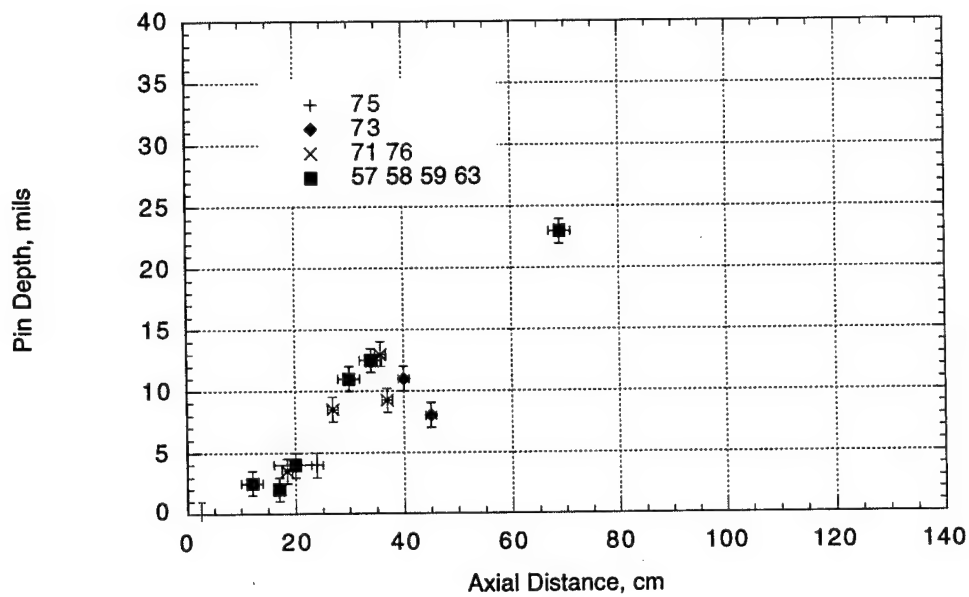


Fig. D4. Wear for row 2, columns 6-7.5.

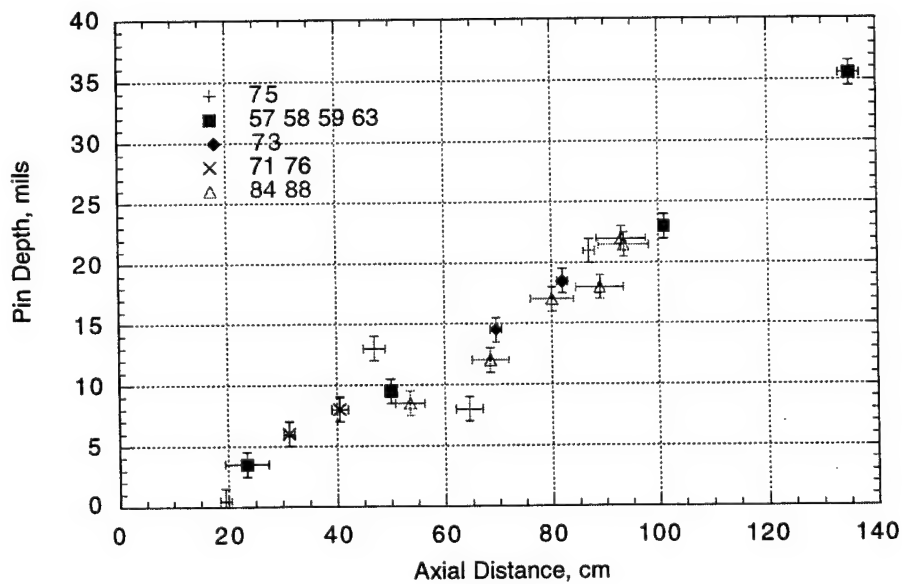


Fig. D5. Wear for row 3, columns 1-4.

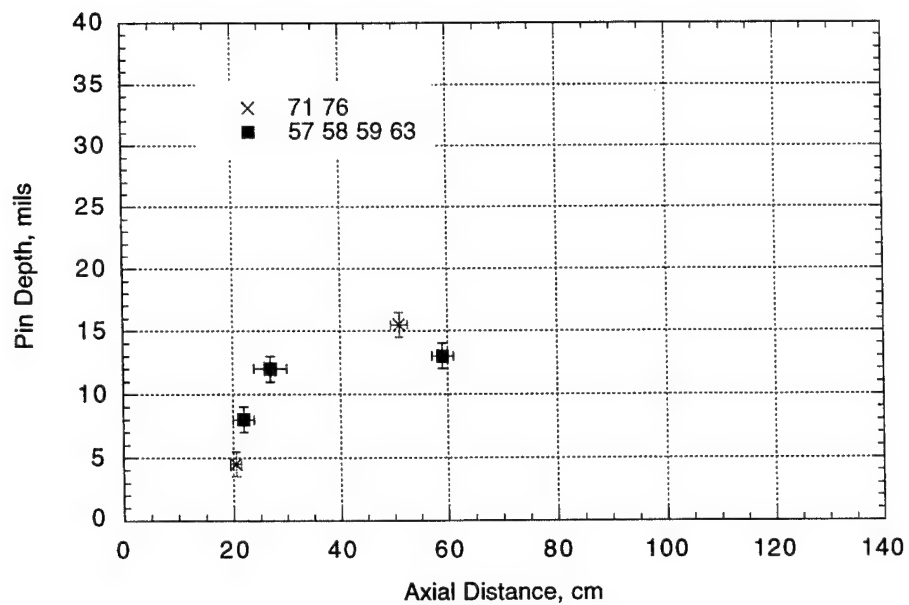


Fig. D6. Wear for row 3, columns 7-9.

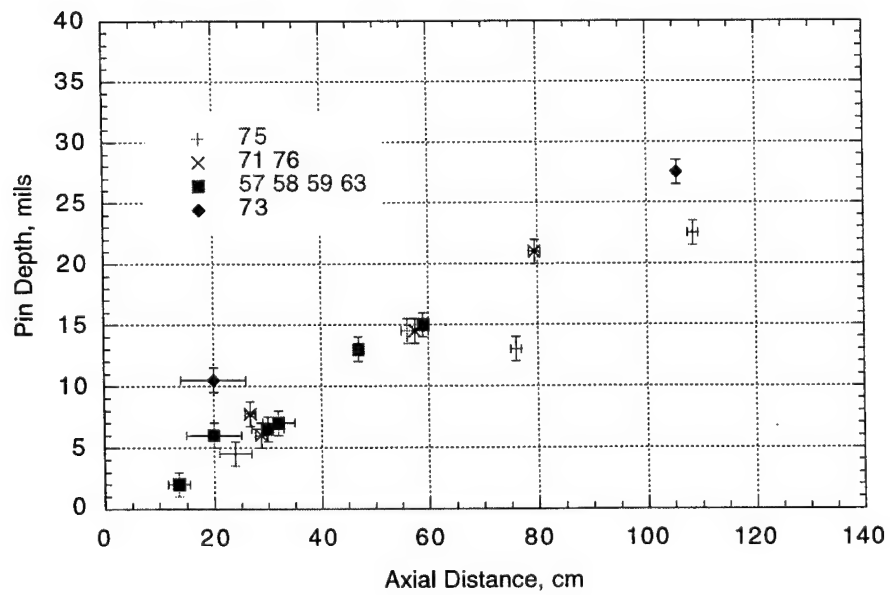


Fig. D7. Wear for row 4, columns 1-3.

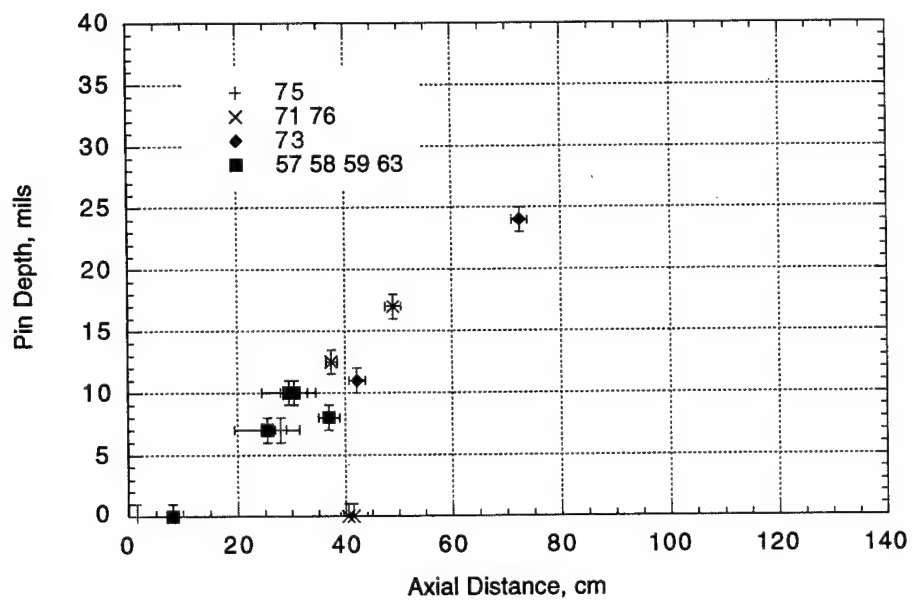


Fig. D8. Wear for row 4, columns 6-9.

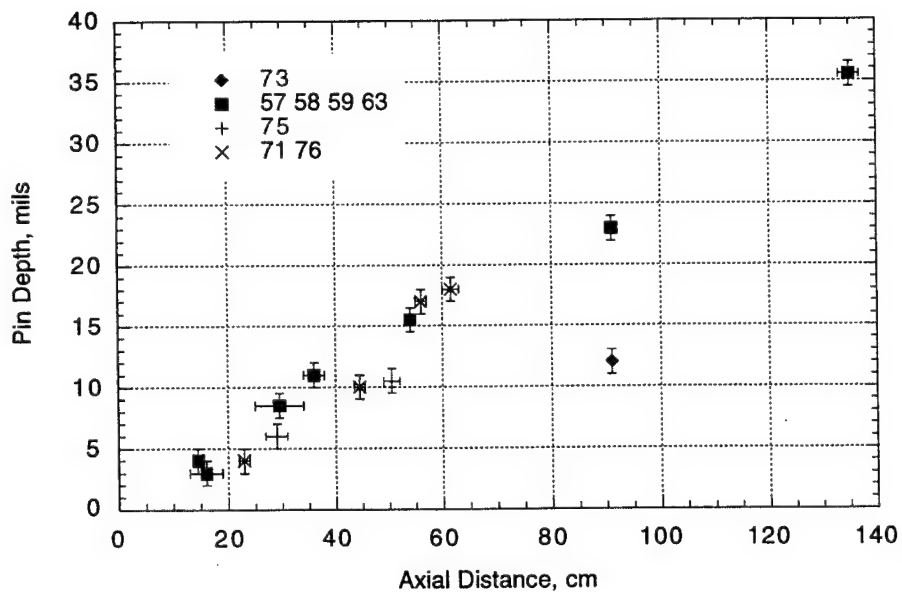


Fig. D9. Wear for row 5, columns 1-3.

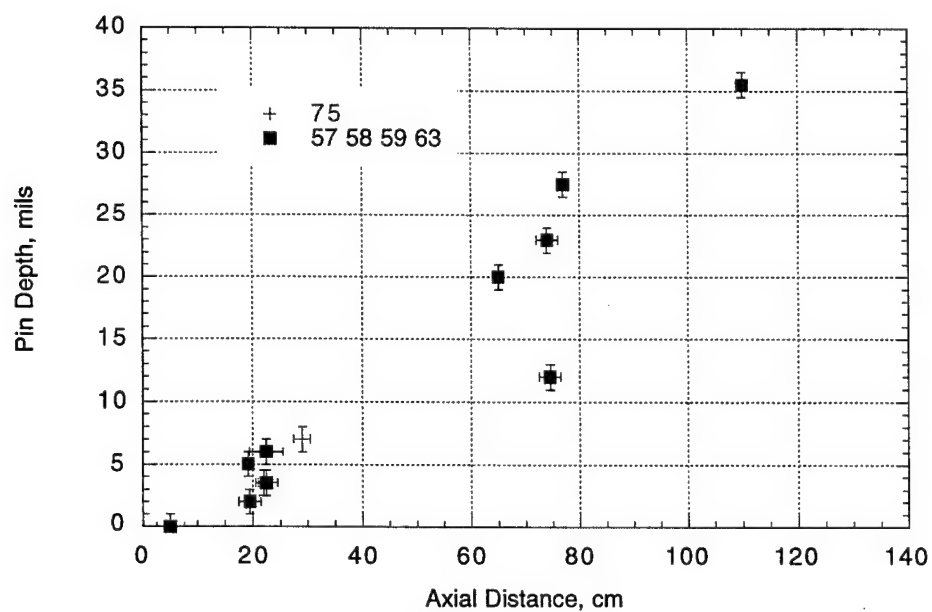


Fig. D10. Wear for row 5, columns 6-8.

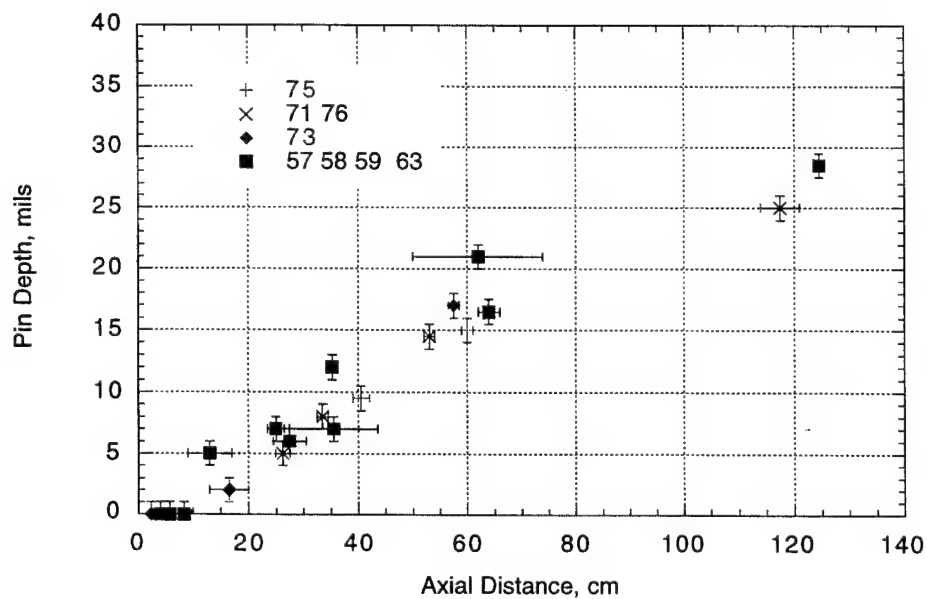


Fig. D11. Wear for row 6, columns 1-4.

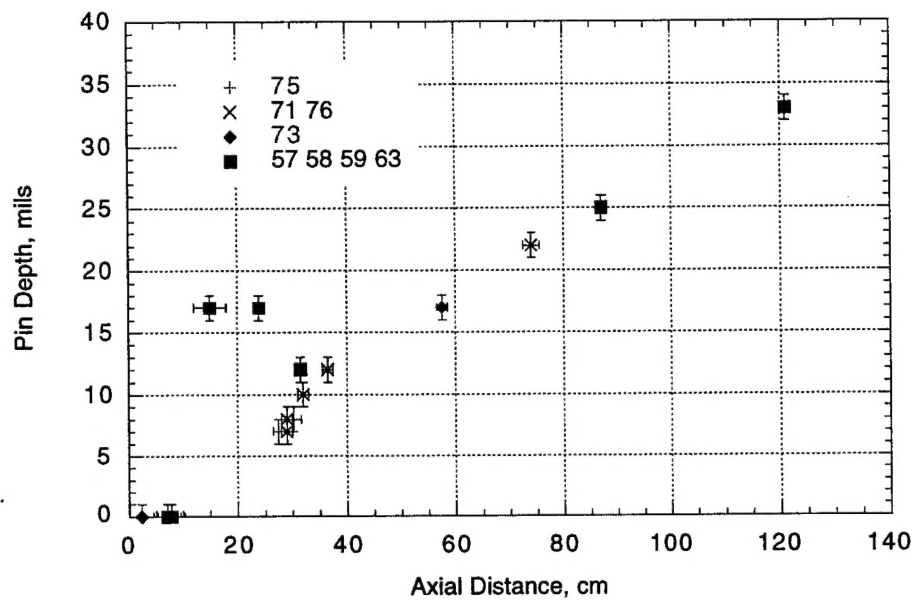


Fig. D12. Wear for row 6, columns 6-9.

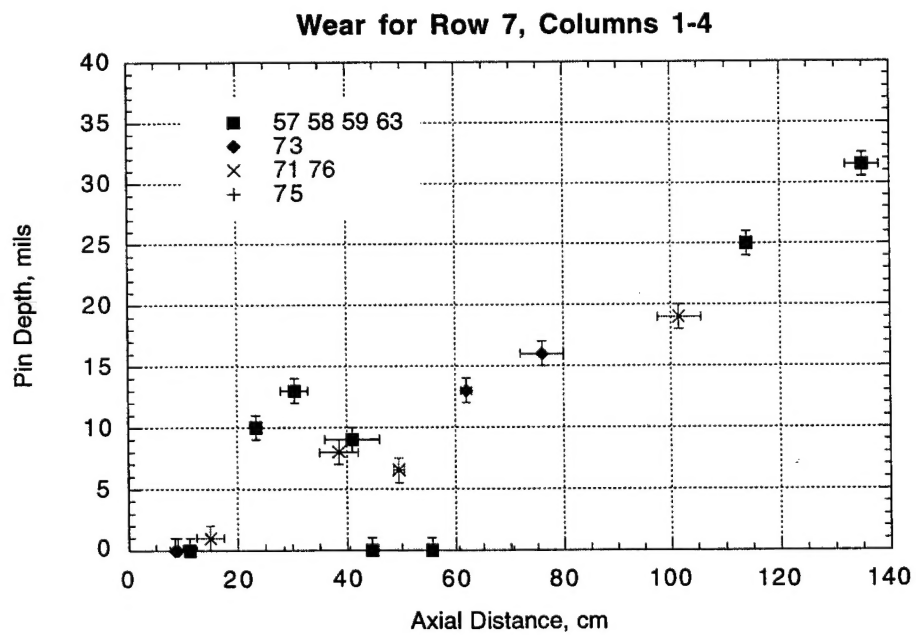


Fig. D13. Wear for row 7, columns 1-4.

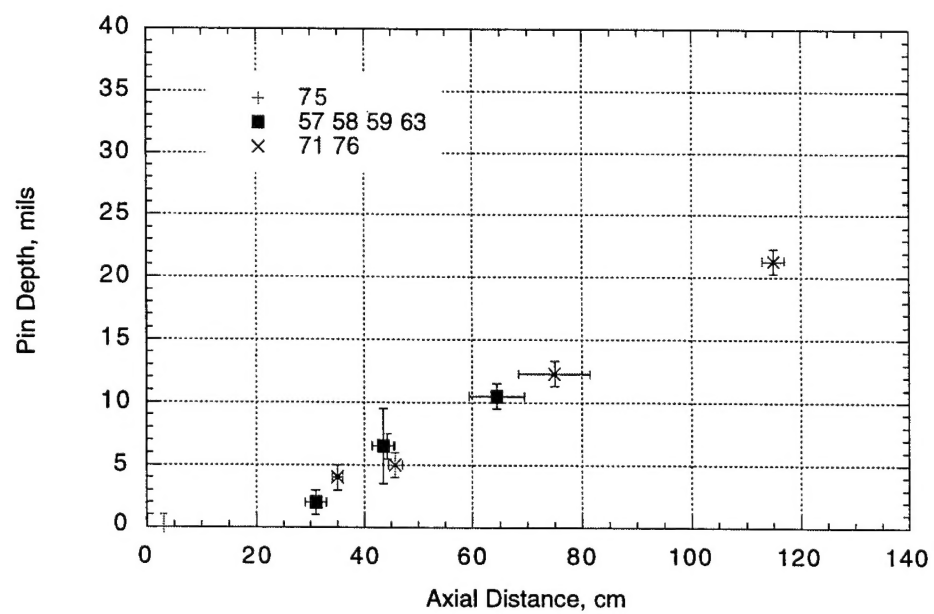


Fig. D14. Wear for row 8, columns 1-4.

Distribution List

Administrator
Defense Technical Information Center
Attn: DTIC-DDA
8725 John J. Kingman Road,
Ste 0944
Ft. Belvoir, VA 22060-6218

Director
US Army Research Lab
ATTN: AMSRL OP SD TA
2800 Powder Mill Road
Adelphi, MD 20783-1145

Director
US Army Research Lab
ATTN: AMSRL OP SD TL
2800 Powder Mill Road
Adelphi, MD 20783-1145

Director
US Army Research Lab
ATTN: AMSRL OP SD TP
2800 Powder Mill Road
Adelphi, MD 20783-1145

Army Research Laboratory
AMSRL-CI-LP
Technical Library 305
Aberdeen Prvg Grd, MD 21005-5066

Mr. Dave Bauer
IAP Research, Incorporated
2763 Culver Avenue
Dayton, OH 45429-3723

Dr. Bruce Burns
U.S Army Research Laboratory
Attn: AMSRL-WT-PD
Bldg. 390
Aberdeen Prvg Grd, MD 21005-5066

Dr. George Chryssomallis
Science Applications International Corp.
3800 W. 80th St., Suite 1090
Bloomington, MN 55431

Dr. Dan Dakin
Science Applications International Corp.
2000 Powell St., Suite 1090
Emeryville, CA 94608

Dr. Harry Fair
Institute for Advanced Technology
The University of Texas at Austin
4030-2 West Braker Lane
Austin, TX 78759

Dr. Scott Fish
Institute for Advanced Technology
The University of Texas at Austin
4030-2 W. Braker Lane
Austin, TX 78759

Dr. Thaddeus Gora
U.S. Army Armament Research,
Development and Engineering Center
Attn: AMSTA-AR-FS Bldg. 94
Picatinny Arsenal, NJ 07806-5000

Dr. Robert Guenther
Army Research Office
P.O. Box 12211
Research Triangle Park, NC 27709-2211

Mr. Albert Horst
Chief, Propulsion and Flight Division
Army Research Laboratory
ATTN: AMSRL -WT-P
Army Research Laboratory
Aberdeen Prvg Grd, MD 21015-5066

Dr. Kuo-Ta Hsieh
Institute for Advanced Technology
The University of Texas at Austin
4030-2 W. Braker Lane
Austin, TX 78759

Dr. Keith A. Jamison
Science Applications International Corp.
1247-B N. Eglin Parkway
P. O. Box 126
Shalimar, FL 32579

Dr. Walter LaBerge
Institute for Advanced Technology
The University of Texas at Austin
4030-2 West Braker Lane
Austin, TX 78759

Dennis Ladd
Commander, TACOM-ARDEC
Attn: AMSTA-AR-FSP-E / Dennis Ladd
Bldg. 354
Picatinny Arsenal, NJ 07806-5000

Dr. Scott Levinson
Institute for Advanced Technology
The University of Texas at Austin
4030-2 W. Braker Lane
Austin, TX 78759

Dr. Hans Mark
Institute for Advanced Technology
The University of Texas at Austin
4030-2 West Braker Lane
Austin, TX 78759

Dr. Ingo W. May
Office of the Director
Army Research Laboratory
ATTN: AMSRL -WT
Army Research Laboratory
Aberdeen Prvg Grd, MD 21015-5066

Distribution List

Dr. Ian McNab
Institute for Advanced Technology
The University of Texas at Austin
4030-2 W. Braker Lane
Austin, TX 78759

Dr. Edward M. Schmidt
U.S. Army Research Laboratory
Attn: AMSRL-WT-B
Aberdeen Prvg Grd, MD 21005-5066

Ms. Rachel Monfredo Gee
Institute for Advanced Technology
The University of Texas at Austin
4030-2 W. Braker Lane
Austin, TX 78759

Mr. Francis Stefani
Institute for Advanced Technology
The University of Texas at Austin
4030-2 W. Braker Ln.
Austin, TX 78759

Dr. Jerry Parker
Institute for Advanced Technology
The University of Texas at Austin
4030-2 W. Braker Lane
Austin, TX 78759

Mr. Patrick Sullivan
Institute for Advanced Technology
The University of Texas at Austin
4030-2 West Braker Lane
Austin, TX 78759

Dr. John Parmentola
SARDA-RT
2511 S. Jefferson Davis Highway
Presidential Towers Bldg., Suite 9000
Arlington, VA 22202-3911

Robert J. Taylor
Lockheed Martin Vought Systems
M/S: WT-21
P.O. Box 650003
Dallas, TX 75265-0003

Dr. Chadee Persad
Institute for Advanced Technology
The University of Texas at Austin
4030-2 W. Braker Lane
Austin, TX 78759

Mr. Alex Zielinski
U.S. Army Research Laboratory
AMSRL-WT-PB, B390, RM 212
Aberdeen Prvg Grd, MD 21005-5066

Dr. John Powell
U.S. Army Research Laboratory
Attn: AMSRL-WT-WD
Bldg. 120
Aberdeen Prvg Grd, MD 21005-5066

Mr. Raymond C. Zowarka
Center for Electromechanics
The University of Texas at Austin
Pickle Research Campus
EME 13, C R 7000
Austin, TX 78712

Mr. Bob Schlenner
U.S. Army Armament Research,
Development and Engineering Center
Attn: AMSTA-AR-CCL
Bldg. 65N
Picatinny Arsenal, NJ 07806-5000